APPLICATION OF MODEL PREDICTIVE CONTROL TO HEATING AND COOLING OF OFF-GRID SHELTERS

A Dissertation
Presented to
The Academic Faculty

by

Sumit K. De

In Partial Fulfillment
of the Requirements for the Degree
of Master of Science in Mechanical Engineering in the
George W. Woodruff School of Mechanical Engineering

Georgia Institute of Technology
December 2017

APPLICATION OF MODEL PREDICTIVE CONTROL TO HEATING AND COOLING OF OFF-GRID SHELTERS

Approved by:

Dr. Yogendra Joshi, Advisor
School of Mechanical Engineering
Georgia Institute of Technology

Dr. Samuel Graham
School of Mechanical Engineering
Georgia Institute of Technology

Dr. Satish Kumar
School of Mechanical Engineering
Georgia Institute of Technology

Date Approved: August 29, 2017

ACKNOWLEDGEMENTS

First and foremost, I would like to thank my advisor, Dr. Yogendra Joshi, for his tremendous support and continuous guidance over the years. I appreciate Dr. Yogendra Joshi for making this thesis and my entire degree come to fruition. Next, I would like to thank Dr. Ashish Sinha for educating me on MPC and always mentoring me. I would also like to thank Brad Stanley at the U.S. Army Communications-Electronics Research, Development and Engineering Center (CERDEC), for his tremendous support with hardware testing and data collection for the project. In addition, I would also like to thank all the colleagues at National Renewable Energy Laboratory (NREL), the U.S. Army Natick Soldier Research, Development and Engineering Center (NSRDEC) and Massachusetts Institute of Technology (MIT) Lincoln Laboratory, who actively assisted in providing and improving the computational model for the thesis. I would also like to thank EOIR Technologies for the guidance with software integration. I would also like to thank my two committee members, Dr. Samuel Graham and Dr. Satish Kumar, for their valuable guidance over the years. I would like to thank my family and friends back home for their continuous support. Also, I would like to thank my friends from METTL Group, MiNDS Group, EMRL Group and FLOID Lab Group for supporting me throughout the years. Lastly, I appreciate the financial support from Office of Naval Research (ONR) throughout my education.

TABLE OF CONTENTS

ACKNOWLEDGEMENTS iii

LIST OF TABLES vii

LIST OF FIGURES viii

LIST OF SYMBOLS AND ABBREVIATIONS xi

ABSTRACT xiii

CHAPTER 1. INTRODUCTION 1

CHAPTER 2. LITERATURE REVIEW 4

2.1 MPC Theory 4
2.1.1 System Model 6
2.1.2 Mathematical Formulation 7
2.1.3 Prediction Horizon 8
2.1.4 Control Horizon 8
2.1.5 Hard and Soft Constraints 9
2.2 MPC Implementation in the Literature 9
2.2.1 Residential and Commercial Heating Ventilation and Air-Conditioning (HVAC) System 9
2.2.2 Military Heating Ventilation and Air-Conditioning (HVAC) System 10
2.3 MPC System Architecture 11
2.4 Shelter Modeling Software 12
2.4.1 EnergyPlus 12
2.4.2 OpenStudio 15
2.5 Mathematical Devising Software 18
2.5.1 MATLAB 18
2.5.2 MLE+ 20
2.6 ECU Controlling Software 22
2.6.1 VirtualBox 23
2.6.2 Linux 23
2.6.2.1 Ubuntu Operating System 24
2.6.3 EIO Application 25

CHAPTER 3. RESEARCH METHODOLOGY 27

3.1 Airbeam Shelter 27
3.2 Environmental Control Units 29
3.2.1 IECU 29
3.2.2 F100 31
3.3 Creation and Validation of EnergyPlus Model 32
3.3.1 Shelter Profile 32
3.3.2 Weather Profile 35
3.3.3 Infiltration Profile 36
3.3.4 ECU Profile 37
3.3.5 Ground-Coupling Profile 38
3.3.6 Interior Load Profile 40
3.3.7 Thermostat Profile 41
3.4 EnergyPlus Framework 41
3.5 MPC Framework 43
3.5.1 Input 1: EnergyPlus model of shelter + ECU 44
3.5.2 Input 2: Thermostat set-point schedule 44
3.5.3 Input 3: Range of input set-point temperature choices 45
3.5.4 MPC workflow components 45
3.5.5 MPC workflow description 47
3.6 Integrated MPC Framework with EIO Application 48
3.6.1 Software development of API 49

CHAPTER 4. SIMULATION RESULTS AND DISCUSSION 54

4.1 Airbeam Shelter with F100 – Thermal Comfort Optimization 54
4.1.1 Loads Applied to the Model 55
4.1.2 Results for February 1 56
4.1.2.1 Main Zone Temperature 56
4.1.2.2 Power Consumption 57
4.1.3 Results for April 1 59
4.1.3.1 Main Zone Temperature 59
4.1.3.2 Power Consumption 60
4.1.4 Results for June 1 – CASE A 61
4.1.4.1 Main Zone Temperature 61
4.1.4.2 Power Consumption 62
4.1.5 Results for June 1 – CASE B 64
4.1.5.1 Main Zone Temperature 64
4.1.5.2 Power Consumption 65
4.1.6 Results for June 1 – CASE C 66
4.1.6.1 Main Zone Temperature 66
4.1.6.2 Power Consumption 67
4.2 Discussion of Results for Airbeam Shelter with F100 – Thermal Comfort Optimization 69
4.3 Airbeam Shelter with F100 – Energy Consumption Optimization 71
4.3.1 Loads Applied to the Model 72
4.3.2 Results for February 1 73
4.3.2.1 Main Zone Temperature 73

4.3.2.2 Power Consumption 74
4.3.3 Results for April 1 76
4.3.3.1 Main Zone Temperature 76
4.3.3.2 Power Consumption 77
4.3.4 Results for June 1 78
4.3.4.1 Main Zone Temperature 78
4.3.4.2 Power Consumption 79
4.4 Discussion of Results for Airbeam Shelter with F100 – Energy Consumption Optimization 81
4.5 Thermal Comfort Optimization – Humidity Level Based 82

CHAPTER 5. FIELD APPLICATION RESULTS AND DISCUSSION 84

5.1 Alaska Shelter with IECU 84
5.1.1 Loads Applied to the Shelter 85
5.1.2 Inconsistencies 88
5.1.2.1 MPC Model and Alaska Shelter 88
5.1.2.2 Run Period 89
5.1.3 Results for MPC versus Manual Control 90
5.1.3.1 Zone Temperature 90
5.1.3.2 Power Consumption 92
5.1.3.3 Zone Temperature and Power Consumption – Superimposed 93
5.2 Discussion of Results for Alaska Shelter with IECU 97
5.3 Verification of Application of MPC versus Manual Control 98
5.3.1 Loads Applied to the Model 98
5.3.2 Results 99
5.3.2.1 Main Zone Temperature 100
5.3.2.2 Power Consumption 101
5.4 Discussion of Results for Verification of MPC Application 104
5.5 Real-Time Load Profile Live-Updates during MPC Operation 105

CHAPTER 6. CONCLUSION & FUTURE WORK 107

6.1 Conclusion 107
6.2 Future Work 109

REFERENCES 111

LIST OF TABLES

Table 1 – IECU Specifications [43] 30

Table 2 – F100 Specifications [44] 32

Table 3 – Airbeam Shelter Material Properties [42] 34

Table 4 – System Health Responses [50] 50

Table 5 – ECU Commands [50] 51

Table 6 – MPC vs. EnergyPlus Net Load (kWh) Comparison – F100 69

Table 7 – MPC vs. EnergyPlus Net Load (kWh) Comparison – F100 81

Table 8 – MPC vs. Manual Control Net Load (kWh) Comparison – IECU 97

Table 9 – June 22 vs. July 21 Net Load (kWh) Comparison – IECU 104

LIST OF FIGURES

Figure 1 – MPC Theory [courtesy of Dr. Ashish Sinha, Senior Hardware/Thermal Engineer, Oracle] 5

Figure 2 – Integration of software to perform MPC 12

Figure 3 – Overall Structure of EnergyPlus [32] 14

Figure 4 – Various Classes of EnergyPlus Objects [32] 15

Figure 5 – OpenStudio SketchUp Plug-In [34] 17

Figure 6 – OpenStudio Application [34] 18

Figure 7 – MATLAB Desktop [36] 20

Figure 8 – MLE+ Interface [37] 22

Figure 9 – VirtualBox Desktop [38] 23

Figure 10 – Ubuntu OS Desktop [39] 25

Figure 11 – EIO Application Desktop [41] 26

Figure 12 – Airbeam Shelter Perspective View 1: L×W×H = 20 ft × 32 ft × 11 ft [42] 28

Figure 13 – Airbeam Shelter Perspective View 2: L×W×H = 20 ft × 32 ft × 11 ft [42] 29

Figure 14 – HDT 60K IECU [43] 30

Figure 15 – HDT 60K F100 [44] 31

Figure 16 – Airbeam Shelter Model [42] 33

Figure 17 – EnergyPlus Control Schematic [courtesy of Dr. Ashish Sinha, Senior Hardware/Thermal Engineer, Oracle] 43

Figure 18 – MPC Inputs [courtesy of Dr. Ashish Sinha, Senior Hardware/Thermal Engineer, Oracle] 45

Figure 19 – MPC Schematic [courtesy of Dr. Ashish Sinha, Senior Hardware/Thermal Engineer, Oracle] 47

Figure 20 – Data Flow Inside MPC [29] 48

Figure 21 – High-Level Overview of Integration 53

Figure 22 – Site Outdoor Dry Air Bulb Temperature – Worcester, MA 55

Figure 23 – MPC vs. EnergyPlus – Main Zone Temperature – FEB 1 57

Figure 24 – MPC vs. EnergyPlus – Cooling Coil Electric Power – FEB 1 58

Figure 25 – MPC vs. EnergyPlus – Heating Coil Electric Power – FEB 1 58

Figure 26 – MPC vs. EnergyPlus – Main Zone Temperature – APR 1 59

Figure 27 – MPC vs. EnergyPlus – Cooling Coil Electric Power – APR 1 60

Figure 28 – MPC vs. EnergyPlus – Heating Coil Electric Power – APR 1 61

Figure 29 – MPC vs. EnergyPlus – Main Zone Temperature – JUN 1 – CASE A 62

Figure 30 – MPC vs. EnergyPlus – Cooling Coil Electric Power – JUN 1 – CASE A 63

Figure 31 – MPC vs. EnergyPlus – Heating Coil Electric Power – JUN 1 – CASE A 63

Figure 32 – MPC vs. EnergyPlus – Main Zone Temperature – JUN 1 – CASE B 64

Figure 33 – MPC vs. EnergyPlus – Cooling Coil Electric Power – JUN 1 – CASE C 65

Figure 34 – MPC vs. EnergyPlus – Heating Coil Electric Power – JUN 1 – CASE C 66

Figure 35 – MPC vs. EnergyPlus – Main Zone Temperature – JUN 1 – CASE C 67

Figure 36 – MPC vs. EnergyPlus – Cooling Coil Electric Power – JUN 1 – CASE C 68

Figure 37 – MPC vs. EnergyPlus – Heating Coil Electric Power – JUN 1 – CASE B 68

Figure 38 – Site Outdoor Dry Air Bulb Temperature – Worcester, MA 72

Figure 39 – MPC vs. EnergyPlus – Main Zone Temperature – FEB 1 74

Figure 40 – MPC vs. EnergyPlus – Cooling Coil Electric Power – FEB 1 75

Figure 41 – MPC vs. EnergyPlus – Heating Coil Electric Power – FEB 1 75

Figure 42 – MPC vs. EnergyPlus – Main Zone Temperature – APR 1 76

Figure 43 – MPC vs. EnergyPlus – Cooling Coil Electric Power – APR 1 77

Figure 44 – MPC vs. EnergyPlus – Heating Coil Electric Power – APR 1 78

Figure 45 – MPC vs. EnergyPlus – Main Zone Temperature – JUN 1 79

Figure 46 – MPC vs. EnergyPlus – Cooling Coil Electric Power – JUN 1 80

Figure 47 – MPC vs. EnergyPlus – Heating Coil Electric Power – JUN 1 80

Figure 48 - Alaska Shelter Perspective View: L×W×H = 20 ft × 32 ft × 11 ft [51] 85

Figure 49 – Actual Weather History of McGuire AFB on June 22, 2017 [52] 86

Figure 50 – Actual Weather History of McGuire AFB on July 21, 2017 [53] 87

Figure 51 – Controller Input for Application of MPC 88

Figure 52 – Manual Control – Zone Temperature – JULY 21 91

Figure 53 – MPC – Zone Temperature - JUNE 22 91

Figure 54 – MPC vs. Manual Control – IECU Power Consumption – JUN 22 93

Figure 55 – Manual Control – Zone Temperature & Power Consumption – Superimposed 95

Figure 56 – MPC – Zone Temperature & Power Consumption – Superimposed 97

Figure 57 – Site Outdoor Dry Air Bulb Temperature – McGuire AFB, NJ 99

Figure 58 – June 22 vs. July 21 – Main Zone Temperature – EnergyPlus Simulations 100

Figure 59 – June 22 vs. July 21 – Unitary System Electric Power – EnergyPlus Simulations 102

Figure 60 – June 22 vs. July 21 – Cooling Coil Electric Power – EnergyPlus Simulations 103

Figure 61 – June 22 vs. July 21 – Heating Coil Electric Power – EnergyPlus Simulations 103

LIST OF SYMBOLS AND ABBREVIATIONS

ACH	Air Changes per Hour or Air Change Rate
AFB	Air Force Base
API	Application Programming Interface
COP	Coefficient of Performance
CTF	Conduction Transfer Function
DoD	Department of Defense
DoE	Department of Energy
ECU	Environmental Control Unit
EIO	Energy Informed Operations
FOB	Forward Operating Base
HVAC	Heating Ventilation and Air Conditioning
MPC	Model Predictive Control
NREL	National Renewable Energy Laboratory
OS	Operating System
PID	Proportional–Integral–Derivative
REST	Representational State Transfer
URL	Uniform Resource Locator

ABSTRACT

An increasing concern at off-grid forward operating bases (FOBs), disaster relief camps, refugee aid camps and other encampments is the rising cost of supplying and sustaining shelters to accommodate the occupant(s). This is due to high risk burdened costs of liquid fuel deliveries, needed for local electricity generation in remote, and often hostile regions, where such contingency bases are located. A significant part of the non-combat mission related energy consumption in such bases is towards the heating and cooling of shelters. The Environmental Control Unit (ECU) for a shelter, consisting of the components and controls of a packaged terminal air conditioner & heat pump, is operated with a simple set-point temperature control. For such shelters, more efficient use of energy can be accomplished by applying a model predictive control (MPC) approach to the ECU. MPC selects the most fuel efficient operation of the shelter ECU, based on shelter size, materials and construction, internal thermal loads, weather profile, including wind speed, solar insolation, infiltration, and ground coupling. The thesis demonstrates a first-of-its-kind, more energy-efficient and more thermally comfort application of the MPC approach on an Alaska soft shell shelter, equipped with an ECU, by performing a combination of MATLAB and EnergyPlus modeling.

CHAPTER 1. INTRODUCTION

Supporting and sustaining operations at off-grid FOBs, disaster relief camps, refugee aid camps and other encampments require enormous supply of transported liquid fuel for onsite generation of electricity. The generated electricity by heavy generators provides power to the various transported systems and equipment at the base. The heating/cooling system for a military off-grid shelter accounts for as much as 80% of electrical energy usage at a typical military outpost [1]. The predicted average risk-burdened cost of a gallon of fuel delivered at the FOB ranges from $15 to up to $600 [1]. This is a key motivation for pioneering new methods for reducing heating/cooling energy usage, without compromising on the effectiveness of the mission.

This thesis investigates the implementation and validation of a model predictive control (MPC) framework to a military shelter and environmental control unit (ECU). MPC is performed on an EnergyPlus exported form of the validated shelter model, for a soft-shell off-grid shelter (HDT AirBeam Model 2032A). The validated shelter model also stores the unit specifications of the paired heating/cooling unit (such as HDT F100 or IECU). A typical MPC simulation obtains system energy usage, and other model output variables for a set of input sequences. Simulations performed for multiple sets of input conditions are sorted to select the most fuel efficient prediction [2]. This chosen prediction is applied for the most immediate time step, and is repeated at every upcoming time step until the end of a user chosen prediction horizon. The programmatic framework will sequentially cycle and choose the set-point temperature for the ECU after choosing the most efficient model based on the system usage, as dictated by the equipment load profile,

electrical load profile, weather profile, convection profile, humidity, solar radiation, infiltration, and other components of heat transfer to the shelter.

Chapter 2 of this thesis provides the supporting literature review of the MPC theory and application in the industry. In addition, it introduces the various software used in this work, which are categorized under shelter modeling, mathematical formulation, and ECU control. The building energy usage simulation tools such as EnergyPlus and OpenStudio, and system response modeling tools such as MATLAB and MLE+ are described. In addition, the integration enabling framework, including VirtualBox software running Linux-based Ubuntu operating system (OS), which ultimately enabled the MPC application interface with the military software EIO Application for communicating with an intelligent environmental control unit (IECU), are also described.

Chapter 3 of this thesis provides the methodology for creating the EnergyPlus model of the shelter and ECU for the simulation, validating the shelter model, defining the variables involved with MPC, choosing hard and soft constraints, and various other procedures in preparation for conducting MPC simulations. Since one form of the results for analysis is quantifying the results obtained with MPC versus results obtained with baseline OpenStudio simulation, detailed workflow of controller for the MPC tool is thoroughly discussed. Also, since this MPC tool was operated at a military FOB for data collection, the procedures undertaken to develop the software interface between MPC framework and military software interface are also discussed.

Chapters 4 & 5 provide the results for MPC model validation by comparing results with corresponding baseline model OpenStudio simulation. Also, the results of the MPC

implementation to an actual ECU compared with conventional manual control on ECU are discussed. Specifically, the ventilated zone temperatures, and the electrical power consumption results under each baseline control and MPC are assessed.

Chapter 6 presents the conclusion of this thesis, along with its significance and contribution to future application.

CHAPTER 2. LITERATURE REVIEW

This chapter provides description of several resources utilized in the research. The foremost focus is on the MPC theory, and its applications in the building energy management literature. The subsequent focus is on the various software used in conceptualization, formulation and application of the MPC tool to an actual ECU/shelter setup. The following software execute the aforementioned processes -

- EnergyPlus simulates the characteristics of a shelter with ECU
- OpenStudio executes baseline EnergyPlus simulations
- MATLAB performs the MPC calculations
- MLE+ executes autonomous EnergyPlus simulation sessions
- VirtualBox generates virtual operating systems
- Linux-based Ubuntu OS facilitates executing EIO Application
- EIO Application electronically controls an actual ECU

The chapter also describes other concepts involved in the process and the inter-relationships between the various simulation tools.

2.1 MPC Theory

MPC is a control technique that considers future system behaviors for a set of anticipated control actions, to determine the most suitable control action to be applied to the system at the 'present' moment [2]. A model of the system is used to predict future system behavior under a given set of control actions. Several control actions are applied to the validated model of the system and the corresponding system behaviors are predicted.

An optimization scheme is subsequently used to weigh various control actions in terms of compliance with control objectives and constraints, and to choose the optimum control action. From the chosen sequence, the control action for the first time interval is applied at the present moment, while the rest of the control actions are discarded, and the entire process is repeated for the next time interval. Figure 1 displays the controller logic of MPC [2].

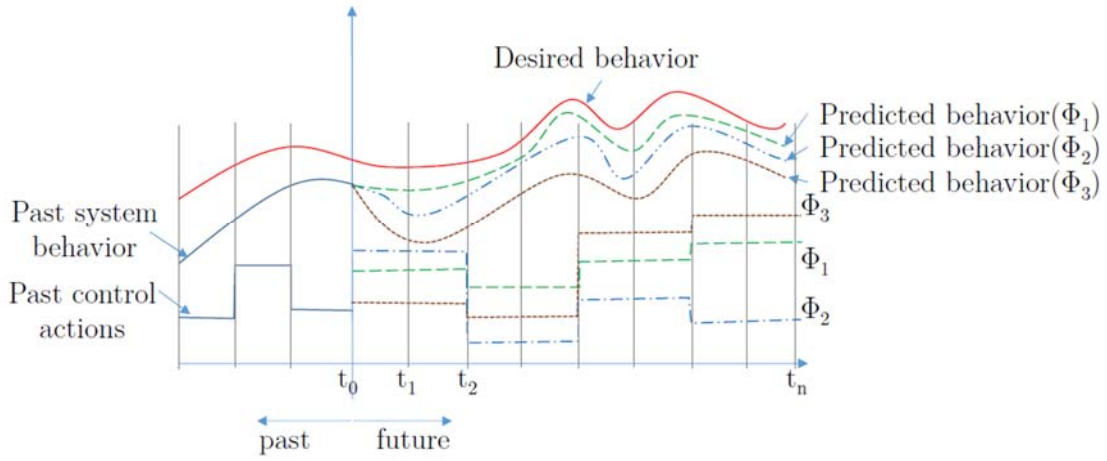

Figure 1 – MPC Theory [courtesy of Dr. Ashish Sinha, Senior Hardware/Thermal Engineer, Oracle]

For the task of controlling a system, with the objective of closely matching its behavior to the desired behavior as shown by red colored line in Figure 1, the system can be controlled by control actions which can be imposed at time instants t_0, t_1,… t_n. The model predictive controller tasked with controlling the system would apply the control action sequences to the system's model, and predict its future behavior for up to n time steps. Figure 1 shows three distinct behaviors of the system for three control action sequences [Φ_1, Φ_2, Φ_3]. With every control action sequence there would be a unique cost

associated, defined in terms of energy use, waste generation, or monetary cost of executing the control actions.

Once the future behaviors are predicted, the controller would select the control action sequence that provides best compliance with the desired behavior, while satisfying cost constraints associated with the control actions. This often requires extensive computing resource for a real system with several inputs and outputs. Thus, several possible combination of control actions need to be assessed to determine the most suitable control action. The first step of the chosen control action sequence is applied to the system as control for the 'current' time step while the control actions for the rest of the time steps are discarded. Thereafter, as time moves forward from $t = t_0$ to $t = t_1$, the entire control process, as described above, is repeated for t_1 with the system behavior now predicted till t_{n+1}.

2.1.1 System Model

System model is critical for the application of predictive control. A model is used in place of a real system to predict system behavior under future control actions. The predicted behavior and the results obtained by predictive control will only be as good as the fidelity of the model with respect to the physical system. There are three main approaches to obtaining a system model (i) white box, i.e. using fundamental physics based equations to obtain system model, (ii) black box, i.e. use of past system input-output data to obtain a system model and (iii) grey box model, a combination of white and black box approaches. It should be noted that models for predictive control can only be discrete in time [2]. The computational exercise required to determine the best control actions moving

forward will always lead to time gap between successive control actions, thus disrupting temporal continuity.

2.1.2 Mathematical Formulation

Physical systems are often represented by state-space mathematical models for the purpose of predictive control. Equations 1 & 2 provide the general form of a state space representation in discrete time -

$$X_{t+1} = AX_t + BU_t \tag{1}$$

$$Y_t = CX_t + DU_t \tag{2}$$

Here X_t, Y_t, U_t are vectors representing the states of the physical system, measured outputs and input (control) signals at time instant t (i.e the current time instant). X_{t+1} represents the 'one step ahead' future system state.

The above set of equations can be transformed to express system outputs at a k step ahead time instant in future, but in terms of current system states and planned control actions over the k time steps. Equations 3 & 4 show the system states for the k step ahead prediction -

$$\begin{bmatrix} X_{t+1} \\ X_{t+2} \\ \dots \\ X_{t+k} \end{bmatrix} = A_1[X_t] + B_1 \begin{bmatrix} U_t \\ U_{t+1} \\ \dots \\ U_{t+k-1} \end{bmatrix} \tag{3}$$

$$\begin{bmatrix} Y_{t+1} \\ Y_{t+2} \\ \dots \\ Y_{t+k} \end{bmatrix} = C_1[X_t] + D_1 \begin{bmatrix} U_t \\ U_{t+1} \\ \dots \\ U_{t+k-1} \end{bmatrix} \quad (4)$$

Equation 4 explicitly represents a set of measured system outputs up to k time steps into future, in terms of known system state at the current time instant t and control action sequence over the future time steps. The matrix containing the various U elements on the right hand side of the equation is a typical control action sequence($\Phi_{i\,=\,1,2,3}$) as shown in Figure 1 and the matrix containing various Y elements on the left side of the equation is the predicted system behavior up to k time steps. Once the system behavior is predicted for a set of control action sequences, an optimization algorithm or a brute force exhaustive search method can be used to choose control action sequence that satisfies cost parameter as well as compliance with the desired behavior. Formulations for this process can be found in the text and is out of scope of this paper.

2.1.3 Prediction Horizon

Prediction horizon is the time extending into future for which system outputs are predicted [2]. In most cases of MPC, this extent of time in future is kept constant. As a result, the future-most time keeps advancing as time progresses. Such a prediction horizon is called a '*receding horizon*'. The process described in Figure 1 has a prediction horizon of n time steps.

2.1.4 Control Horizon

Control horizon is the number of slabs into which the prediction horizon is divided for future control actions to be held constant [2]. This reduces the complexity associated with multiple combinations of control actions for each time step. In Figure 1 if $n = 8$ is considered, the control horizon equates to 4 and equally divides over the prediction horizon, i.e. 4 slabs of time and each containing two time steps. Control actions can be seen to be constant within a slab.

2.1.5 Hard and Soft Constraints

Hard and soft constraints describe the flexibility a predictive controller has while choosing suitable control action sequences [2]. For a system with energy use as a cost of control action, lower limits of energy use can be applied as a hard or a soft constraint. While a hard constraint cannot be breached, thus leading to unsolvable control problems in some cases, a soft constraint can be breached to maintain continuous operations.

2.2 MPC Implementation in the Literature

To support the implementation and application of MPC approach to an actual ECU providing ventilation to a shelter at a FOB, it is crucial to understand the relevancy and efficiency of the tool in the current industry. Both theoretical and experimental approaches of MPC are considered for assessing the benefits of the work.

2.2.1 Residential and Commercial Heating Ventilation and Air-Conditioning (HVAC) System

The fundamentals of MPC have been successfully implemented into industrial applications. As per several literature sources, MPC is already a tested and implemented

control mechanism for optimizing HVAC energy consumption for both residential and commercial applications [3 - 23]. Moreover, researchers have validated the competency of MPC controllers for multiple input/output type building heater system as compared to conventional on-off controller as well as PID (proportional–integral–derivative) controller [24]. Authors such as Hazyuk et al. [25], Rehrl and Horn [26], Sturzenegger et al. [27] and Gruber et al. [28] have also reinforced the superiority of MPC over PID control and any traditional control for typical HVAC control needs, which involve multiple input-output systems.

2.2.2 Military Heating Ventilation and Air-Conditioning (HVAC) System

Beyond application of MPC to residential and commercial systems, the control approach has also been studied for its application to soft shell military shelters. Since the military HVAC system is nearly identical in its control framework to a residential or commercial HVAC system, results described in the literature show favourable outcomes for MPC application to the HVAC system of military shelters. Application of MPC on military soft shelter ECUs has been studied to demonstrate energy savings of up to 12%, and peak power reduction of up to 18% [29]. The approach considers Base-X 305 Military soft shelter with a 6 Ton ColPro ECU, both products of *HDT Global* [29]. Another study with the same shelter and ECU from *HDT Global* supports suitable functionality of the MPC approach to both a singular model of the combined shelter with ECU and independent models of shelter and ECU [30]. Thus, favorable literature data of theoretical studies supporting energy savings, as well as unrestricted approaches using MPC, especially on military soft-shell shelters, establish the applicability of the approach for testing on a physical ECU with a shelter at a FOB.

2.3 MPC System Architecture

MPC framework is hosted by MATLAB with syntax for MLE+ within its script. The syntax encloses EnergyPlus model while the EnergyPlus model encloses the EnergyPlus weather file. EIO Application is the military graphic user interface (GUI) software for controlling multiple hardware at a FOB via the micro-grid. With electrical power locally generated by generators using liquid fuel, the micro-grid device distributes the generator power to the various electronic equipment at a FOB. Additionally, MATLAB is a Windows OS software, while EIO Application is a Linux-based Ubuntu OS software. VirtualBox application allows for a virtual machine to have a dedicated Ubuntu OS to install and launch EIO Application. Moreover, the EIO Application is a web-based software which uses the internet server to generate logs, update statuses and control devices via the micro-grid. The hardware connection via an Ethernet cable among the micro-grid and all devices as well as the dedicated laptop for the EIO Application and MPC establishes the complete software-to-hardware systems architecture of the control. Figure 2 provides an operating overview of the final integrated workflow between MPC and EIO Application.

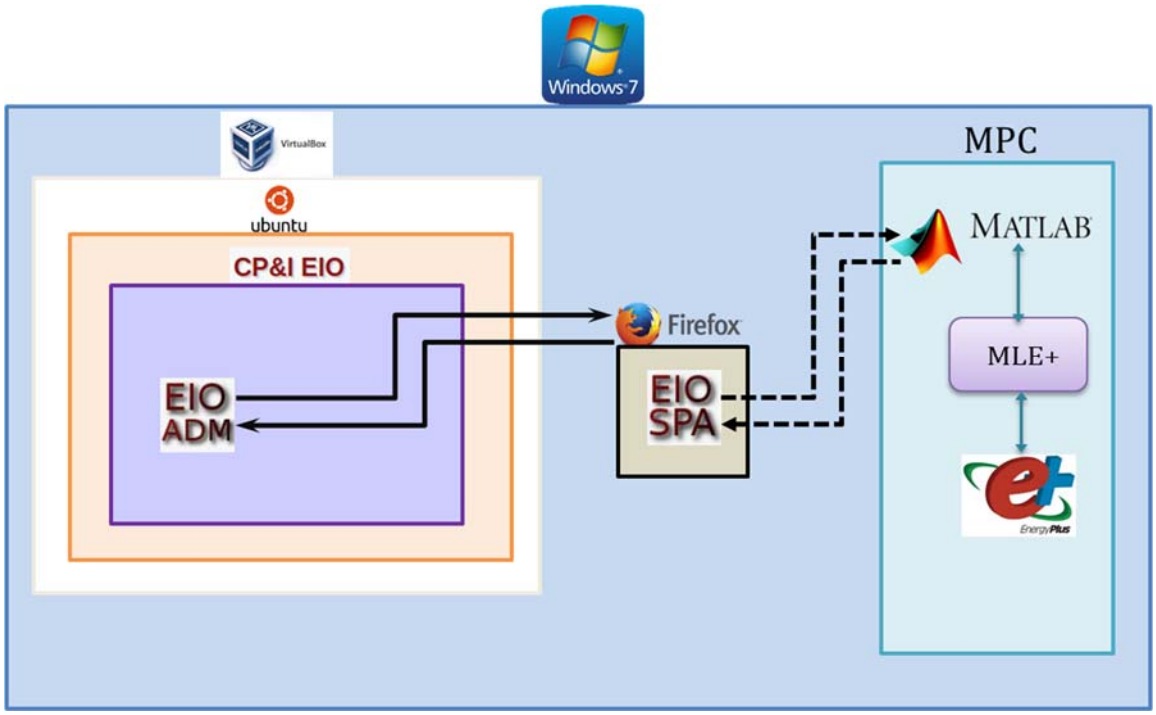

Figure 2 – Integration of software to perform MPC

2.4 Shelter Modeling Software

The first category of software discussed in this chapter is shelter modeling. The models are created in EnergyPlus and controlled in OpenStudio GUI. SketchUp tool serves as the software for architecturally constructing the model, to be defined and functionalized by EnergyPlus.

2.4.1 EnergyPlus

The United States Department of Energy (DoE) simulation software known as EnergyPlus is an energy analysis and thermal load simulation program released in early 2001. EnergyPlus effectively replaced two previously used building energy simulation programs: BLAST (Building Loads Analysis and System Thermodynamics) and DOE-2 [31]. Both programs written in FORTRAN over two decades ago; BLAST uses a heat

transfer balance method for its simulations whereas DOE-2 uses a room weighting factor approach in its simulations [31]. Upon conceptualization of the EnergyPlus software in 1996, U.S. Department of Energy (DOE), CERL, University of Illinois, Lawrence Berkeley National Laboratory (LBNL), Oklahoma State University, and Gaud Analytics released the beta version of EnergyPlus in 1999 and the first version of EnergyPlus in 2001 [31].

The simulation code of EnergyPlus is written in C++ [32]. The software performs simulations, and simultaneously calculates the heating and cooling load requirements necessary for maintaining temperature thermostat set-point(s). Calculations are based upon the physical architecture of the housing, the heating/cooling system, the interior load profile of the housing and the exterior load profile of the surrounding. More functionalities of the software are integration and simultaneous solution for coupled systems, iterative calculations for building responses and simulation time-steps in the range from hourly to sub-hourly. Heat transfer approach taken by the simulations involves energy balance involving both radiation and convection effects in both interior and exterior surfaces. However, major assumptions such as uniform surface temperatures, uniform wave irradiation and one-dimensional heat condition simplify as well as restrict the energy balance model. Other functionalities of EnergyPlus includes transient heat conduction, three-dimensional finite difference ground analytical techniques, layer-by-layer integration of moisture adsorption/desorption into conduction transfer functions, and effective moisture penetration depth model (EMPD). The thermal comfort models are based on the activity, inside dry bulb, and humidity in the environment. The abilities of EnergyPlus to configure complex heating/cooling systems and to produce high fidelity simulation results make it a proper simulation tool for the purpose of building/shelter housing load analysis

[32]. Figure 3 describes the workflow within EnergyPlus, in which independent simulation objects for the heat and mass balance equations and the independent simulation objects for the building system calculations interact to determine the final results. Final results are typically viewed in user-prescribed set of output variable objects.

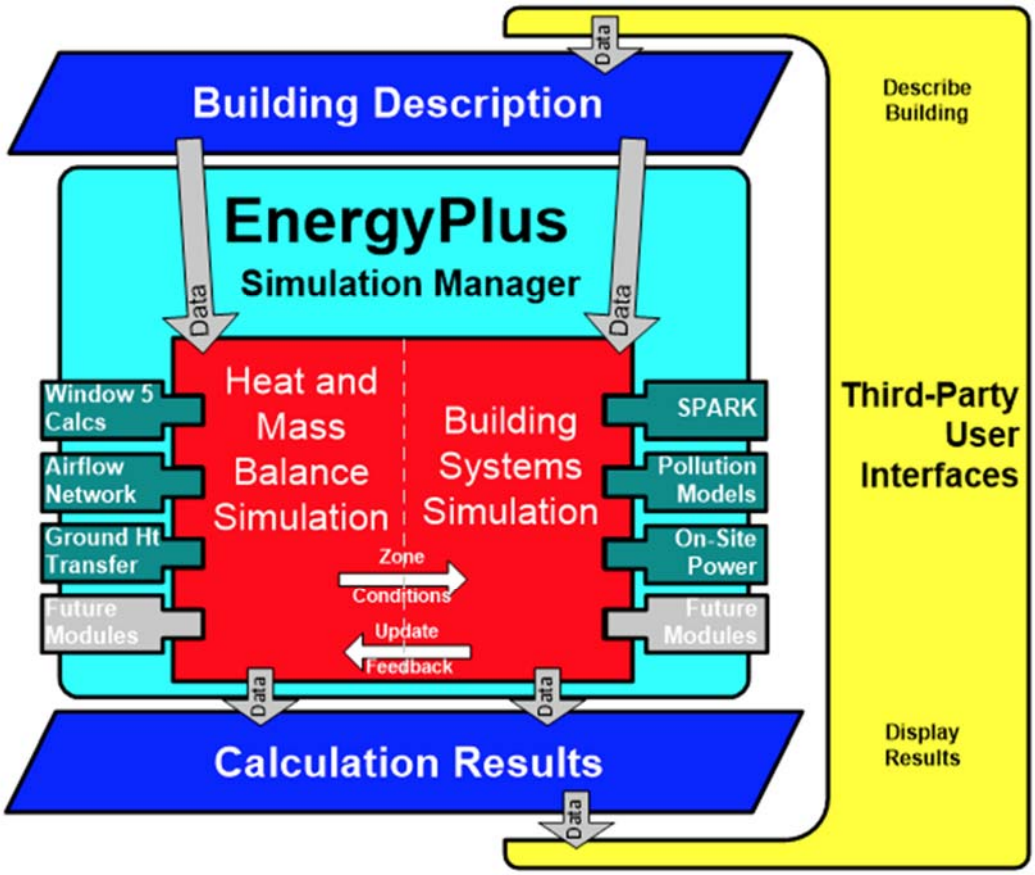

Figure 3 – Overall Structure of EnergyPlus [32]

The software has multiple objects, which categorically function under the many conceptual modules. The modules, which operate the calculations are sky, shading, daylighting, window glass, Conduction Transfer Function (CTF) calculation, airflow network, photo-voltaic, condenser loop, plant loop, zone equipment and air loop. The distribution of the modules is shown in the Figure 4 [32]. These independent modules

contain independent objects of numerical and binary class data which only interact among each other through within the integrated solution manager [32]. The integrated solution manager is divided into surface heat balance manager, air heat balance manager and building systems simulation manager.

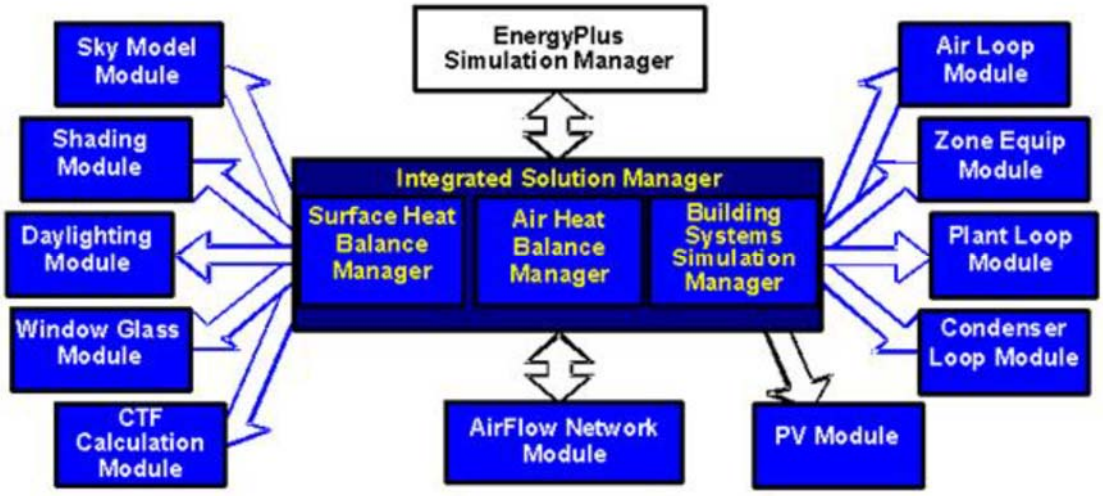

Figure 4 – Various Classes of EnergyPlus Objects [32]

2.4.2 OpenStudio

The graphical user interface (GUI) of EnergyPlus capable of performing energy modeling is known as OpenStudio [33]. The software is written in C++ programming language and developed by NREL, Lawrence Berkeley National Laboratory (LBNL), Oak Ridge National Laboratory (ORNL), Pacific Northwest Laboratory (PNNL) and Argonne National Laboratory (ANL). The software supports the whole building energy simulation for the U.S. Department of Energy (DoE) by regulating the simulation tools EnergyPlus and Radiance. Radiance is an advanced daylight analysis simulation program. The

application has extensions such as OpenStudio SketchUp Plug-in, ResultsViewer, and the Parametric Analysis Tool [34].

OpenStudio software is paired with 3D geometry building open-source software known as SketchUp. The modeling tool starts with OpenStudio SketchUp Plug-in to create 3D geometry shelter envelope and assign surface and other definitions to the structure. SketchUp Plug-in also allows the geometry to interface with OpenStudio allowing a GUI control to the architectural components of the shelter model. Furthermore, OpenStudio provides the interactive setup in creating a building energy model, including setting up the site weather profile, the units of measurement, the schedules, the constructions, the internal loads, the space type, the facility, the spaces, thermal zone, heating/cooling systems, and measures which are shown on the left menu in Figure 5. Upon launch of simulation under the GUI tool, the software automatically scans for objects or components prescribed in one or all of the classified programs such as Ruby, EnergyPlus, and Radiance [34]. The programs work interactively to pass data from the hard-coded EnergyPlus calculations to the interface of OpenStudio.

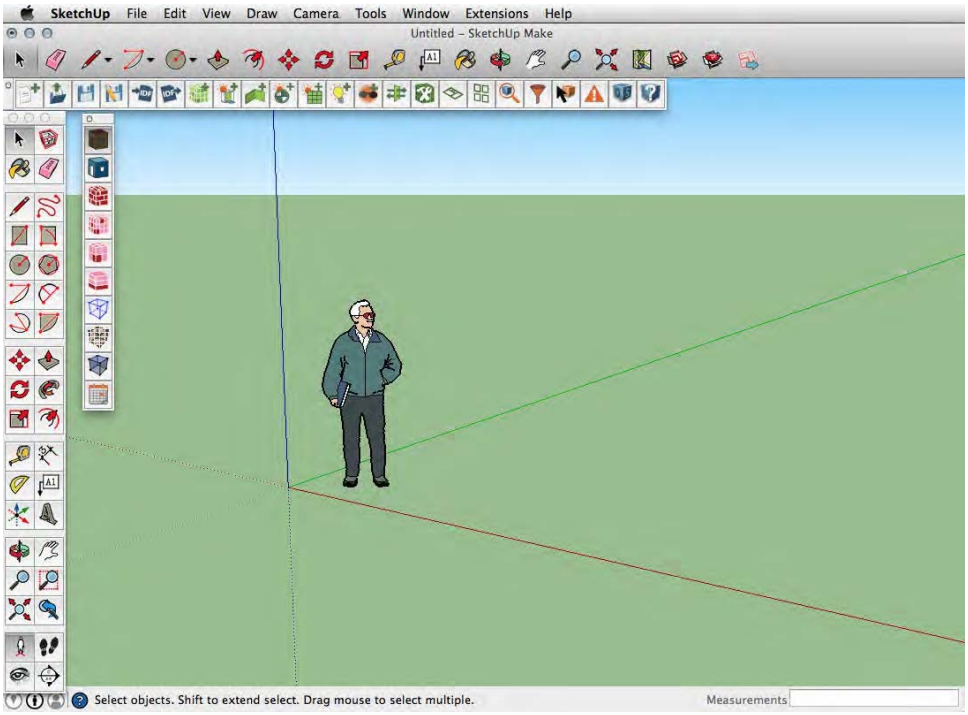

Figure 5 – OpenStudio SketchUp Plug-In [34]

The OpenStudio model can represent an entire shelter energy model encompassing the heating/cooling system or it can be an individual component of the shelter energy model. Regardless of the content, the GUI feature of the software will allow EnergyPlus simulations to perform the prescribed calculations. OpenStudio model is hierarchical and object-oriented that serves as a container for Model Objects, which are also processed by EnergyPlus in the format of input data dictionary (IDD) objects [35]. The OpenStudio Model Objects are assorted control components for the simulation which are simulation settings, output data, resources, site and location, geometry, building loads, advanced daylighting, heating/cooling systems, and economics [35]. The GUI front panel of the software is shown in Figure 6.

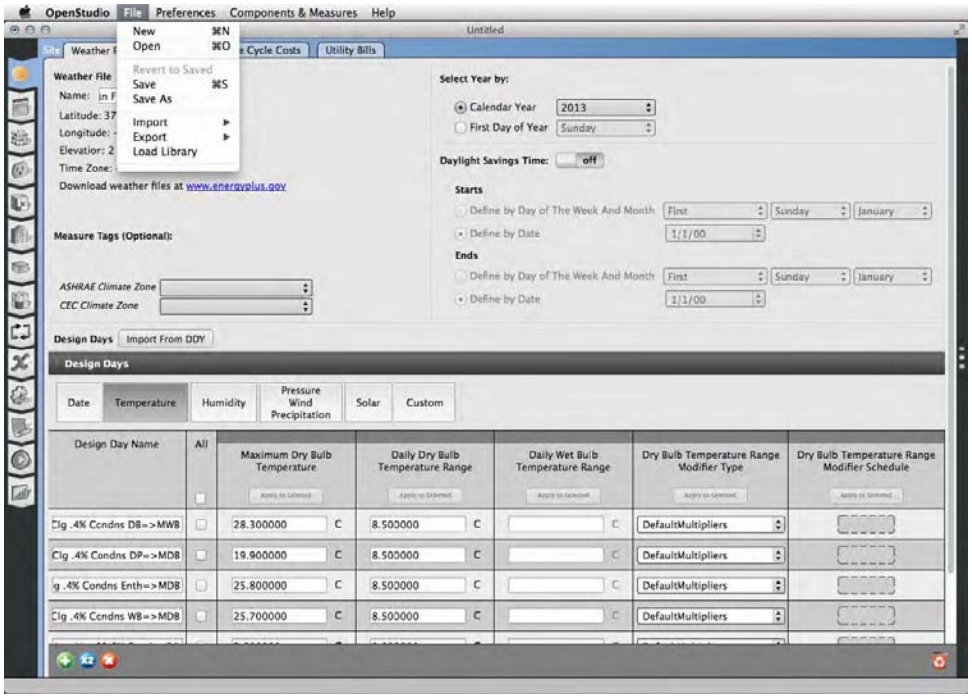

Figure 6 – OpenStudio Application [34]

2.5 Mathematical Devising Software

The second category of software discussed in this chapter is mathematical devising. The MPC optimization calculations are performed in MATLAB and the input for the MPC controller are obtained from MLE+ controlling the EnergyPlus model. The controller for the MPC primarily resides in MATLAB to autonomously initiate EnergyPlus simulation sessions to assess the outputs for selecting the corresponding optimum input.

2.5.1 MATLAB

The MATLAB software is a widely used platform which has optimized for solving engineering and scientific problems. It is a matrix-based language written in C, C++ and Java which is used for but not limited to machine learning, signal processing, image processing, computer vision, communications, computational finance, control design and

robotics [36]. Features of the software such as built-in graphics facilitate graphical visualization of data and built-in toolboxes or functions facilitate all forms of mathematical and statistical analyses [36]. Additionally, a MATLAB script can be integrated with other software languages which can enable deployment of algorithms and applications within web, enterprise and production systems [36].

There are multifold applications of the MATLAB software. It is acknowledged as a high-level language for scientific and engineering computing with a desktop environment tuned for iterative exploration, design, and problem-solving [36]. Moreover, the program can suitably execute graphics for visualizing data and tools for creating custom plots, applications for curve fitting, data classification, signal analysis, control system tuning, and many other tasks [36]. In addition, interface with external software(s) via application programming interface (API) can be executed with C/C++, Java, .NET, Python, SQL, Hadoop, and Microsoft Excel [36].

MATLAB version R2017a is the latest release of the software which is used for this thesis. The MATLAB desktop is trivially organized for the ease of access to open coding scripts, enter input commands and view output data. The desktop shown in Figure 7, includes three panels namely Current Folder, Command Window and Workspace [36]. The saved scripts and their corresponding output data after a cycle of run are stored in the Current Folder panel of the desktop [36]. The Command Window panel is characterized by the symbol or prompt ">>" which designates the command line for entering commands [36]. The Workspace panel is used to access and explore the saved data after a completed run or imported external data [36]. MATLAB stores any variables to the workspace and displays the result in the Command Window.

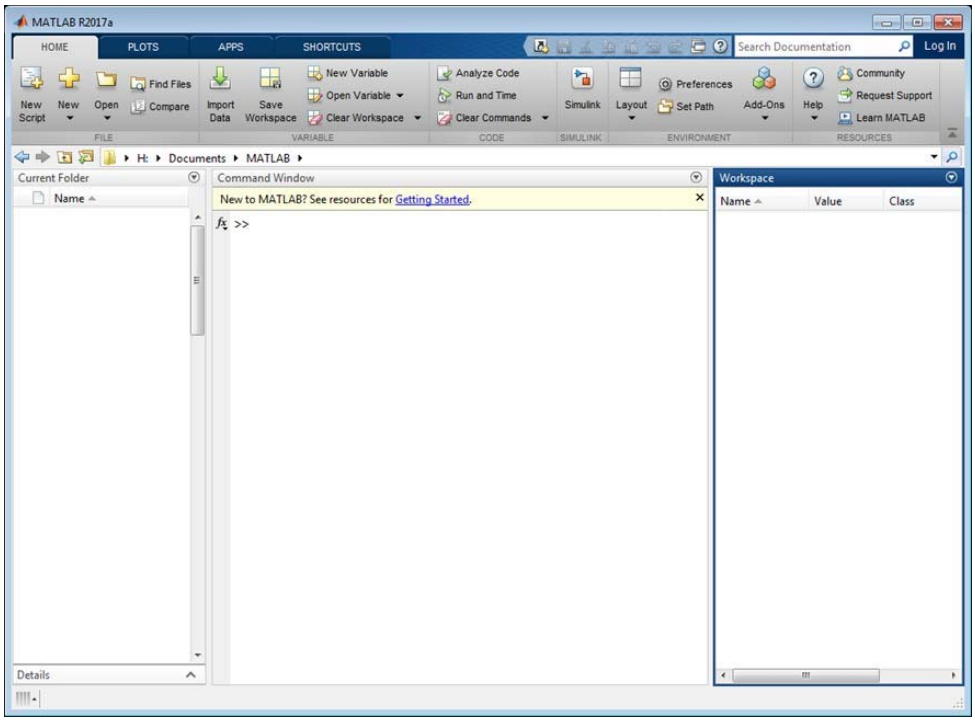

Figure 7 – MATLAB Desktop [36]

2.5.2 MLE+

The platform MLE+ serves the principal purpose of interfacing the building simulation software EnergyPlus with mathematical modeling software MATLAB. It utilizes the simulation capabilities of building energy software tool EnergyPlus, while explicitly manipulating the MATLAB environment for control design [37]. With integrated support for system identification, control design, optimization, simulation analysis and communication between software applications and building equipment, MLE+ is able to facilitate the processes of building simulation and controller formulation [37]. The system identification component uses a mathematical model to generate or establish a correlation between a discrete set of input-output data [37]. However, for the most precise and accurate results for building simulation, the original EnergyPlus model of the investigated shelter

or building predicates highest fidelity. MLE+ is a tool designed for co-simulation and analysis for energy-efficient building automation design by capitalizing the high-fidelity building simulation capabilities of EnergyPlus and the scientific computation and design capabilities of Matlab for controller design [37].

A building simulation tool such as EnergyPlus uses high fidelity physical models for heat and mass transfer across solid walls, radiation from surfaces, coupling of air and water loops, thermal comfort, fenestrations, daylighting control, weather conditions, atmospheric pollution, occupancy and heating/cooling equipment [37]. The access to full information of the building improves its simulated estimate of the energy requirements in terms of heating and cooling loads, interior environmental conditions and building automation operation cost [37]. The high-fidelity EnergyPlus simulations lack capability for algorithm development, optimization, control synthesis and model-based design [37]. In addition, EnergyPlus also lacks the capability to directly interface with the scientific computation software MATLAB [37]. The approach for imposing feedback control to the EnergyPlus model is by using MLE+ operator for integration. The co-simulation capabilities of MLE+ extend to other software and utilities, which are shown in a schematic flowchart of Figure 8.

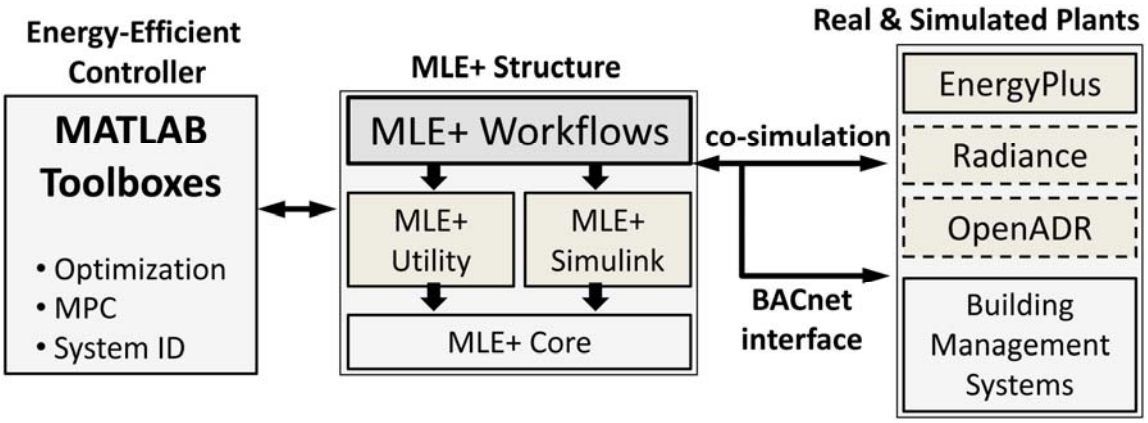

Figure 8 – MLE+ Interface [37]

MLE+ has the capability to dictate informed actions by comparing, and expeditiously simulating scenarios of different control algorithm implementations across a range of building model parameters [37]. Also, it has the capability to facilitate identification and validation of simplified models from high order physical models [37]. Optimizing parameters of a provided shelter model for successfully designing advanced controllers such as MPC is the primary reason for administering the MLE+ interface in this thesis.

2.6 ECU Controlling Software

The third category of software discussed in this chapter is ECU controlling. The software for remotely controlling an ECU is the EIO Application. To be able to install and ultimately use/access the controllable features of the EIO Application, Linux-based Ubuntu Operating System needs to be configured as a virtual desktop inside VirtualBox. Once the communication between the virtual desktop EIO Application and host desktop with MATLAB is developed, the MPC optimization tool will be able to dictate the corresponding output of the chosen input to the ECU hardware.

2.6.1 *VirtualBox*

The software is a cross-platform virtualization tool which allows multiple operating systems to be installed and operated in the form of individual virtual machines [38]. Allotted disk space and memory of the host desktop or operating system dictates the performance of the virtual desktop [38]. In VirtualBox, a virtual machine platform can be created which is a special environment where the guest virtual operating system is installed, stored and accessed. Figure 9 shows the front panel of the software where on the left toolbar, the configured desktops are listed for launching and accessing the virtual machines.

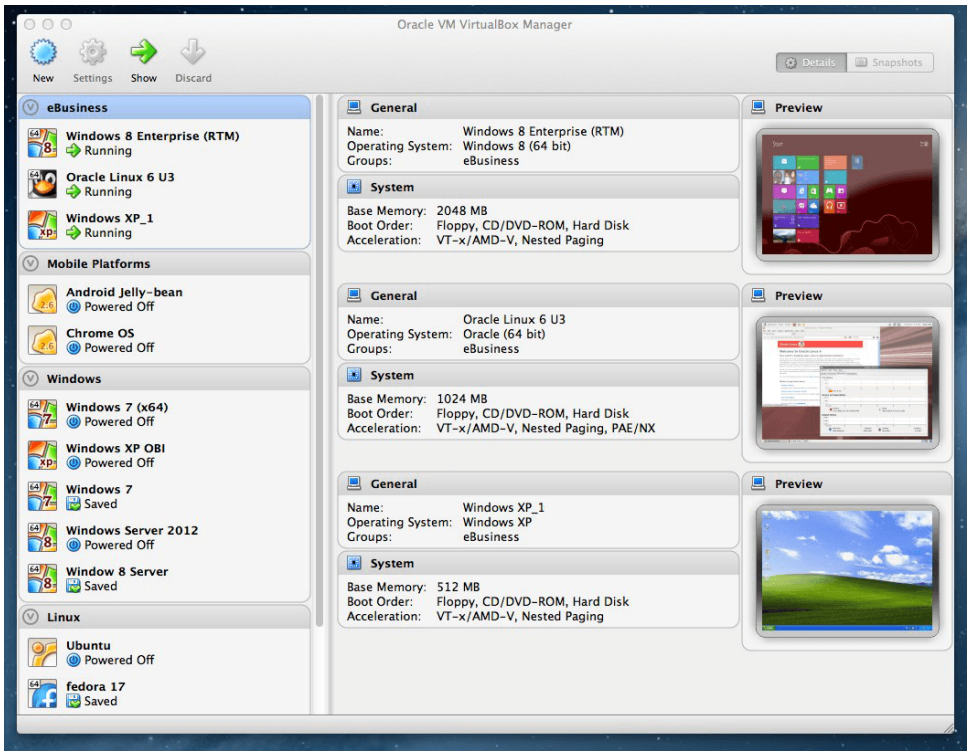

Figure 9 – VirtualBox Desktop [38]

2.6.2 *Linux*

Linux is a separate OS than Windows OS. Linux is an OS which is member of the UNIX family [39]. It is a widely commercialized OS which hosts the Android system for smartphones and computer system of modern in-car technology [39]. Since Linux was designed with the backdrop of security and hardware compatibility, its core benefit is it is incredibly flexible and can be configured to run on ideally any device [39]. Hence, the application of Linux is found ranging from micro-computers and cellphones to the largest super-computers [39]. Linux-based OS distributions which are widely used but not limited to the listed few are Knoppix, Ubuntu, Fedora and several others existing and upcoming in the industry of software development [39].

2.6.2.1 Ubuntu Operating System

For the scope of this thesis project, Ubuntu OS version 14.04 serves as the host desktop for the military software used to communicate with the hardware via micro-grid. This is the application for the OS because of the security and hardware compatibility features ensured by its Linux background. Ubuntu OS is based on the foundation of Linux, with Linux kernel serving as the core or its autonomous controller [39]. Allocation of computing resources such as memory and processor for the Ubuntu OS is handled by Linux. In theory, Ubuntu OS is similar to Windows OS because both are desktops which enable visually-orientation using the concept of GUI control [39]. This simply means that features such as the mouse to navigate the desktop, open applications, move files and perform most other tasks are facilitated by the OS. The desktop of Ubuntu OS is shown in Figure 10 where the applications reside on the left side taskbar similar to a Windows desktop where the applications reside under the Windows key.

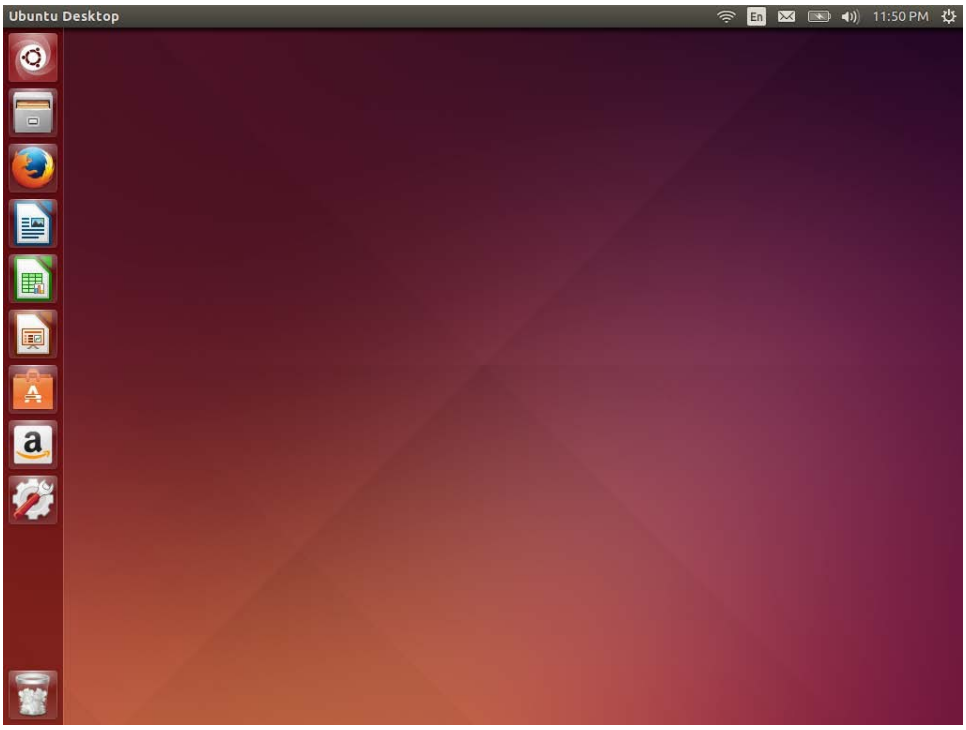

Figure 10 – Ubuntu OS Desktop [39]

2.6.3 EIO Application

The software is the military GUI control system for the micro-grid and all the electronic systems at the base. Figure 11 shows that the EIO (Energy Informed Operations) Application consists of an interactive monitor display to manage the Army micro-grid containing power resources such as generators, ECUs and other equipment [40]. The EIO application component "EIO ADM" launches the GUI control and while the component "EIO SPA" serves as the GUI control [41]. Since, EIO Application communicates to each of the connected devices via a networking server, the GUI front panel of the software is accessed through the web browser [41].

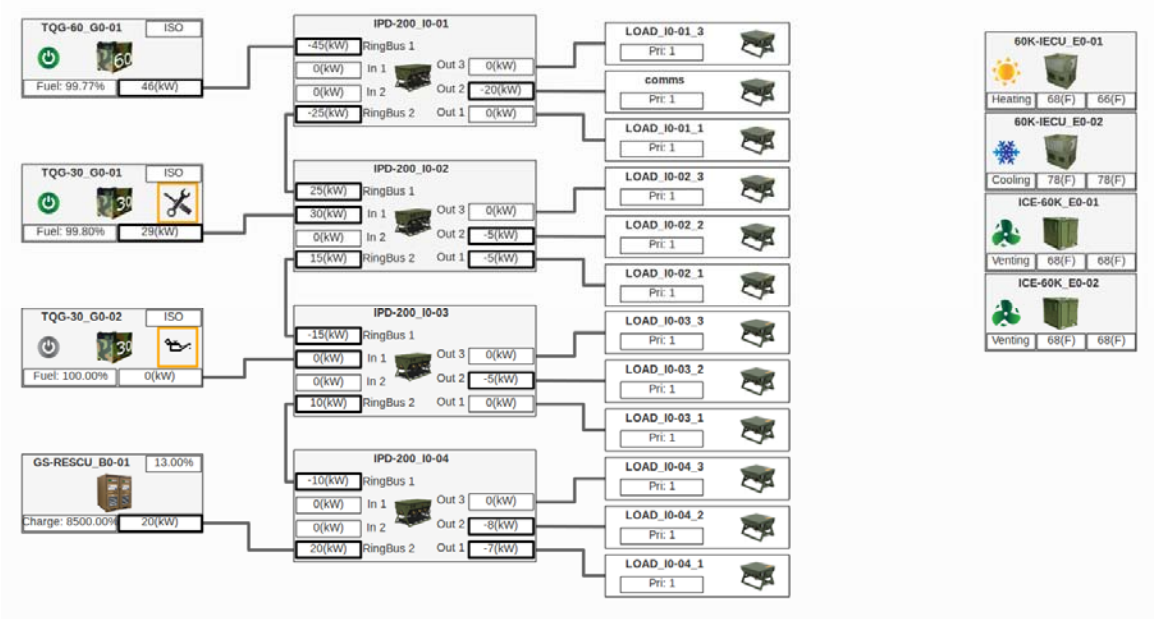

Figure 11 – EIO Application Desktop [41]

One of the major functionalities of the software is it allows interface with any external program or software to enable sending and receiving data signals. Hence, this feature allows an external program to autonomously control an ECU. The software-to-software interface is established by the development of the API of both EIO Application and the external software [40]. All data exchange occurring with the EIO Sensor Sever takes place via REST (Representational State Transfer) API in JSON (JavaScript Object Notation) format [40]. To interface the MPC framework to the EIO App, the host software MATLAB for the MPC framework needs to be modified for performing the control on actual ECU hardware. As a result, MATLAB program is able to receive and send JSON strings as the signals for altering settings on the ECU.

CHAPTER 3. RESEARCH METHODOLOGY

This chapter contains the introduction to the studied shelter and ECUs, which includes creation and validation of the EnergyPlus model. In addition, description of the EnergyPlus model configured shelter and ECU, description of the MPC framework and description of the MPC framework integrated with EIO Application workflow are also discussed in the chapter.

3.1 Airbeam Shelter

The physical tent structure modeled in EnergyPlus is representative of the soft-wall tactical shelter manufactured by HDT Global called HDT AirBeam Model 2032A. The shelter dimensions for the length and width are 20 ft by 32 ft (6.1 m by 9.8 m), while the height is 11 ft high (3.35 m) [42]. The pressurized “air beam” in this shelter provides actual shape and support to the physical structure. The interior space is a singular zone serves as the wide and unobstructed space. It can be used for command and control space, maintenance activities, or other soldier billeting [42]. The shelter architecture is characterized by a standard interior liner and no energy-efficiency features except a vestibule [42]. Figures 12 & 13 show the side-perspective and front-perspective views of the Airbeam shelter respectively.

Figure 12 – Airbeam Shelter Perspective View 1: L×W×H = 20 ft × 32 ft × 11 ft [42]

The shelter consists of 2 independent interior zones or spaces, separated by a standard door, which is regenerated in the EnergyPlus model. The 2 zones are identified as "Main Zone" which is the actual ventilated space and "Vestibule" which is the walkway for entering the ventilated space. Unlike the Main Zone, Vestibule does not have its own dedicated heating/cooling system, which is regenerated in the EnergyPlus model as well. Figure 12 highlights the Vestibule zone of the Airbeam shelter, which serves as the front entrance to the shelter.

Figure 13 – Airbeam Shelter Perspective View 2: L×W×H = 20 ft × 32 ft × 11 ft [42]

3.2 Environmental Control Units

The heating/cooling units used by the military are introduced in this section. Both units discussed are from the same manufacturer and roughly the same heating/cooling capacity.

3.2.1 IECU

The ECU model in EnergyPlus is representative of the Improved Environmental Control Unit (IECU) manufactured by *HDT Global*. The 5 ton unit, displayed in Figure 14, has a 60,000 BTU/h cooling capacity and 30,000 BTU/h heating capacity [43]. The unit is equipped with non-ozone depleting refrigerant R-410A for its cooling cycle and electric heating coil for the heating cycle [43].

Figure 14 – HDT 60K IECU [43]

The unit specifications provided by the manufacturer are listed in the Table 1. These values are entered into the EnergyPlus model object of the ECU.

Table 1 – IECU Specifications [43]

Specification Type	Specification Value
Refrigerant	R-410A
Total cooling capacity	18.2 kW ≈ 62,000 BTU/hr
Sensible cooling capacity	12.3 kW ≈ 42,000 BTU/hr
Heating capacity	8.8 kW ≈ 30,000 BTU/hr
Air flow rate	1,700 CFM
Rated COP	1.7

3.2.2 F100

Another ECU model in EnergyPlus is representative of the F100 unit manufactured by HDT Global. The 5 ton unit, displayed in Figure 15, has a 58,000 BTU/h cooling capacity and 34,140 BTU/h heating capacity [44]. The unit is equipped with non-ozone depleting refrigerant HFC-410A for its cooling cycle and electric heating coil for the heating cycle [44].

Figure 15 – HDT 60K F100 [44]

The unit specifications provided by the manufacturer are listed in the Table 2. These values are entered into the EnergyPlus model object of the ECU.

Table 2 – F100 Specifications [44]

Specification Type	Specification Value
Refrigerant	HFC-410A
Total cooling capacity	17 kW ≈ 58,000 BTU/hr
Sensible cooling capacity	11.4 kW ≈ 39,000 BTU/hr
Heating capacity	10 kW ≈ 34,410 BTU/hr
Air flow rate	1,900 CFM
Rated COP	1.5

3.3 Creation and Validation of EnergyPlus Model

For the application of this thesis, the baseline model of the Airbeam shelter with either one of the ECUs was created, validated and provided by NREL. This section of the chapter will briefly discuss the origins and verification of many of the components, necessary for a validating a model. The model is completed to match every EnergyPlus applicable parameter/variable. The shelter components dominate the model, which is coupled with the specifications and performance curve profiles of the ECU.

3.3.1 Shelter Profile

The baseline model of the shelter for this thesis was developed in EnergyPlus Version 8.1 (DoE 2014a) by NREL. It was based upon engineering drawings from the manufacturer, specifications of envelope material, measurements of material property, specification sheets of ECU, field measurements and observations [42]. Surrounding the

ventilated main zone, the air gaps which form the beam structure between the inner and outer liners were modeled in the software as individual zones. The air flow in this gap was set to a constant value of about 1 CFM (0.00049 m3/s) [42]. NREL performed laboratory experiments to determine the surface properties of the inner shell, outer liner and shade fly of the Airbeam shelter while manufacturer and literature data provided precise estimates for thermal resistance properties. The completed and validated EnergyPlus model of the shelter is shown in Figure 16 through the SketchUp desktop.

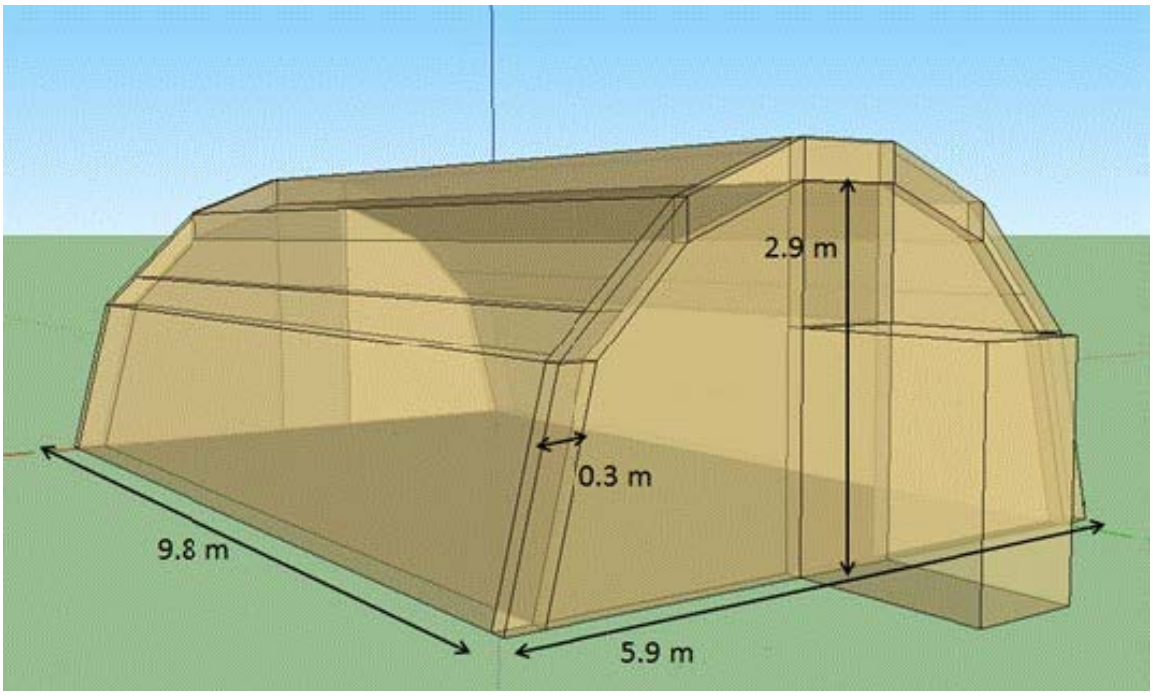

Figure 16 – Airbeam Shelter Model [42]

Important shelter specifications provided in the paper sourcing from manufacturing literature and engineering tables for similar materials are listed in the table. These variables serve as key input to the conductive heat transfer calculations for the model. Upon creation of the baseline model of the shelter by NREL, it is subsequently validated by comparing field-measured data of the off grid shelter for various variables such as ventilated space

temperature, cooling load profile, heating load profile and various other sensitivity analyses [45]. The various material properties of the Airbeam Shelter are tabulated in Table 3. The thermal absorptance entry of the floor has the value 0.72 based upon surface property of polystyrene for cooling season experiments [42]. It also has the value 0.742 for the same entry, based upon surface property of standard floor material for heating season experiments [42].

Table 3 – Airbeam Shelter Material Properties [42]

Property	Units	Exterior Shell		Inner Liner		Floor
		Outer Surface	Inner Surface	Outer Surface	Inner Surface	Inner Surface
Roughness	-	Medium Smooth	Medium Smooth	Medium Smooth	Medium Smooth	Medium Smooth
Thermal absorptance	Fraction	0.897	0.90	0.889	0.889	0.72/0.742
Solar absorptance	Fraction	0.571	0.9	0.13	0.13	0.2
Visible absorptance		0.6	0.9	0.13	0.13	0.2
Thermal resistance	m^2K/W	0.0088		0.0088		0.5/0.0176

The shelter structure is also equipped with a shade fly which serves as shade from direct solar radiation. It is a tan colored mesh, supported 6-12 inches above the shelter [42]. The shade fly is also integrated into a model by NREL for solid or partial shading of direct

and diffuse solar radiation [42]. The shade fly model does not include transmittance as a function of solar angle of incidence, partial blocking of infrared heat exchange occurring between the outer fabric of the shelter and sky, and infrared heat loss effect of solar radiation striking the shading fabric [42]. Moreover, the shading model is unable to model the accurate convective thermal conditions between the outer surface of the shelter and the shading fabric [42].

3.3.2 Weather Profile

Accurate models of a shelter energy usage crucially depend on object entries under the classifications of weather, atmosphere and solar radiation. Since the validity of the inputs from the weather profile are contingent upon the location, the EnergyPlus model needs to be assigned with the accurate weather file.

For the weather inputs, EnergyPlus requires a specific input file format, known as EnergyPlus Weather file (EPW) [32]. The EPW file contains hourly information of meteorological and solar radiation data sets for a whole year, including dry bulb temperature (℃), dew point temperature (℃), relative humidity (%), atmospheric pressure in (Pa), solar heat flux (Wh/m^2), radiation heat flux (Wh/m^2), wind speed (m/s), wind direction (degrees) and many other categories [46]. These components serve as key variables in the convective and radiative heat transfer calculations for the model. In case of availability of recorded weather data of the geographical site, the meteorological weather file can be populated and in theory, replaced with the measured data. However, this process is usually inconsistent, because of several missing entries of the measured data needed for completely populating the EPW file. The historically measured meteorological weather

data is openly available on the EnergyPlus website for more than 2,000 different geographical locations around the globe.

The weather data for the thesis is used from 2 locations for 2 separate studies. The first weather data is of the McGuire Air Force Base (AFB) in New Jersey which is nearest to the geographical location of Ft. Dix. Another weather data is of Worcester, Massachusetts which is nearest to the geographical location of Base Camp Integration Lab (BCIL). As previously stated, validation of EnergyPlus shelter is strongly dependent on the accuracy, precision and abundancy of the local field-measured weather.

3.3.3 Infiltration Profile

Infiltration is a major heat transfer component associated with creating an accurate model of a shelter. In an operating base, it is common to have air supply and return ducts placed outside the shelter in an unconditioned space. Depending on the mechanical system, there might be leakage which causes pressure difference that could led to increase in envelope infiltration.

For a model-type estimation of the infiltration, the EnergyPlus object called "ZoneInfiltration:EffectiveLeakageArea" is used for the Airbeam shelter. This object operates using the Sherman-Grimsrud's effective leakage area model, described in the ASHRAE Handbook of Fundamentals [42]. The model is based on user-defined effective leakage area (ELA) and coefficients for temperature between inside and outside temperature and wind-speed variables [42]. The equation considers the stack or temperature coefficient (C_s) in units of $(L/s)^2/(cm^4 \cdot K)$, wind pressure coefficient (C_w) in units of $(L/s)^2/(cm^4 \cdot (m/s)^2)$, scheduled fractional multiplier (F_{sch}), average local wind

speed (V_w) in units of m/s, average inside-to-outside temperature difference (ΔT) in units of °C and equivalent leakage area in units of cm^4. The resultant expression is defined as the infiltration in units of air change rate (ACH) which is shown in Equation 5 -

$$Infiltration = F_{sch} * \frac{ELA}{1000} * \sqrt{(C_s \cdot \Delta T + C_w \cdot V_w^2)} \quad (5)$$

This modeled form of infiltration is validated in the literature using field-measured data taken and studied for calibration.

3.3.4 ECU Profile

The ECU objects of the EnergyPlus model are populated with all the unit specifications provided by the manufacturer, out of which major ones are listed in Tables 1 & 2. Typical ECU objects are distributed into cooling coil component, heating coil component, fan component and performance curves component. Performance curves are the numerical data which simulate the performance of the heating/cooling equipment [47].

Regeneration of the precise model of the heating/cooling system using various heating/cooling system templates, plus additional nonexistent inputs results in the ECU performance as close to the actual system. The list of inputs includes the major unit specifications of the ECU namely cooling capacity, heating capacity, rated COP, rated sensible heat ratio, fan efficiency and flow rate. The final input is in the form of cooling performance curves, which are data sets of quadratic or biquadratic curves determined by regression analysis on tabular data for a particular equipment performance metric [47]. This performance metric is typically consists of important cooling coil characteristics and

energy input ratio data for various combinations of temperature data [47]. The regression analysis determines the equation coefficients which are the primary input to all performance curve objects [47]. In the workflow of EnergyPlus, a performance curve generates a plot in 3D space on which the desired output values of cooling capacity can be spatially determined for each individual or aggregate combinations of outdoor dry bulb temperature and return air wet bulb temperature [45]. The performance curve input to an EnergyPlus model can be in the form of curve coefficients or set of discrete data input-output data points which define a coarser curve [47]. Ideal input for a valid shelter model is typically in the EnergyPlus object form of curve coefficients [47]. Hence at each simulation time step, the software is able to determine the discretely characteristic outputs of the heating/cooling system for a given condition of current wet bulb and dry bulb temperatures.

In order to validate the ECU performance with a shelter using field-measured data, thorough specifications as well as performance characteristics defined by performance curves need to be provided by the manufacturer. Typically, the data set for the curves are recorded upon conducting extensive physical experiments using a form of test chamber under various combinations of environmental conditions [45].

3.3.5 Ground-Coupling Profile

Another important component for accurately modeling a shelter is regenerating and validating the effects of ground temperature and the resultant heat transfer through the floor surface. Regardless of the width of the layer of material adjacent to the ground, the heat

transfer effects through the floor surface are extremely significant in determining overall thermal energy performance of the shelter.

A typical approach for modeling the ground-coupling of the shelter is to populate the floor construction objects of the shelter with the precise material layers and properties subjective to the assembled shelter. For the baseline EnergyPlus model of a shelter, the approach with ground condition involves assigning a floor construction object of 1 meter depth of soil as the outermost layer of material of floor construction [45]. Furthermore, the EnergyPlus object known as "OtherSideCoefficient" specifies the surface temperature of the outer surface, which physically represents the center of mass point of soil at 1 meter underground, as the actual ground temperature at 1 meter depth [48]. The monthly averaged ground temperature data at different depths for different geographical locations are obtained from the EPW weather file of the location [48].

A thin layer of defined floor liner typically results in an unstable simulation and causes calculation convergence error for termination of the simulation [42]. To resolve the issue, EnergyPlus provides a module or object based on the correlation founded by Kusuda and Achenbach (1965) [49]. The "GroundTemperature:Undisturbed:KusudaAchenbach" object requires input of the soil thermal conductivity, density and specific heat. The correlation considers the average annual soil surface temperature ($\overline{T_s}$) in units of ℃, amplitude of the soil temperature change throughout the year ($\Delta\overline{T_s}$) in units of ℃, phase shift of minimum surface temperature (θ) in units of days, thermal diffusivity of the ground (α) in units of m^2/days, and time constant (τ) value of 365 days. The resultant expression is soil surface temperature or undisturbed ground temperature as a function of time and depth ($T(z,t)$) in units of ℃ which is shown in Equation 6 -

$$T(z,t) = \overline{T_s} - \Delta\overline{T_s} \cdot e^{-z\cdot\sqrt{\frac{\pi}{\alpha\tau}}} \cdot \cos\left(\frac{2\pi t}{\alpha t} - \theta\right) \quad (6)$$

The thermal diffusivity is converted to unit of m^2/days by multiplying 86,400 seconds (equivalent to a day). The module autonomously calculates the input of soil temperature amplitude, average soil surface temperature and phase shift value using the EPW input of monthly ground temperature value at 0.5m depth provided by the "GroundTemperature:Shallow object" [45].

3.3.6 Interior Load Profile

Another important component for accurately modeling a shelter is regenerating and validating the effects of interior load in the ventilated and all other adjacent spaces. The interior loads are generated in the form of but not limited to shelter occupancy, interior lighting and plugged interior equipment. All the loads of this category can be tangibly quantified and any variance among them can be addressed by the creation of schedules. The dissipating heat generated by any plugged equipment or lighting is acknowledged as a proportion of both convective and radiative mode of heat transfer to the surroundings. The rated values for the equipment under this load type are in Watt (W).

The heat generated by the occupants is included in the present analysis. The heat dissipation from the human body is measured in Mets, a unit for the amount of heat emanating from a unit surface area of the human body in unit time [30]. In the literature, 1 Mets equates to 58 W/m^2. The occupant thermal loading can vary from 0.8 mets while resting, 2-3 Mets while walking, and 10-14 Mets while performing any type of strenuous

physical activity [30]. Assuming average human body surface area to be 2 m^2, the mets to heat diffusion data were converted to the uniform unit of Watt (W).

For the purpose of validation using field-measured data, the exact rated power consumption values for the equipment and lighting needs to be determined. Additionally, the exact occupancy of the shelter also needs to be determined. Since the mere values will not be sufficient to model the interior load profile, an estimated or pre-recorded schedule of each of the load types also needs to be accounted in creation of the EnergyPlus model. The validation of the EnergyPlus model is strongly dependent on the accuracy, precision and abundancy of the range of inputs under this category.

3.3.7 Thermostat Profile

The last category of the component responsible for accurately modeling and validating a shelter is the operating thermostat schedule for the heating and cooling set-points. This object in the EnergyPlus model as well as the physical set-up of ECU with shelter, serves as the temperature constraints or bounds which dictate the comfort criteria of the ventilated space.

User chosen thermostat schedule needs to be exactly regenerated in the EnergyPlus model to establish the exact temperature constraints of the space for validating the model. Without the knowledge of the dictating temperature bounds for a ventilated space under the backdrop of a functioning ECU, the model creation will remain incomplete for any form of simulation, as well as validation study.

3.4 EnergyPlus Framework

Independent EnergyPlus simulations with the provided inputs for shelter, ECU, weather and all other profiles ultimately generate the results for baseline heating and cooling system control. Baseline heating and cooling system control within EnergyPlus is characterized by a simple control mechanism. The user-chosen thermostat heating & cooling set-points dictate the constraints for the ventilated space temperature. In its control logic, the shelter return air temperature needs to match the raw thermostat set-point temperature. Hence, the ECU set-point temperature is the operating raw thermostat set-point temperature.

The control schematic for the EnergyPlus control is shown in Figure 17 where the purple connections serve as the air loop for the system, while the green connections serve as the control loop for the system. For a thermostat set-point schedule prescribed by the user, the ECU assesses return air shelter temperature as with the weather loads, interior loads, ground-coupling and infiltration loads, to determine the appropriate cooling or heating cycle for activation. The thermostat set-point schedule serves as the ECU set-point temperature for performing the control. Hence, the appropriate heating or cooling cycle dictates the selection of the corresponding thermostat set-point temperature, and the corresponding cooling coil or heating coil for activation. The performance curves instantly establish the corresponding output capacity of cooling or heating for the inputs/model states of outdoor dry bulb temperature and return air wet bulb temperature. Subsequently, the coil object is engaged at the determined capacity to initiate the cooling or heating of the supply air, to theoretically match the dictating thermostat set-point temperature. The supply air flow rate is modulated by the fan object to cool or heat the space. This completes

1 entire simulation loop, followed by a repetition of the control performed on the basis of the return air shelter temperature.

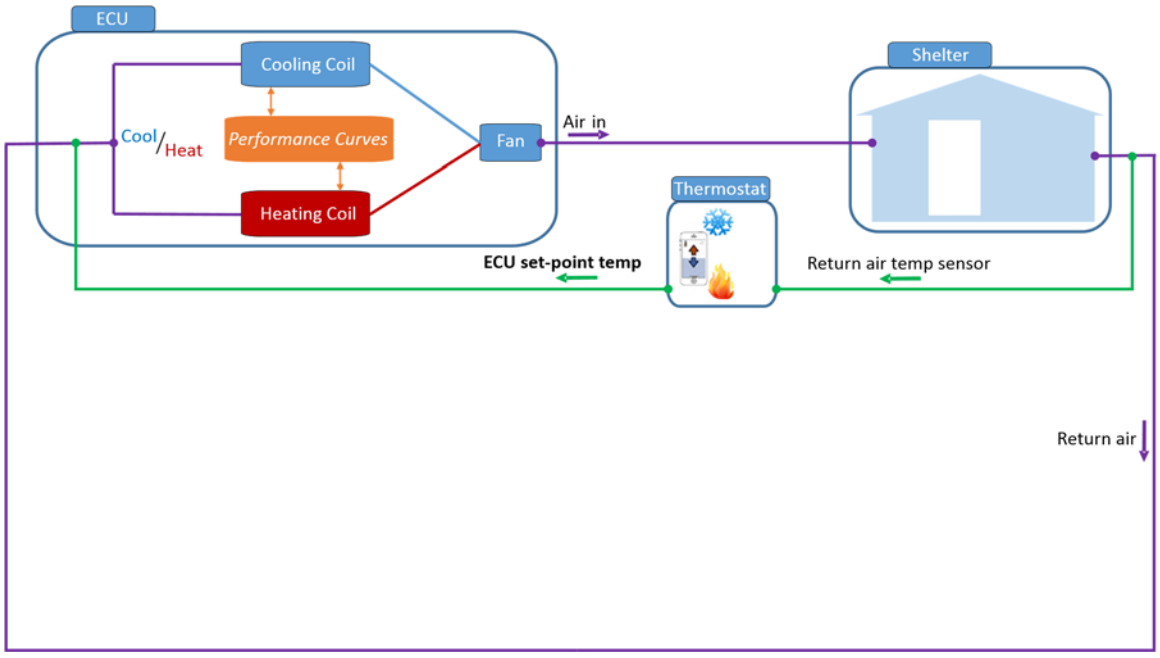

Figure 17 – EnergyPlus Control Schematic [courtesy of Dr. Ashish Sinha, Senior Hardware/Thermal Engineer, Oracle]

3.5 MPC Framework

The MPC framework performs the operation of sorting and selecting the most energy-efficient temperature set-point for the ECU, which occur after analyzing the anticipated model behavior to a designated thermostat set-point schedule for the shelter. The framework consists of the 3 major inputs to the predictive controller: calibrated EnergyPlus model of the shelter with ECU, thermostat set-point schedule for the shelter and a range of input temperature set-points for the ECU. The 3 inputs to the framework are categorized into four types ranging between system states, uncontrollable disturbances to the system, controllable inputs to the system and range of inputs to be tested for with the

controller. The resultant output from these inputs is the selected case from the list of range of inputs to be tested with the controller.

3.5.1 Input 1: EnergyPlus model of shelter + ECU

This input falls under the category of system states and uncontrollable disturbances to the system. System states encompass all the known and validated discrete specifications or information of the shelter and of the ECU. The EnergyPlus model contains every determined data of the "state of the system" in the correct numerical and binary forms within EnergyPlus objects. The data includes the specifications and performance curves of the ECU, architectural components, material and heat transfer properties of the shelter structure, infiltration and ground coupling of the shelter, and interior load profile. The input type disturbances encompass all the weather related inputs in the form of EnergyPlus weather file or EPW data. The data includes dry bulb temperature, dew point temperature, relative humidity, atmospheric pressure, solar heat flux, radiation heat flux, wind speed, wind direction and many other categories. Figure 18 classifies this input to the MPC tool as the "system states" and "disturbances".

3.5.2 Input 2: Thermostat set-point schedule

This input falls under the category of controllable inputs to the system. The typical soldier chosen thermostat schedule for heating set-points and cooling set-points serve as the input to the system. This thermostat input is processed as the bound or constraint for the ventilated space temperature when the MPC is sorting the selections from all the anticipated system responses, corresponding to their range of inputs to the controller. Figure 18 classifies this input to the MPC tool as the "controllable inputs".

3.5.3 *Input 3: Range of input set-point temperature choices*

This input category falls under the category of range of inputs to be tested for with the controller. This is the driving input because it is a range of temperature values for the controller to perform multiple MPC simulations for each individual temperature value. The immediate step after this stage in the controller is to post-process the resultant responses by sorting and selecting under the backdrop of reducing energy consumption and satisfying thermostat temperature bounds. Figure 18 classifies this input to the MPC tool as the "range of input ECU set-point temps".

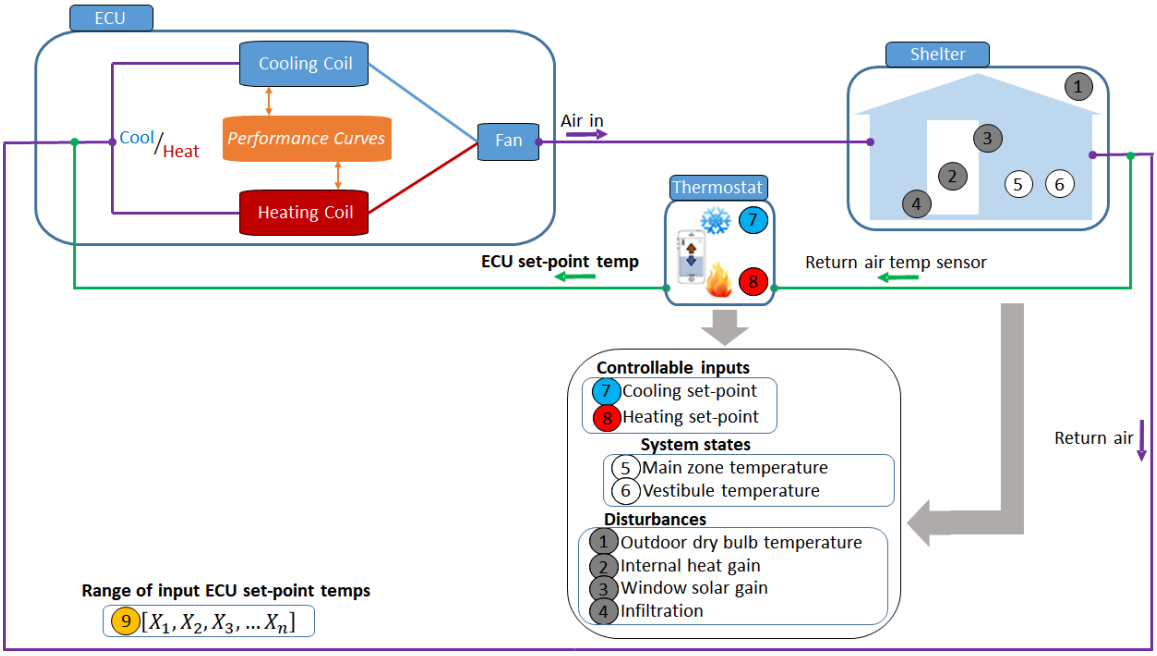

Figure 18 – MPC Inputs [courtesy of Dr. Ashish Sinha, Senior Hardware/Thermal Engineer, Oracle]

3.5.4 *MPC workflow components*

MPC framework is hosted by the software MATLAB which contains MLE+ syntax within its script to launch EnergyPlus sessions and pass data to as well as receive data from

the completed simulations. In technical terms, the workflow consists of an outside operator "while loop" which conditionally terminates the simulation cycle at the end of the chosen period. Inside the loop, a "for loop" operator launches, completes individual EnergyPlus sessions with each of the discrete choices of input set-point temperatures to obtain and store various output variables. These output variables are EnergyPlus sensor objects within the software which measure or typically calculate the numerical average of the designated variable. Since the chosen backdrop of this MPC framework is reduction of energy consumption, the primary output variables extracted from the EnergyPlus simulations and outside the "for loop" are Unitary System Electric Power, Cooling Coil Electric Power, Heating Coil Electric Power and Zone Mean Air Temperature.

While the rest of the outputs are assessed under their original values, the Zone Mean Air Temperature output variable is further evaluated to determine the resultant temperature overshoot as compared with the thermostat temperature set-point schedule. The last stage of the workflow is the "sortrows" feature or command which recursively sorts the rows of a matrix in ascending order based on the elements in the first column. In the case when the first column contains repeated elements, the command sorts according to the next column and repeats this behavior for succeeding equal values [36]. This command instantly sorts and selects the most energy-efficient case from the tested input set-point temperatures and proceeds with passing the data as a command to complete the EnergyPlus session as a continuation of the simulation cycle. Figure 19 diagrammatically highlights the overridden conventional ECU set-point temperature by MPC, while maintaining the hard constraints of the user-chosen thermostat set-point schedule.

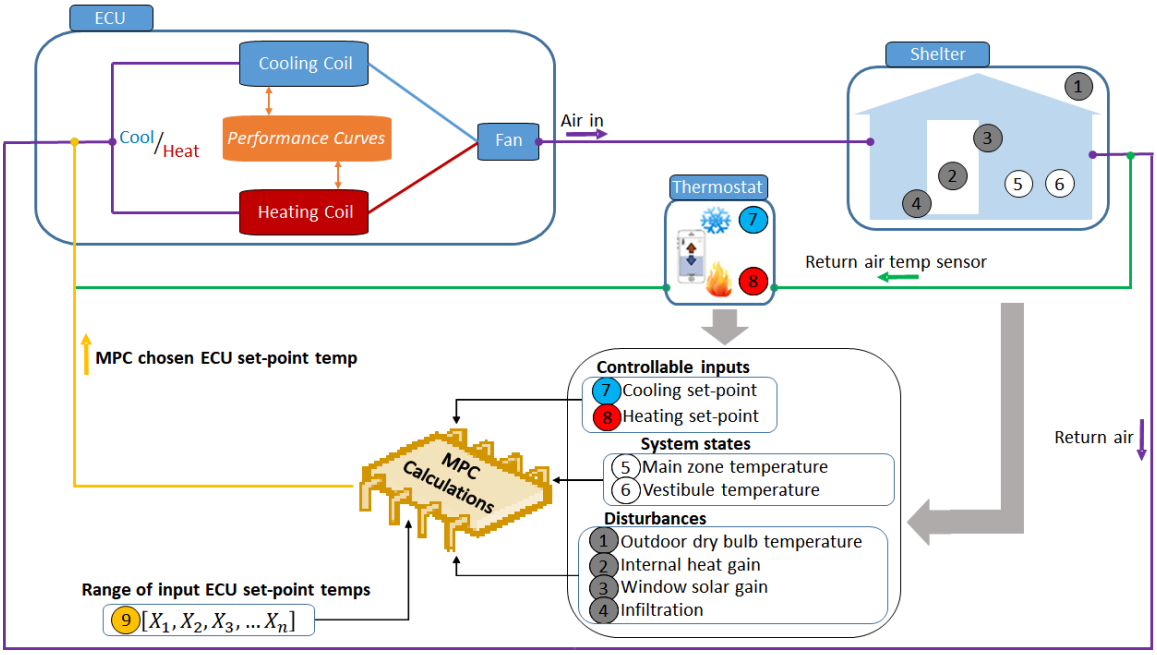

Figure 19 – MPC Schematic [courtesy of Dr. Ashish Sinha, Senior Hardware/Thermal Engineer, Oracle]

3.5.5 MPC workflow description

The workflow begins with an input model and input thermostat set-point schedule to initiate the first EnergyPlus session. However, this initiated EnergyPlus session remains static as it is missing the third input which is the selected input set-point temperature. The next sequence in the workflow is a fresh and separate launch of another EnergyPlus session with the first case of the input set-point temperature choice, which results in extraction and storage of the data upon completion of the simulation. Subsequently, this EnergyPlus session terminates and exits to launch the next session with the next case of the input set-point temperature choice. This iterative portion of the workflow ends with the completion of the simulation of the last input set-point temperature choice. Next stage in the workflow is characterized by sorting of all the output data from the multiple EnergyPlus sessions and selection of the most energy-efficient temperature set-point case which also does not have

any temperature overshoot outside the constraints of the thermostat schedule. The final selected temperature set-point is finally supplied as an input data to the first initiated yet static EnergyPlus session to complete the first run of MPC at the corresponding time-step. Next occurrence in this recursive workflow is the repetition of the entire sequence which continues until the end of the run period for the MPC simulation. This workflow is diagrammatically displayed in Figure 20 which details the optimization function performed by the "sortrows" command inside MATLAB. The "system model" in the diagram represents the EnergyPlus model input to the MPC controller.

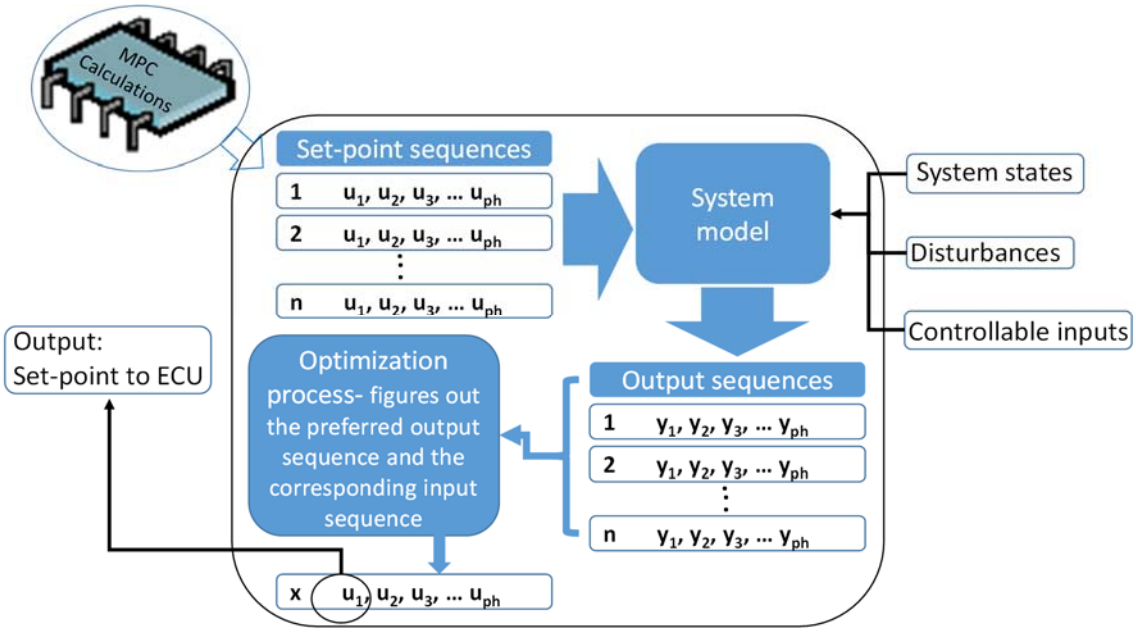

Figure 20 – Data Flow Inside MPC [29]

3.6 Integrated MPC Framework with EIO Application

The next application of the output from the MPC framework is it needs to be properly communicated to an actual ECU in the form of a command or signal at the immediate instant. This particular task requires the major challenge of integration between

the software for MPC and the software for micro-grid. The micro-grid serves as the hardware for distributing generator power to the various electronic equipment at an FOB. The electronic equipment are typically laundry system, dishwasher system and heating/cooling system designated by an ECU. The development of the application programming interface (API) between the software for MPC framework and software for micro-grid accomplished the ultimate task of controlling the ECU.

3.6.1 Software development of API

First objective of the interface is to obtain the current status data of the ECU from the EIO Application and the second objective of the interface is to send signals to modify the status of the ECU. After enabling the "host-only networking" feature of the Ubuntu OS virtual machine settings inside VirtualBox, the ability to access the EIO Application GUI webpage from the host Windows desktop became possible. In order to obtain the specific device IDs, sensor IDs and the sensor values or current readings from the EIO Application but outside its GUI webpage, REST calls need to be made at specific web addresses or URLs (Uniform Resource Locators) [40]. The known statuses of "system health responses" of the ECU are pre-determined by the developers, which are listed as "registers" for accessing individual entries [50]. Table 4 lists all the major system status objects for the ECU. Notably, "Register 2007" reads the temperature set-point, "Register 2003" reads the ECU mode status and "Register 2001" reads the temperature of air leaving shelter and returning to ECU, which is simply the return air shelter temperature.

Table 4 – System Health Responses [50]

Register	Object Name	Units	Explanation
2001	TempEvapIn	Degrees Fahrenheit	Evaporator inlet temperature
2002	TempEvapCoil	Degrees Fahrenheit	Evaporator coil temperature
2003	ECUStatus	N/A	Current ECU Operating Status: • 0 = Off • 1 = Venting • 2 = Cooling • 3 = Heating
2004	OpTime	Hours	Operational hours since last maintenance period.
2005	HPCO	N/A	Compressor high pressure cutoff status. • 0 = Cutoff Inactive • 1 = Cutoff Actuated
2006	LPCO	N/A	Compressor high pressure cutoff status. • 0 = Cutoff Inactive • 1 = Cutoff Actuated
2007	TempSetpoint	Degrees Fahrenheit	The currently programmed temperature set-point.
2008	RemoteControlStatus	N/A	Indicates whether remote control of the ECU is enabled. • 0 = Not Enabled • 1 = Enabled

In addition, the known applicable commands to the ECU are also pre-determined by the developers [50]. These objects are also referred to as "registers" for accessing individual entries. Table 5 lists the important commands to the ECU. Evidently, "Register 3001" alters the ECU mode and "Register 4001" alters the ECU set-point temperature value.

Table 5 – ECU Commands [50]

Register	Object Name	Object Type	Units	Explanation
3001	ECUStatus	ECU Control	N/A	Current ECU Operating Status: • 0 = Off • 1 = Venting • 2 = Cooling • 3 = Heating
4001	TempSetpoint	ECU Set Point	Degrees Fahrenheit	Target temperature set-point for the return air

The first step in developing the API of MATLAB with EIO Application is to be able to receive current status data of the ECU. The API of EIO Application allows access to URLs which are sorted by the device type and its breakdown of sensors with their corresponding statuses or data. Using the command "urlread" in MATLAB, the HTML (HyperText Markup Language) web content from the specified URL can be downloaded into character vector of class JSON (JavaScript Object Notation) strings [36]. The string data can be parsed into MATLAB structure objects by using the command "JSON.parse" only when its script is already present in the current folder of MATLAB [36]. Upon conversion to structure objects, the individual device IDs with their corresponding sensors

IDs and sensor data can be accessed and converted to numerical class double for storage and usage.

The second step in developing the API of MATLAB with EIO Application is to be able to send signals to modify the current state of the ECU. Using the command “web” inside MATLAB, the URL specified with the new temperature set-point for the ECU or the new mode of the ECU will open in the MATLAB web browser and simultaneously send the command to the ECU [36]. This fabrication of URL is another API feature of the EIO Application which is pre-existing for developers to access the hardware connected to the micro-grid via a third-party controller.

The finalized integration is successfully able to perform autonomous operation on the ECU. Figure 21 provides the high-level overview of the integrated framework working as a singular tool. The blue plant represents the Windows desktop, which largely contains the entire MPC framework consisting of MATLAB, MLE+ and EnergyPlus. The purple plant represents the Ubuntu desktop, which primarily contains the EIO Application. In addition, the purple plant also hosts the system health response and control command interfaces of the EIO Application. The grey objects represent the minimal hardware at the operating base, namely micro-grid, ECU and the shelter. With the developed API of MATLAB with respect to the API of EIO Application, the sending and receiving of signals in the form of the “registers” is ultimately possible.

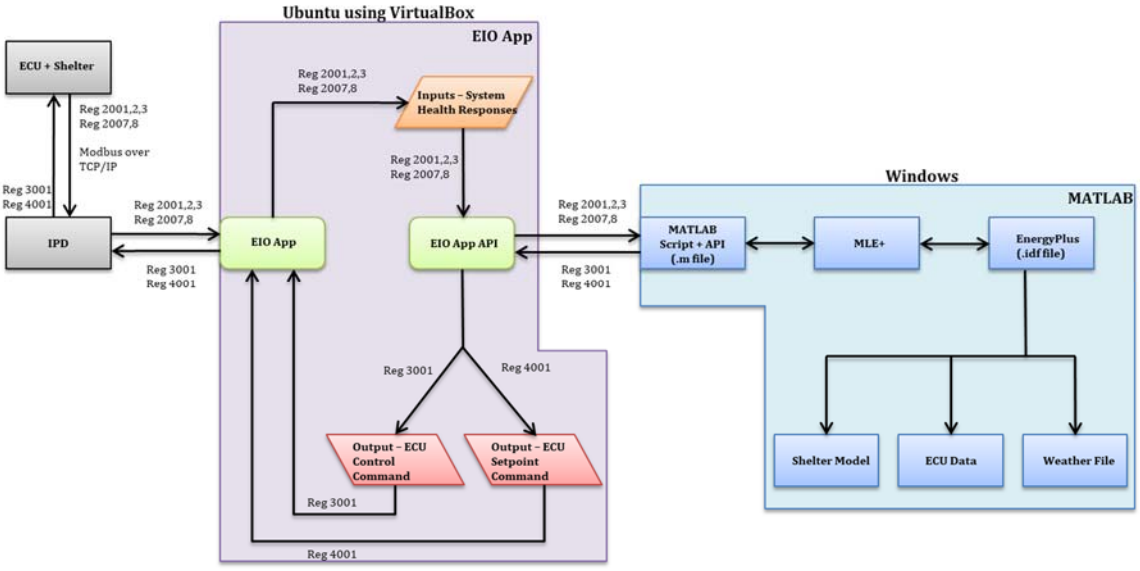

Figure 21 – High-Level Overview of Integration

CHAPTER 4. SIMULATION RESULTS AND DISCUSSION

This chapter presents the results and analyses associated with the simulations performed for the thesis. The MPC model validation is presented by comparing results with corresponding baseline model OpenStudio simulation. Specifically, the ventilated zone temperature results and the electrical power consumption results are the two types of output variables compared in the analysis. Hence, the outputs from the MPC simulation compared with baseline OpenStudio simulation are assessed.

4.1 Airbeam Shelter with F100 – Thermal Comfort Optimization

The Airbeam shelter model equipped with F100 is tested for MPC simulations, as well as EnergyPlus simulations. For all simulation cases with both MPC and EnergyPlus, doubled F100 units/dual capacity F100 unit is used to account for unmet hours of load in the baseline EnergyPlus model of the ECU. Due to its ease of use, OpenStudio software is used to perform the simulations for the EnergyPlus cases. For all simulation cases with MPC, the foremost optimization sequence in the controller is zero temperature overshoot outside the constraints of the thermostat schedule. This sorting sequence is followed by the optimization sequence of least energy consumption by the ECU during the operation of its fan, heating cycle and cooling cycle. Hence, the thermal comfort defined by nonexistence of ventilated temperature overshoot is the priority of the MPC controller. The testing is done for three separate weather days which represent three separate seasons. Also, the time-step for all simulations in the study is set to 15 minutes. In the case of the MPC simulations, the prediction horizon parameter for all simulations in the study is set to 30 minutes. The simulations correspond to the weather of Worcester, MA.

4.1.1 Loads Applied to the Model

Since the simulations are performed for three separate days representing three separate seasons, the environmental load profile is significantly differentiated by the chosen day of the weather file. The dates February 1st, April 1st and June 1st correspond to winter, spring and summer seasons respectively. Figure 22 shows the outdoor dry air bulb temperature input to the model, which is extracted from the EPW file. The internal loads to the model are constant 24 hour input values of 500 W for electronics equipment load, 1,000 W for lighting load and occupancy of 11 people which equates to 1,320 W occupancy load. The range of input ECU set-point temperatures for driving the MPC controller is integer values from 17-28 °C.

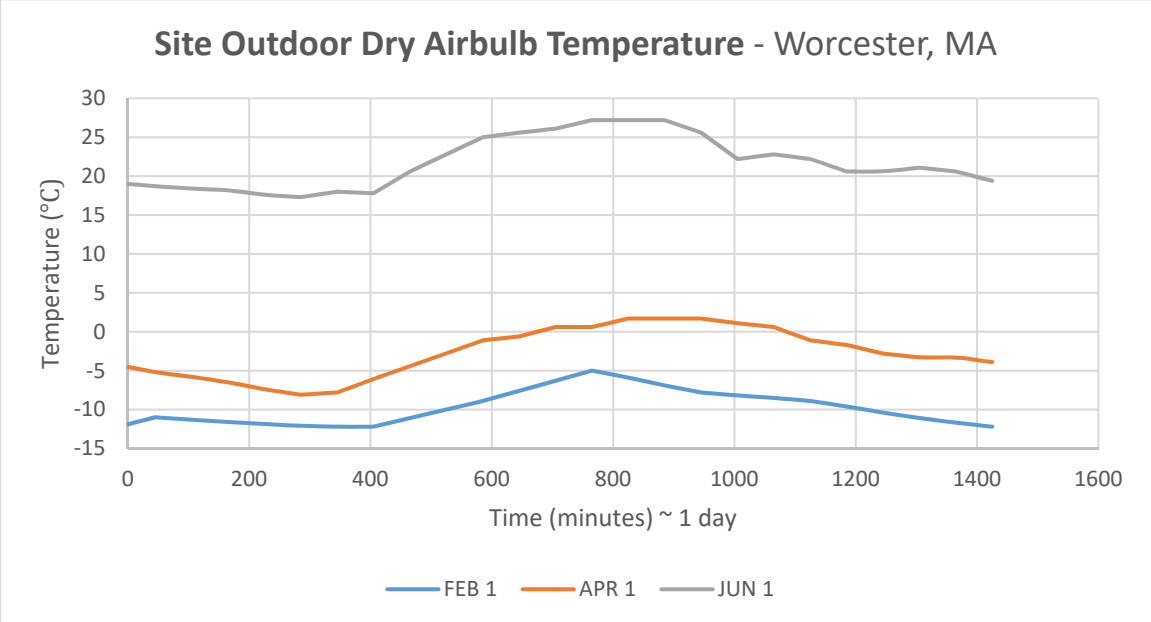

Figure 22 – Site Outdoor Dry Air Bulb Temperature – Worcester, MA

4.1.2 Results for February 1

The first set of results presented is for the February 1st case in Worcester, MA. With the thermostat set-point schedule entered into the model as a hard constraint, the resultant EnergyPlus and MPC predictions of ventilated shelter temperature and equivalent ECU power consumption are compared.

4.1.2.1 Main Zone Temperature

Figure 23 shows the resultant Main Zone temperature from both EnergyPlus and MPC simulations. Green line represents EnergyPlus while orange line represents MPC. The red and blue lines represent the hard constraints of thermostat heating set-point and cooling set-point respectively. Also, dashed purple line represents the site outdoor dry air bulb temperature. By observation, it is evident that for the winter season simulation date, both controller models roughly overlap the thermostat heating set-point temperature.

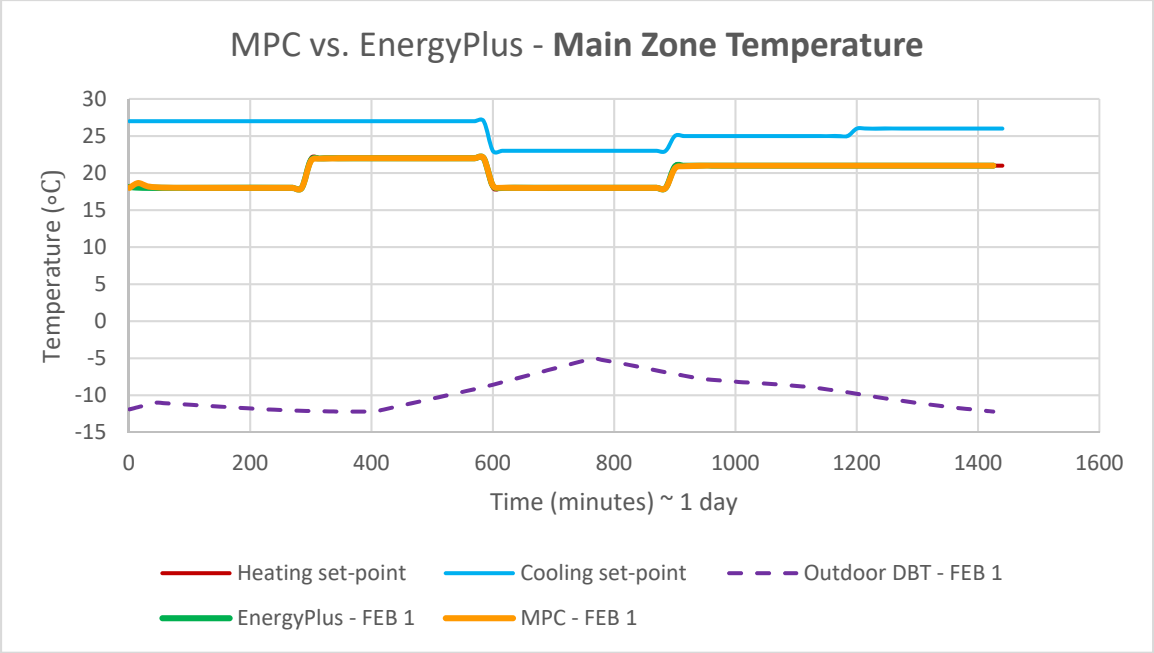

Figure 23 – MPC vs. EnergyPlus – Main Zone Temperature – FEB 1

4.1.2.2 Power Consumption

For both EnergyPlus and MPC simulations, Figures 24 & 25 show the resultant cooling coil electric power and heating coil electric power respectively. On both figures, red line represents EnergyPlus while blue line represents MPC. By observation, it is evident that for the winter season simulation date, the cooling coil electric power is negligible while heating coil electric power is active throughout the 24 hours. By comparison, MPC outperforms EnergyPlus by consuming less power throughout the operating cycle of the ECU.

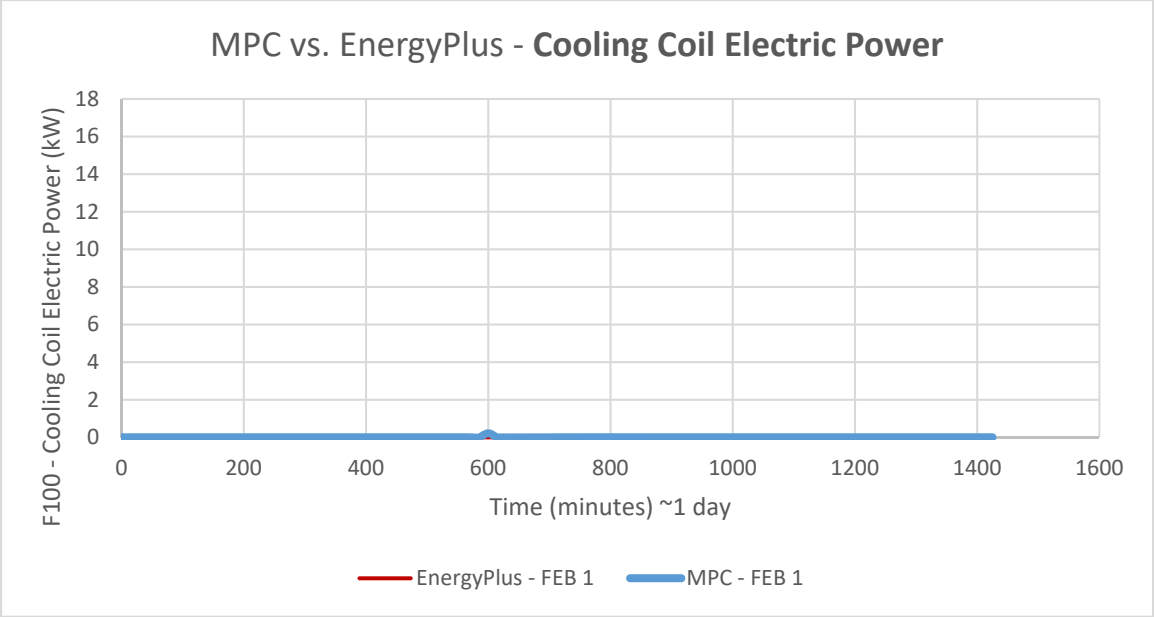

Figure 24 – MPC vs. EnergyPlus – Cooling Coil Electric Power – FEB 1

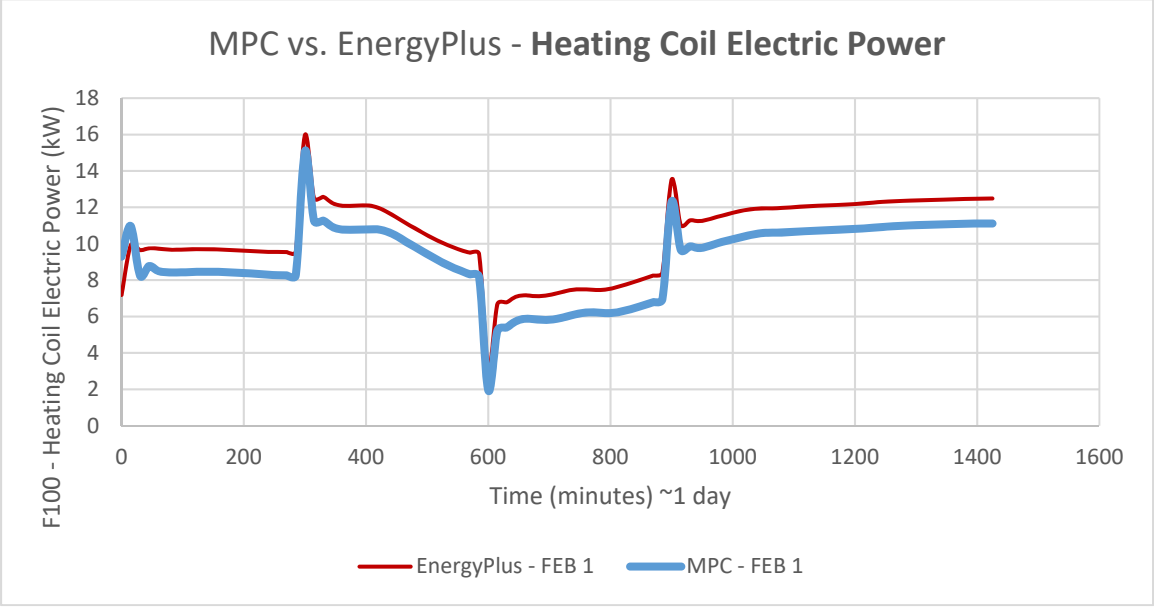

Figure 25 – MPC vs. EnergyPlus – Heating Coil Electric Power – FEB 1

4.1.3 Results for April 1

The second set of results presented is for the April 1st case in Worcester, MA. With the thermostat set-point schedule entered into the model as a hard constraint, the resultant EnergyPlus and MPC predictions of ventilated shelter temperature and equivalent ECU power consumption are compared.

4.1.3.1 Main Zone Temperature

Figure 26 shows the resultant Main Zone temperature from both EnergyPlus and MPC simulations. By observation, it is evident that for the spring season simulation date, both controller models tend to overlap the thermostat heating set-point temperature.

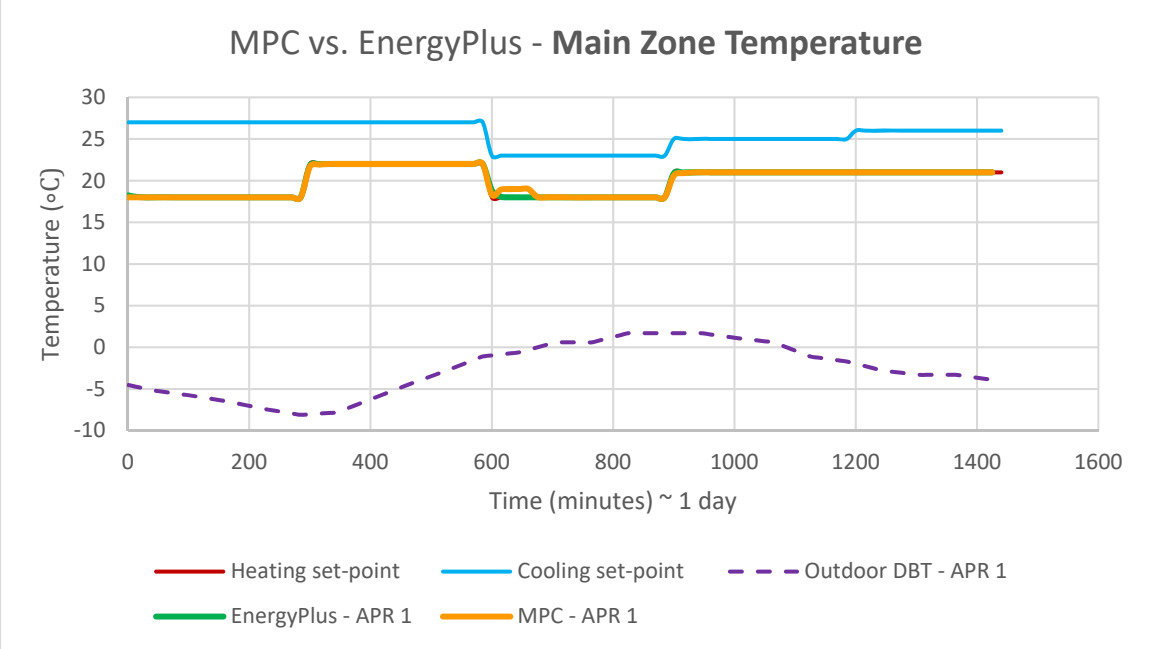

Figure 26 – MPC vs. EnergyPlus – Main Zone Temperature – APR 1

4.1.3.2 Power Consumption

For both EnergyPlus and MPC simulations, Figures 27 & 28 show the resultant cooling coil electric power and heating coil electric power respectively. By observation, it is evident that for the spring season simulation date, the cooling coil electric power is negligible while heating coil electric power is active throughout the 24 hours. By comparison, MPC outperforms EnergyPlus by consuming less power throughout the operating cycle of the ECU.

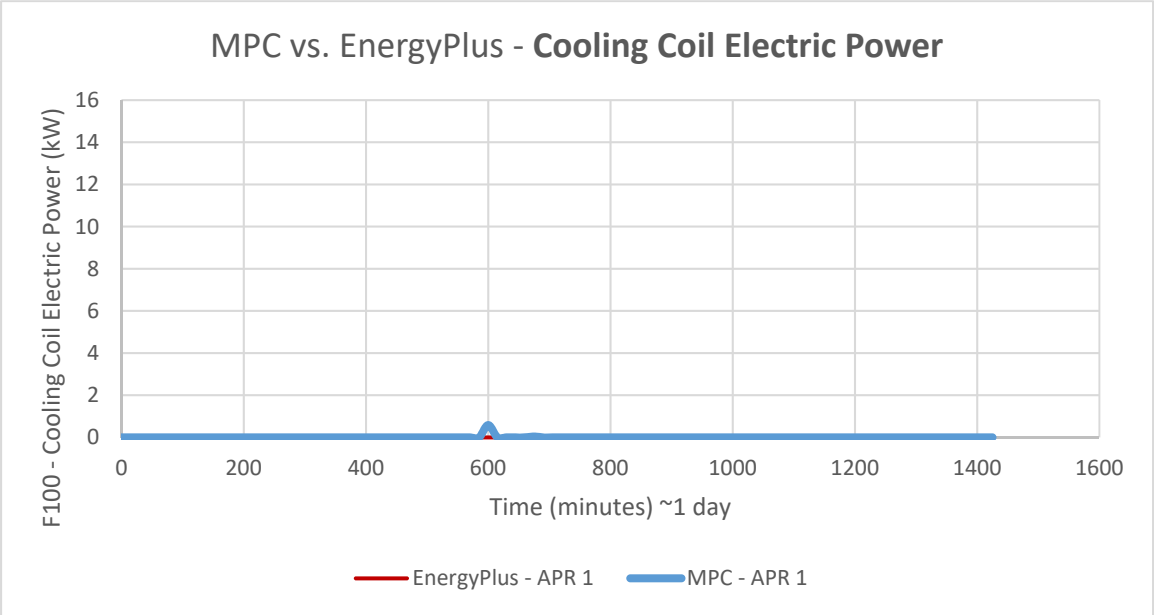

Figure 27 – MPC vs. EnergyPlus – Cooling Coil Electric Power – APR 1

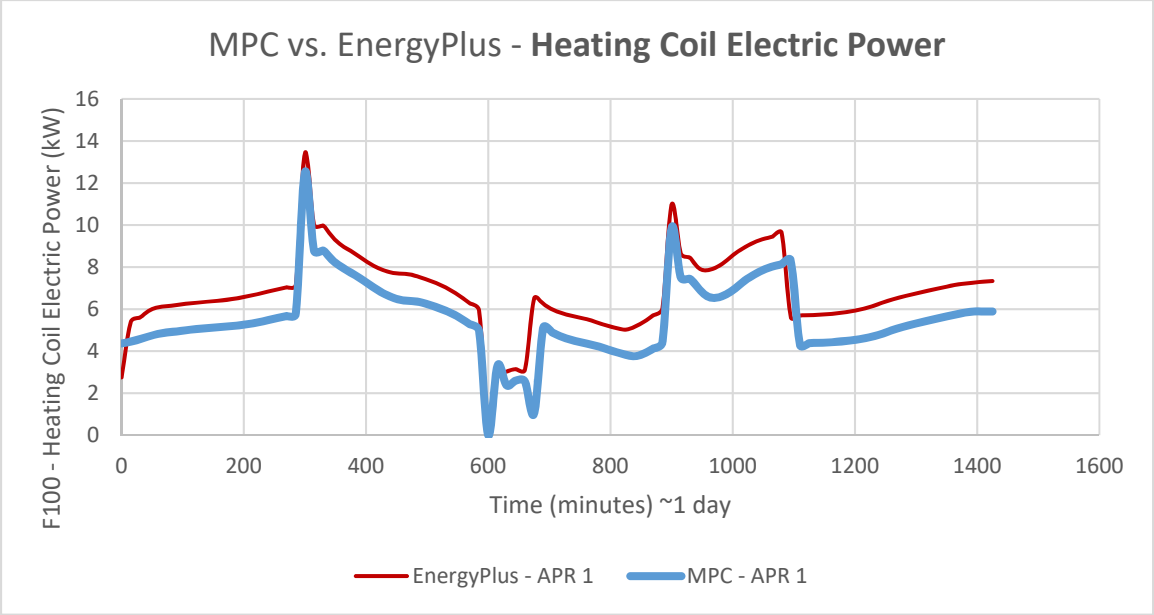

Figure 28 – MPC vs. EnergyPlus – Heating Coil Electric Power – APR 1

4.1.4 Results for June 1 – CASE A

The third set of results presented is for the June 1st case in Worcester, MA with an initial thermostat set-point temperature for MPC set at 21℃. Unlike February and April cases, this initial thermostat set-point temperature for MPC simulation varies from initial thermostat set-point temperature for EnergyPlus simulation. With the thermostat set-point schedule entered into the model as a hard constraint, the resultant EnergyPlus and MPC predictions of ventilated shelter temperature and equivalent ECU power consumption are compared.

4.1.4.1 Main Zone Temperature

Figure 29 shows the resultant Main Zone temperature from both EnergyPlus and MPC simulations. By observation, it is evident that for the summer season simulation date, both controller models tend to overlap the thermostat cooling set-point temperature.

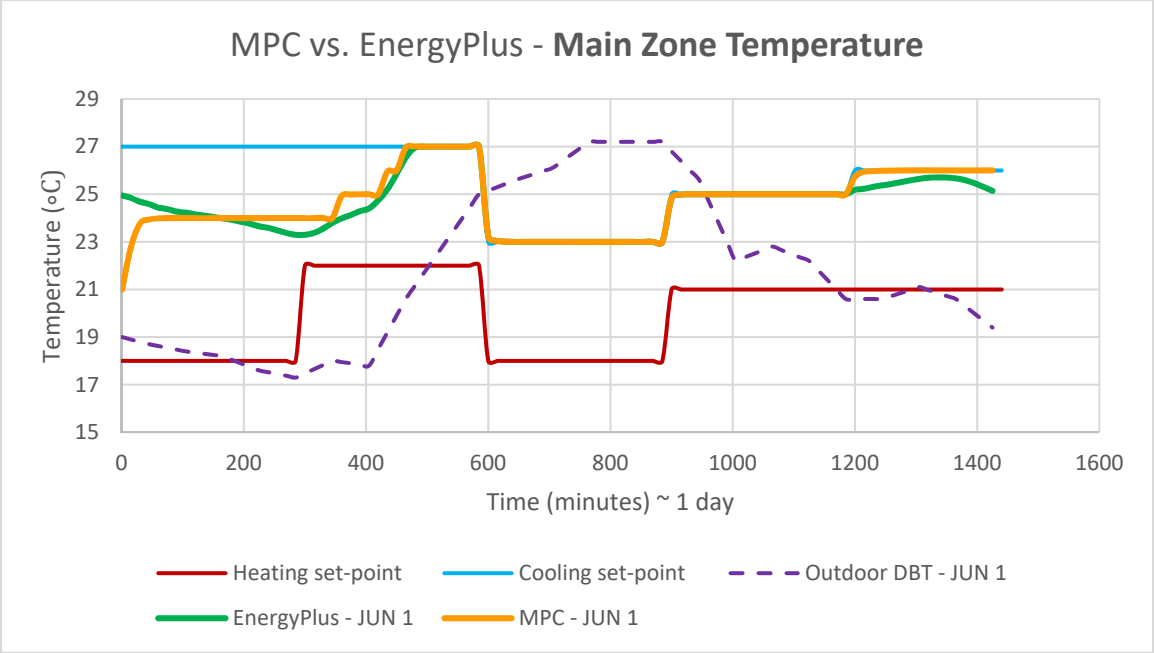

Figure 29 – MPC vs. EnergyPlus – Main Zone Temperature – JUN 1 – CASE A

4.1.4.2 Power Consumption

For both EnergyPlus and MPC simulations, Figures 30 & 31 show the resultant cooling coil electric power and heating coil electric power respectively. By observation, it is evident that for the summer season simulation date, the cooling coil electric power is active throughout the 24 hours while heating coil electric power is nearly negligible. By comparison, MPC slightly outperforms EnergyPlus in its cooling coil electric power consumption. This is due to consuming less power throughout the operating cycle of the ECU. However, the heating coil electric power consumption of MPC exceeds the heating coil electric power consumption of EnergyPlus.

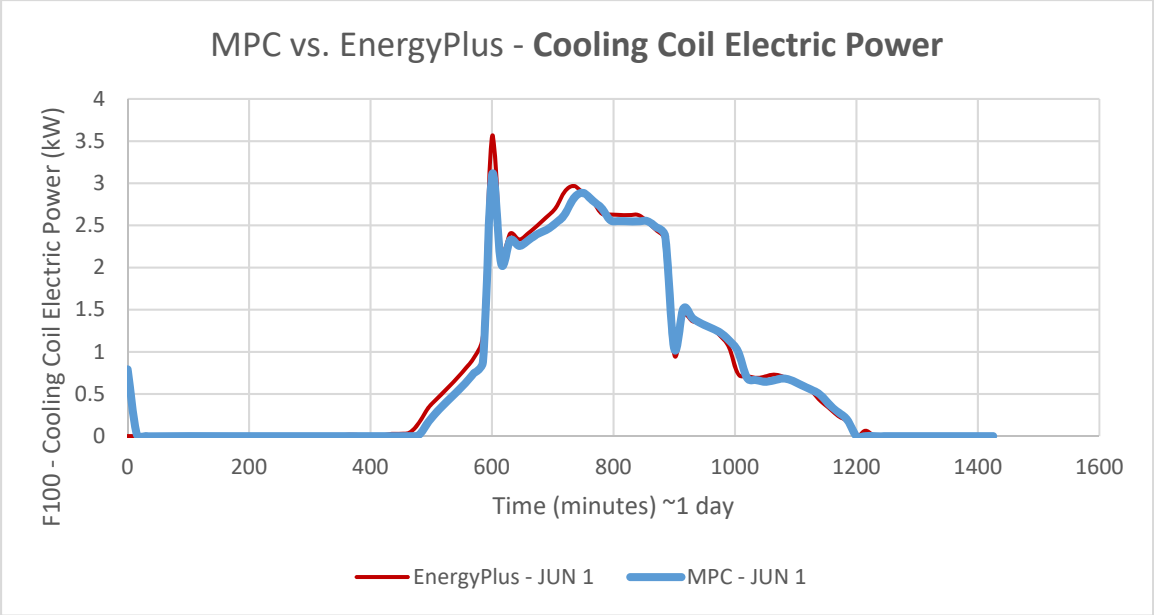

Figure 30 – MPC vs. EnergyPlus – Cooling Coil Electric Power – JUN 1 – CASE A

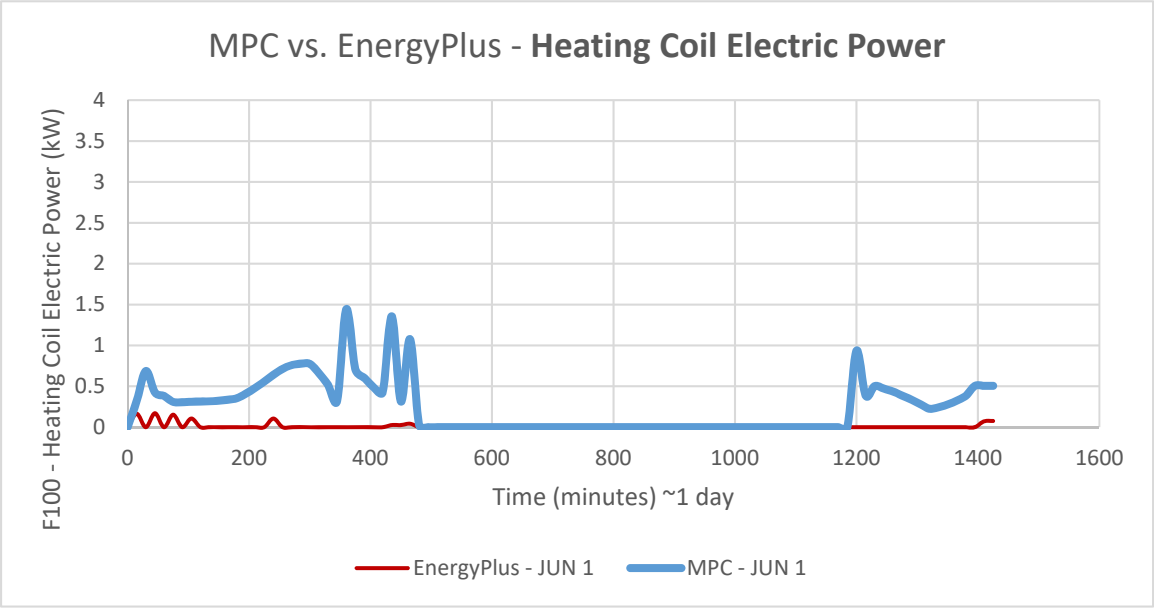

Figure 31 – MPC vs. EnergyPlus – Heating Coil Electric Power – JUN 1 – CASE A

4.1.5 Results for June 1 – CASE B

The fourth set of results presented is for the June 1st case in Worcester, MA with an initial thermostat set-point temperature for MPC set as the same value as initial thermostat set-point temperature for EnergyPlus (25℃). With the thermostat set-point schedule entered into the model as a hard constraint, the resultant EnergyPlus and MPC predictions of ventilated shelter temperature and equivalent ECU power consumption are compared.

4.1.5.1 Main Zone Temperature

Figure 32 shows the resultant Main Zone temperature from both EnergyPlus and MPC simulations. By observation, it is evident that for the summer season simulation date, both controller models tend to overlap the thermostat cooling set-point temperature.

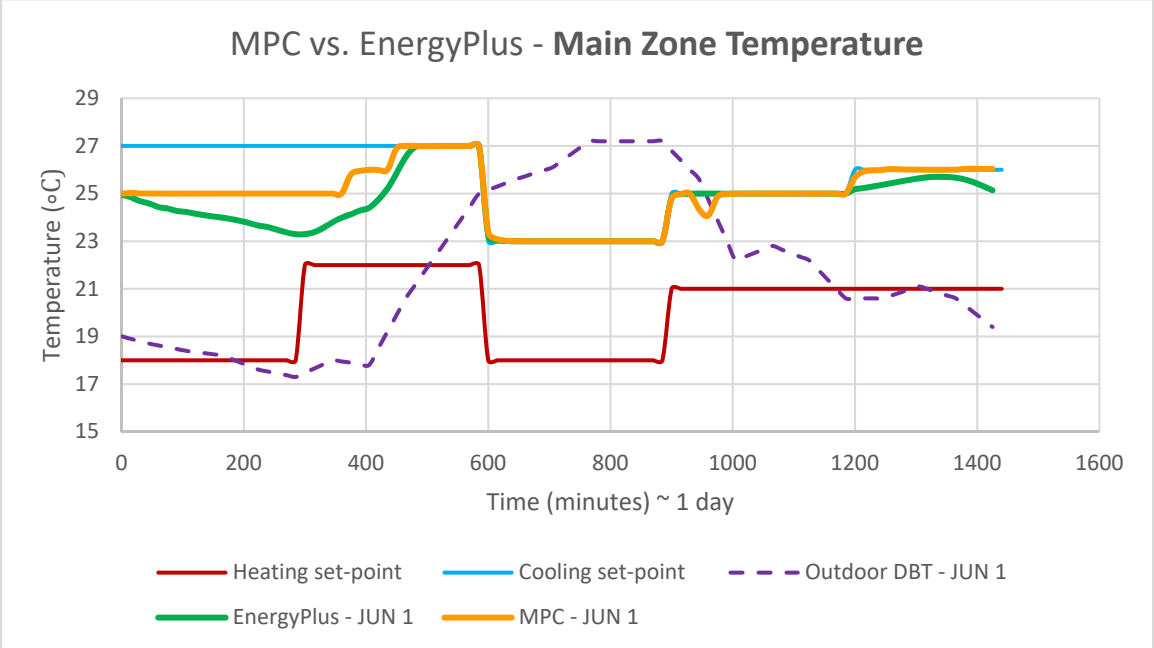

Figure 32 – MPC vs. EnergyPlus – Main Zone Temperature – JUN 1 – CASE B

4.1.5.2 Power Consumption

For both EnergyPlus and MPC simulations, Figures 33 & 34 show the resultant cooling coil electric power and heating coil electric power respectively. By comparison, EnergyPlus slightly outperforms MPC in its cooling coil electric power consumption. Moreover, the heating coil electric power consumption of MPC exceeds the heating coil electric power consumption of EnergyPlus.

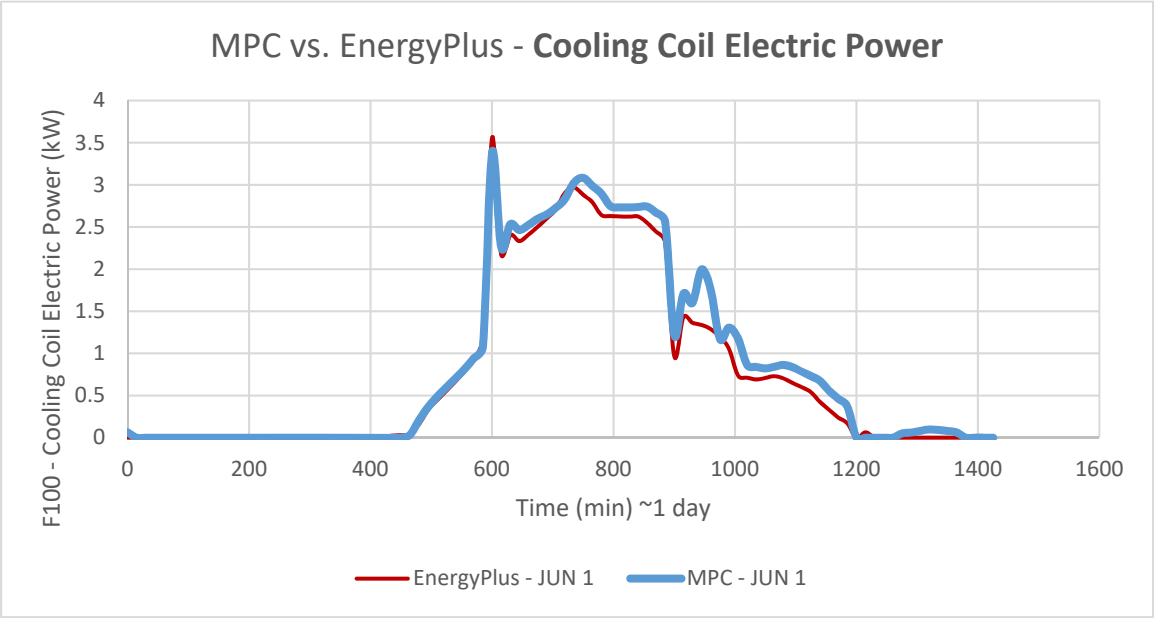

Figure 33 – MPC vs. EnergyPlus – Cooling Coil Electric Power – JUN 1 – CASE C

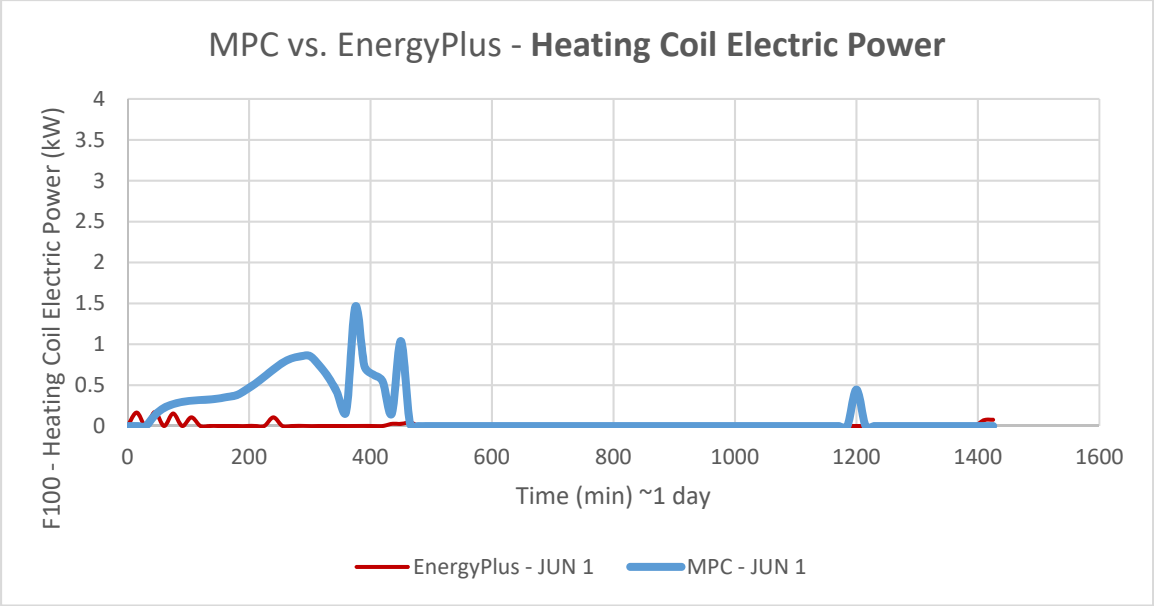

Figure 34 – MPC vs. EnergyPlus – Heating Coil Electric Power – JUN 1 – CASE C

4.1.6 Results for June 1 – CASE C

The fourth set of results presented is for the June 1st case in Worcester, MA with an initial thermostat set-point temperature for MPC set as 18 ℃. With the thermostat set-point schedule entered into the model as a hard constraint, the resultant EnergyPlus and MPC predictions of ventilated shelter temperature and equivalent ECU power consumption are compared.

4.1.6.1 Main Zone Temperature

Figure 35 shows the resultant Main Zone temperature from both EnergyPlus and MPC simulations. By observation, it is evident that for the summer season simulation date, both controller models tend to overlap the thermostat cooling set-point temperature.

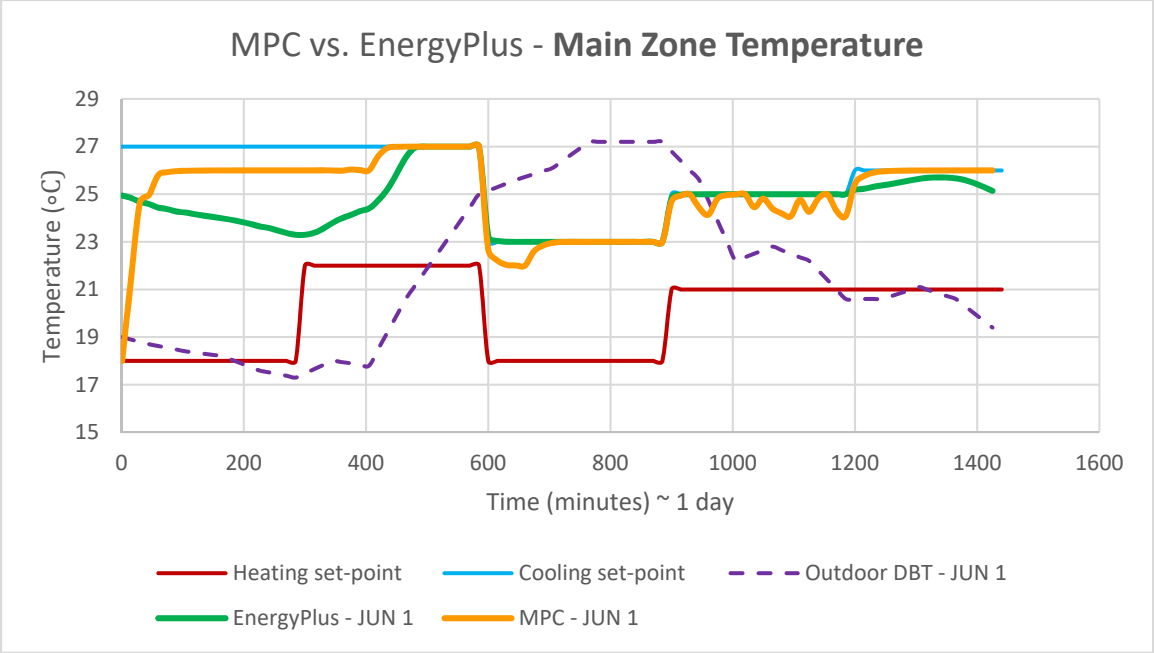

Figure 35 – MPC vs. EnergyPlus – Main Zone Temperature – JUN 1 – CASE C

4.1.6.2 Power Consumption

For both EnergyPlus and MPC simulations, Figures 36 & 37 show the resultant cooling coil electric power and heating coil electric power respectively. By comparison, EnergyPlus largely outperforms MPC in its cooling coil electric power consumption. Moreover, the heating coil electric power consumption of MPC exceeds the heating coil electric power consumption of EnergyPlus.

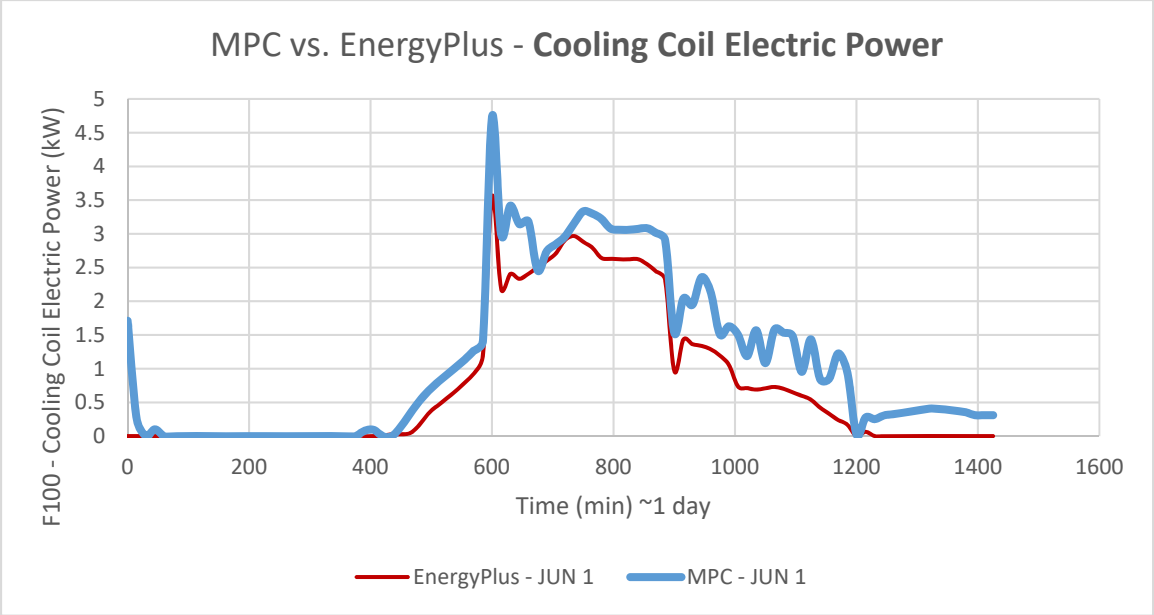

Figure 36 – MPC vs. EnergyPlus – Cooling Coil Electric Power – JUN 1 – CASE C

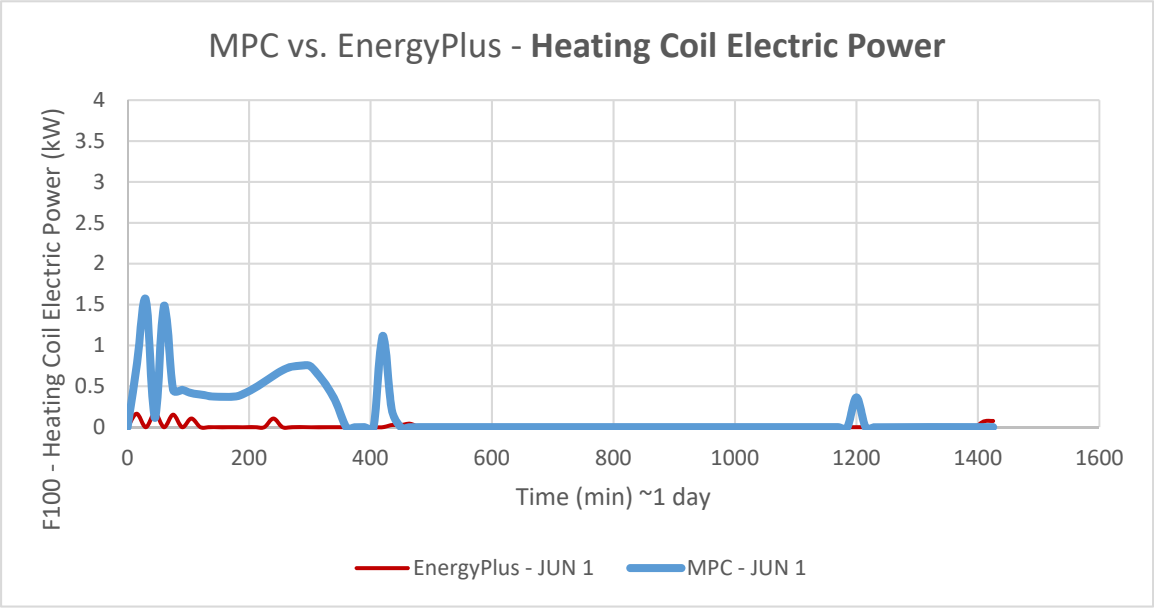

Figure 37 – MPC vs. EnergyPlus – Heating Coil Electric Power – JUN 1 – CASE B

4.2 Discussion of Results for Airbeam Shelter with F100 – Thermal Comfort Optimization

The results obtained for the shelter and ECU combination are further analyzed by determining the net kWh of each MPC and EnergyPlus simulation for the run period of 24 hours. The approach of trapezoidal numerical integration resulted in the values shown in Table 6.

Table 6 – MPC vs. EnergyPlus Net Load (kWh) Comparison – F100

Day	Net Load (kWh)	MPC	EnergyPlus
February 1st	Cooling	3.3	0.0
	Heating	13049.7	14844.0
April 1st	Cooling	9.4	0.0
	Heating	7920.9	9647.5
June 1st – CASE A	Cooling	1071.0	1107.8
	Heating	358.4	13.6
June 1st – CASE B	Cooling	1218.8	1107.8
	Heating	231.8	13.6
June 1st – CASE C	Cooling	1599.9	1107.8
	Heating	228.5	13.6

For winter season day of February 1st, net heating load with MPC is about 1794.3 kWh lower than net heating load with EnergyPlus. However, the temperatures for both simulation methods tend to overlap each other without much difference. This is because MPC is instantaneously selecting the integer set-point, whereas E+ is incrementally increasing or decreasing to reach the set-point which results in higher heating power draw by E+. But since the simulation time-step is a coarse value of 15 minutes, the transient change in temperature with EnergyPlus is not captured.

For spring season day of April 1st, net heating load with MPC is about 1726.6 kWh lower than net heating load with EnergyPlus. However, the temperatures for both simulation methods tend to slightly overlap each other without much difference. This is again because MPC is instantaneously selecting the integer set-point, whereas E+ is incrementally increasing or decreasing to reach the set-point which results in higher heating power draw by E+. As stated before, since the simulation time-step is a coarse value of 15 minutes, the transient change in temperature with EnergyPlus is not captured.

For summer season day of June 1st, net cooling load with MPC is about 36.8 kWh lower than net cooling load with EnergyPlus for Case A. However, net heating load with MPC is about 344.8 kWh higher than net heating load with EnergyPlus. Even though the cooling electric power consumption is lower with MPC, the overall power consumption savings are much higher with EnergyPlus. The reason for the higher net heating load with MPC at the initial few time-steps of the simulation is because the starting set-point for MPC simulations is set to a low integer value of 21 °C. Due to this, the Main Zone requires heating inside the space to reach the favorable thermostat cooling set-point bound.

For Cases B & C of summer season day of June 1st, net cooling load and heating load with MPC exceed the net cooling load and heating load with EnergyPlus. For Case B, the differences between the net cooling coil and heating coil loads of MPC versus EnergyPlus are 111.0 kWh and 218.3 kWh respectively. For Case C, the differences between the net cooling coil and heating coil loads of MPC versus EnergyPlus are 492.0 kWh and 214.9 kWh respectively. These discrepancies between each of the cases occur due to the small prediction horizon and variable factors of the model. Thus, Case A is the most ideal for the summer season day study with lower cooling coil electric power load with MPC.

4.3 Airbeam Shelter with F100 – Energy Consumption Optimization

The Airbeam shelter model equipped with F100 is tested for MPC simulations, as well as EnergyPlus simulations. For all simulation cases with both MPC and EnergyPlus, doubled F100 units/dual capacity F100 unit is used to account for unmet hours of load in the baseline EnergyPlus model of the ECU. Due to its ease of use, OpenStudio software is used to perform the simulations for the EnergyPlus cases. For all simulation cases with MPC, the foremost optimization sequence in the controller is least energy consumption by the ECU during the operation of its fan, heating cycle and cooling cycle. This sorting sequence is followed by the optimization sequence of zero temperature overshoot outside the constraints of the thermostat schedule. Hence, the most energy-efficient usage of the ECU is the priority of the MPC controller. The testing is done for three separate weather days which represent three separate seasons. Also, the time-step for all simulations in the study is set to 15 minutes. In the case of the MPC simulations, the prediction horizon

parameter for all simulations in the study is set to 30 minutes. The simulations correspond to the weather of Worcester, MA.

4.3.1 Loads Applied to the Model

Since the simulations are performed for three separate days representing three separate seasons, the environmental load profile is significantly differentiated by the chosen day of the weather file. The dates February 1st, April 1st and June 1st correspond to winter, spring and summer seasons respectively. Figure 38 shows the outdoor dry air bulb temperature input to the model, which is extracted from the EPW file. The internal loads to the model are constant 24 hour input values of 500 W for electronics equipment load, 1,000 W for lighting load and occupancy of 11 people which equates to 1,320 W occupancy load. The range of input ECU set-point temperatures for driving the MPC controller is integer values from 17-28 °C.

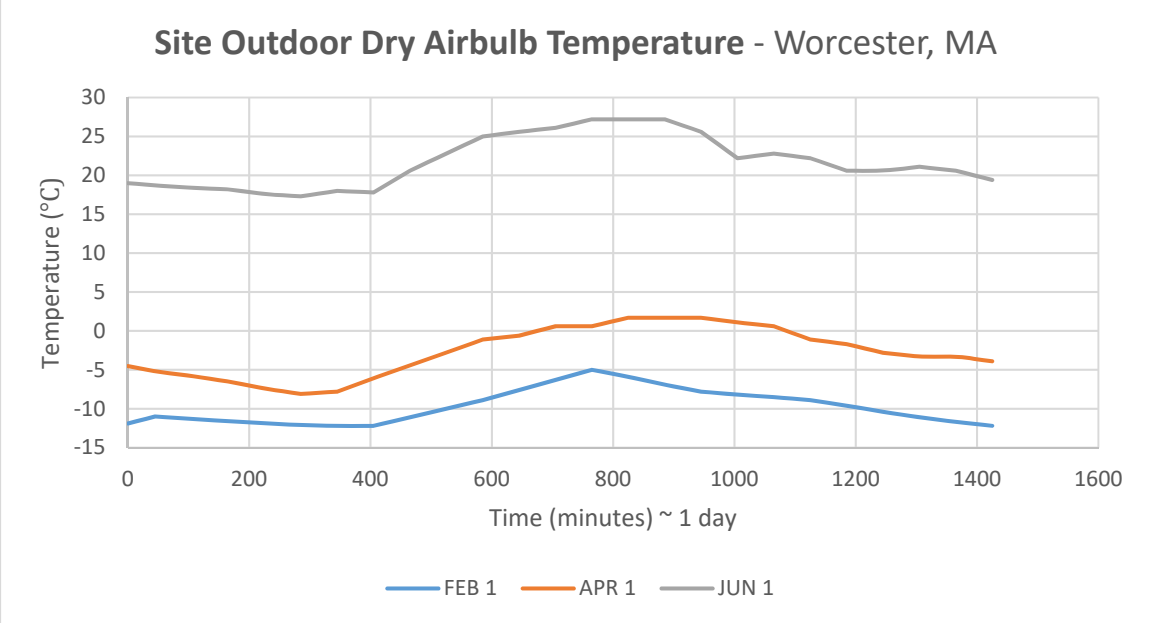

Figure 38 – Site Outdoor Dry Air Bulb Temperature – Worcester, MA

4.3.2 Results for February 1

The first set of results presented is for the February 1st case in Worcester, MA. With the thermostat set-point schedule entered into the model as a hard constraint, the resultant EnergyPlus and MPC predictions of ventilated shelter temperature and equivalent ECU power consumption are compared.

4.3.2.1 Main Zone Temperature

Figure 39 shows the resultant Main Zone temperature from both EnergyPlus and MPC simulations. Green line represents EnergyPlus while orange line represents MPC. The red and blue lines represent the hard constraints of thermostat heating set-point and cooling set-point respectively. Also, dashed purple line represents the site outdoor dry air bulb temperature. By observation, it is evident that for the winter season simulation date, EnergyPlus controller model closely overlaps the thermostat heating set-point temperature while the MPC controller model remains outside the heating set-point temperature bound of the thermostat.

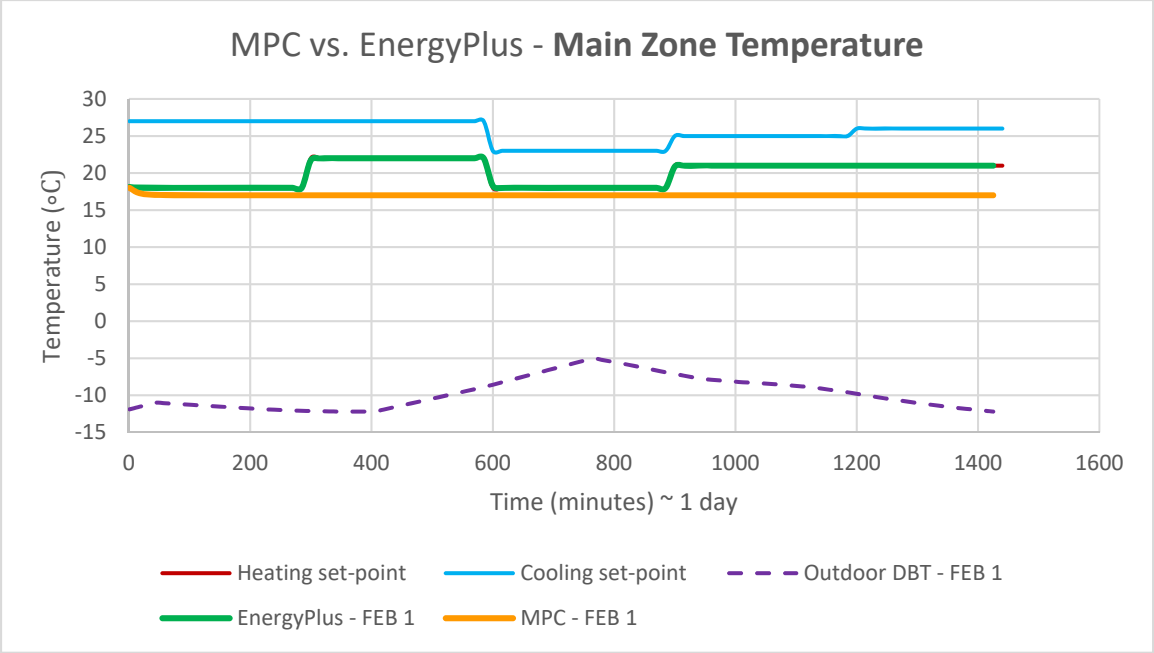

Figure 39 – MPC vs. EnergyPlus – Main Zone Temperature – FEB 1

4.3.2.2 Power Consumption

For both EnergyPlus and MPC simulations, Figures 40 & 41 show the resultant cooling coil electric power and heating coil electric power respectively. On both figures, red line represents EnergyPlus while blue line represents MPC. By observation, it is evident that for the winter season simulation date, the cooling coil electric power is negligible while heating coil electric power is active throughout the 24 hours. By comparison, MPC significantly outperforms EnergyPlus by consuming less power throughout the operating cycle of the ECU.

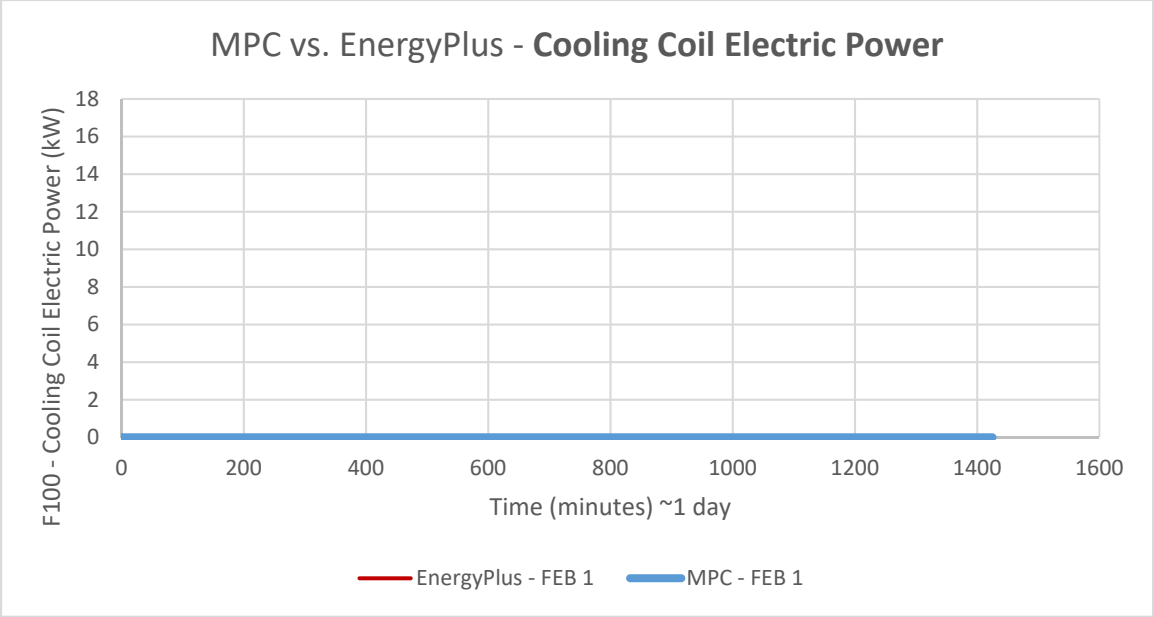

Figure 40 – MPC vs. EnergyPlus – Cooling Coil Electric Power – FEB 1

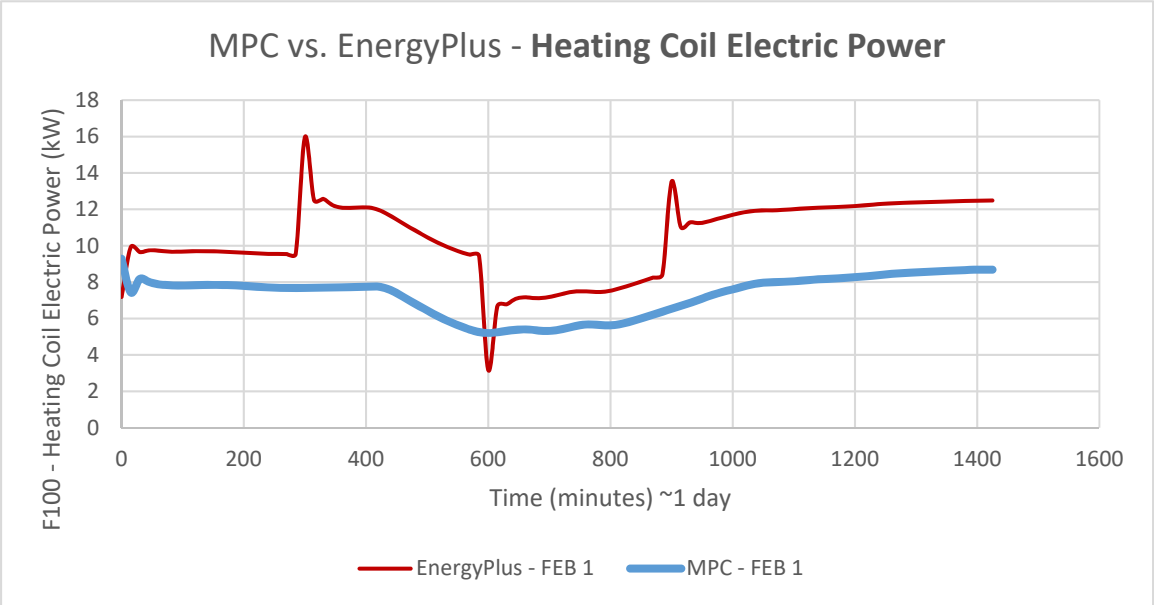

Figure 41 – MPC vs. EnergyPlus – Heating Coil Electric Power – FEB 1

4.3.3 Results for April 1

The second set of results presented is for the April 1st case in Worcester, MA. With the thermostat set-point schedule entered into the model as a hard constraint, the resultant EnergyPlus and MPC predictions of ventilated shelter temperature and equivalent ECU power consumption are compared.

4.3.3.1 Main Zone Temperature

Figure 42 shows the resultant Main Zone temperature from both EnergyPlus and MPC simulations. By observation, it is evident that for the spring season simulation date, EnergyPlus controller model closely overlaps the thermostat heating set-point temperature while the MPC controller model remains outside the heating set-point temperature bound of the thermostat.

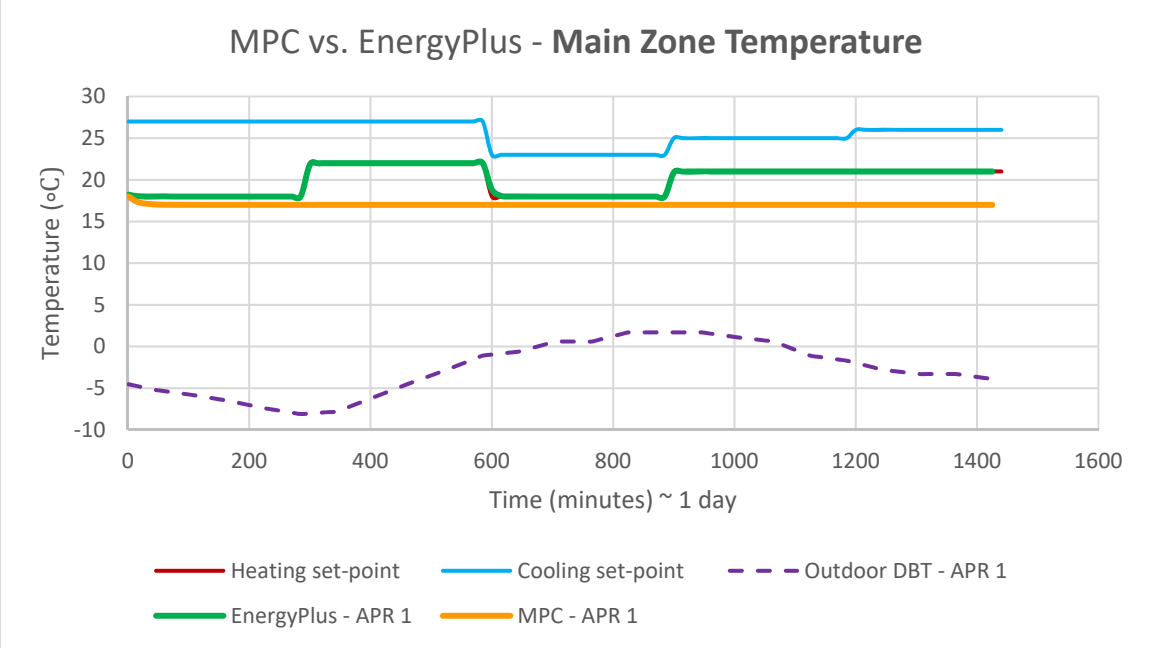

Figure 42 – MPC vs. EnergyPlus – Main Zone Temperature – APR 1

4.3.3.2 Power Consumption

For both EnergyPlus and MPC simulations, Figures 43 & 44 show the resultant cooling coil electric power and heating coil electric power respectively. By observation, it is evident that for the spring season simulation date, the cooling coil electric power is negligible while heating coil electric power is active throughout the 24 hours. By comparison, MPC significantly outperforms EnergyPlus by consuming less power throughout the operating cycle of the ECU.

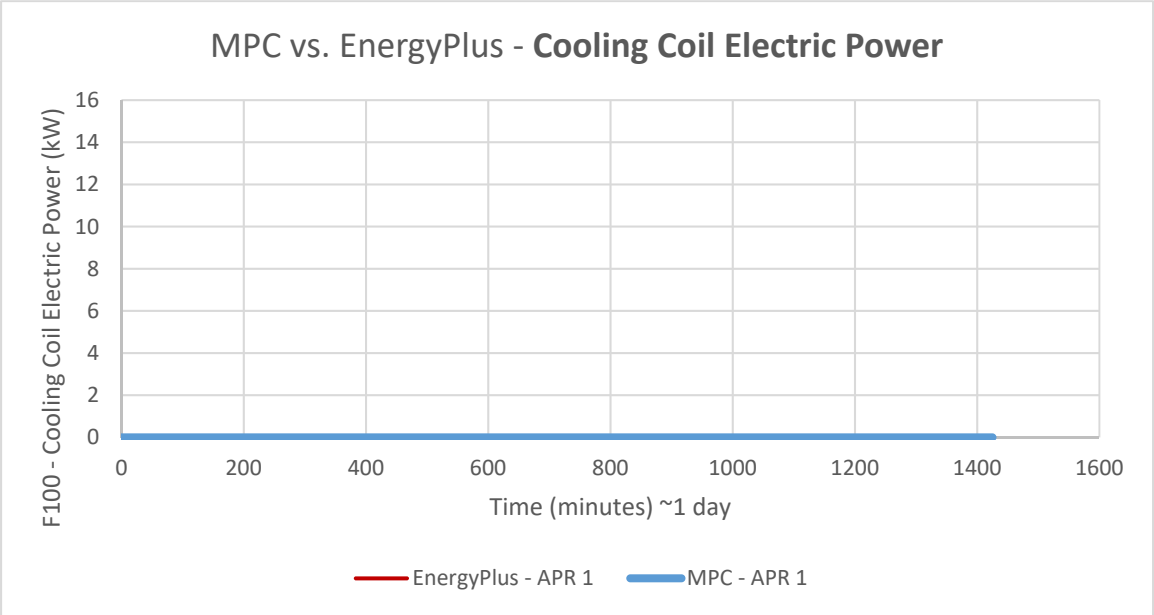

Figure 43 – MPC vs. EnergyPlus – Cooling Coil Electric Power – APR 1

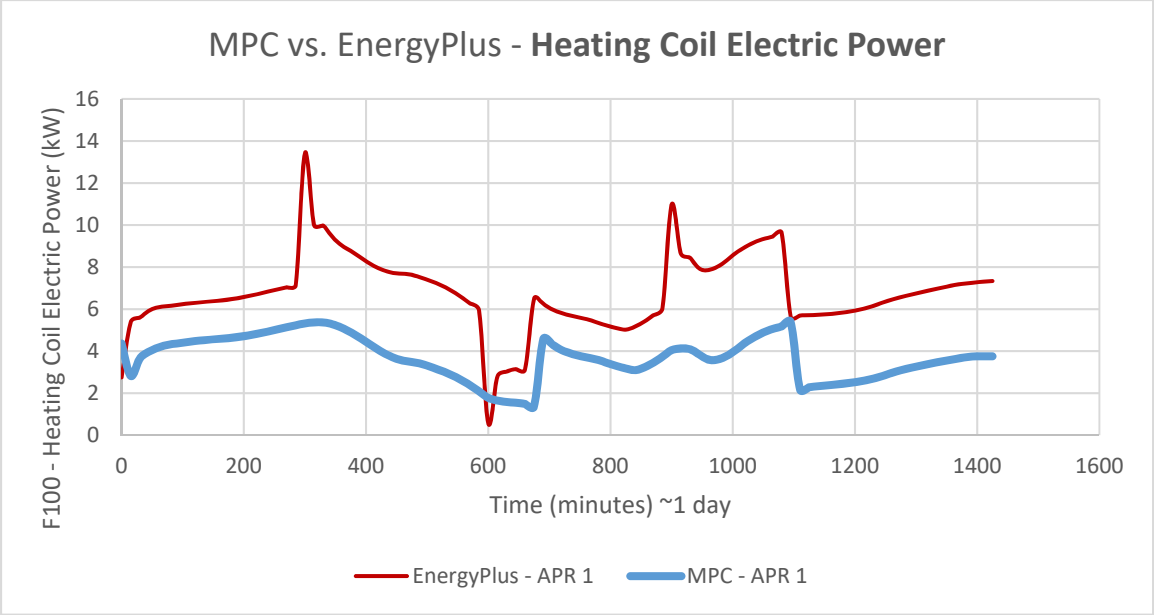

Figure 44 – MPC vs. EnergyPlus – Heating Coil Electric Power – APR 1

4.3.4 Results for June 1

The third set of results presented is for the June 1st case in Worcester, MA with an initial thermostat set-point temperature for set as the same value as initial thermostat set-point temperature for EnergyPlus (25℃). Similar to February and April cases, this initial thermostat set-point temperature for MPC simulation matches with initial thermostat set-point temperature for EnergyPlus simulation. With the thermostat set-point schedule entered into the model as a hard constraint, the resultant EnergyPlus and MPC predictions of ventilated shelter temperature and equivalent ECU power consumption are compared.

4.3.4.1 Main Zone Temperature

Figure 45 shows the resultant Main Zone temperature from both EnergyPlus and MPC simulations. By observation, it is evident that for the summer season simulation date, EnergyPlus controller model closely overlaps the thermostat cooling set-point temperature

while the MPC controller model remains both inside and outside the cooling set-point temperature bound of the thermostat.

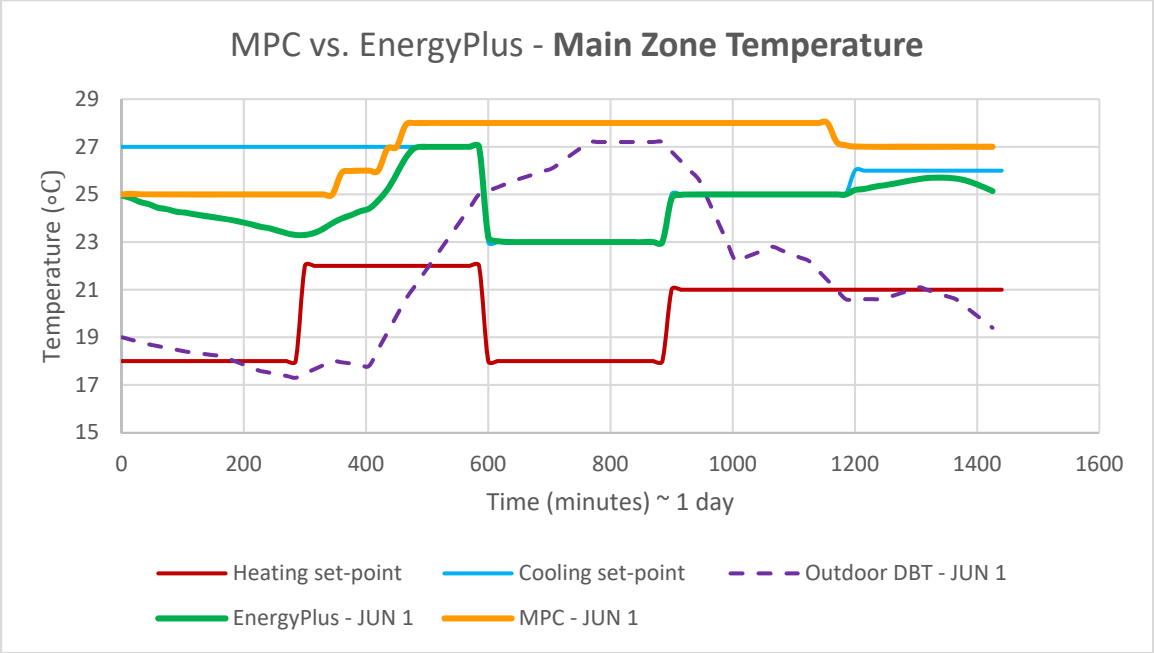

Figure 45 – MPC vs. EnergyPlus – Main Zone Temperature – JUN 1

4.3.4.2 Power Consumption

For both EnergyPlus and MPC simulations, Figures 46 & 47 show the resultant cooling coil electric power and heating coil electric power respectively. By observation, it is evident that for the summer season simulation date, the cooling coil electric power is active throughout the 24 hours while heating coil electric power is nearly negligible. By comparison, MPC significantly outperforms EnergyPlus in its cooling coil electric power consumption. This is due to consuming less power throughout the operating cycle of the ECU. However, the heating coil electric power consumption of MPC exceeds the heating coil electric power consumption of EnergyPlus.

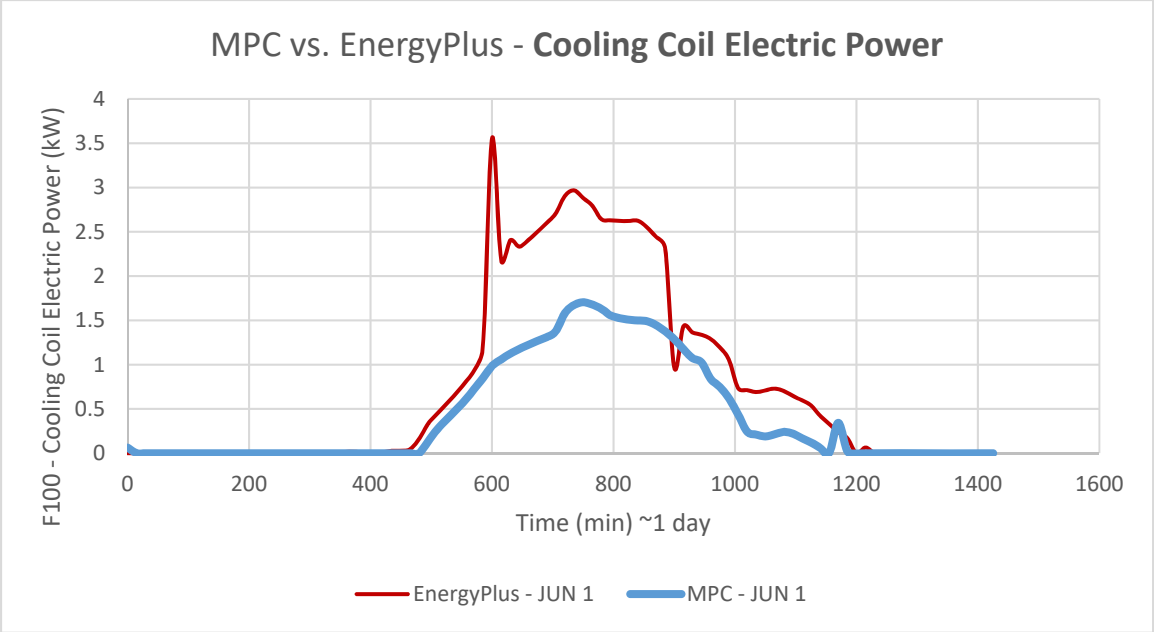

Figure 46 – MPC vs. EnergyPlus – Cooling Coil Electric Power – JUN 1

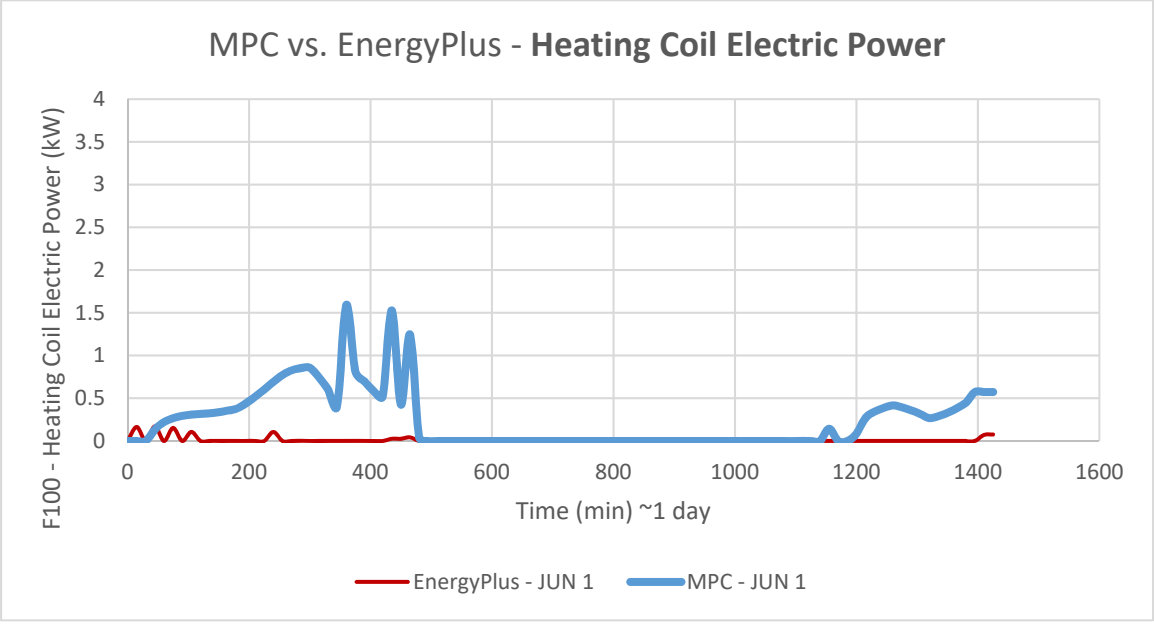

Figure 47 – MPC vs. EnergyPlus – Heating Coil Electric Power – JUN 1

4.4 Discussion of Results for Airbeam Shelter with F100 – Energy Consumption Optimization

The results obtained for the shelter and ECU combination are further analyzed by determining the net kWh of each MPC and EnergyPlus simulation for the run period of 24 hours. The approach of trapezoidal numerical integration resulted in the values shown in Table 7.

Table 7 – MPC vs. EnergyPlus Net Load (kWh) Comparison – F100

Day	Net Load (kWh)	MPC	EnergyPlus
February 1st	Cooling	0.0	0.0
	Heating	10347.8	14844.0
April 1st	Cooling	0.0	0.0
	Heating	5270.9	9647.5
June 1st	Cooling	613.6	1107.8
	Heating	353.6	13.6

For winter season day of February 1st, net heating load with MPC is about 4496.2 kWh lower than net heating load with EnergyPlus. Since the most energy-efficient usage of the ECU is the priority of the MPC controller, the ventilated zone temperature of the MPC simulation case does not meet the thermal comfort criteria and does not overlap the EnergyPlus simulation case.

For spring season day of April 1st, net heating load with MPC is about 4376.6 kWh lower than net heating load with EnergyPlus. Since the most energy-efficient usage of the ECU is the priority of the MPC controller, the ventilated zone temperature of the MPC simulation case does not meet the thermal comfort criteria and does not overlap the EnergyPlus simulation case.

For summer season day of June 1st, net cooling load with MPC is about 494.2 kWh lower than net cooling load with EnergyPlus. However, net heating load with MPC is about 340.0 kWh higher than net heating load with EnergyPlus. Even though the heating electric power consumption is lower with EnergyPlus, the overall power consumption savings are much higher with MPC. Since the most energy-efficient usage of the ECU is the priority of the MPC controller, the ventilated zone temperature of the MPC simulation case does not meet the thermal comfort criteria and does not overlap the EnergyPlus simulation case.

4.5 Thermal Comfort Optimization – Humidity Level Based

Another possible and important foremost optimization sequence in the MPC controller is relative humidity level in the ventilated zone. This criterion would support the prioritization of the thermal comfort defined by low/median/high humidity level in ventilated zone. Since the relative humidity level is subjective to the geographical weather location and comfort level of the occupant, the selection of the optimum relative humidity in the zone is ultimately contingent upon the thermal comfort needs of the occupant(s). In the controller, this sorting sequence will be followed by the optimization sequence of zero temperature overshoot outside the constraints of the thermostat schedule and the most energy-efficient usage of the ECU during the operation of its fan, heating cycle and cooling

cycle. The MPC controller currently has the functionality to support relative humidity based control of the ECU. Similarly, the same functional approach is also possible with an MPC modulated mass flow rate for higher energy-efficiency usage of the ECU.

CHAPTER 5. FIELD APPLICATION RESULTS AND DISCUSSION

This chapter presents the results and analysis associated with the physical application performed of the MPC tool. For the analysis, the results of the MPC implementation to an actual ECU compared with conventional manual control on ECU are also discussed.

5.1 Alaska Shelter with IECU

The Alaska 3239 Shelter equipped with IECU is tested for MPC as well as manual control. For application case with MPC, doubled IECUs/dual capacity IECU is used to account for unmet hours of load in the baseline EnergyPlus model of the ECU. The testing is done for the summer season dates of July 21 for manual control and June 22 for MPC. The control run-period for both cases is 50 minute, performed around 12:35pm – 1:35pm. Figure 48 shows the perspective view of the shelter, notably identical in dimensions and architecture to an Airbeam shelter. The shelter is equipped with vinyl material for the entire tent structure and aluminum frame for support [51]. Due to the unavailability of a validated Alaska shelter model, the valid model of the baseline Airbeam shelter provided by NREL serves as the input model to the controller for the MPC application.

Figure 48 - Alaska Shelter Perspective View: L×W×H = 20 ft × 32 ft × 11 ft [51]

5.1.1 Loads Applied to the Shelter

Since the tests were performed at Range 1, Ft. Dix, NJ, the historical weather data for the McGuire AFB, NJ was used in the MPC application. This is because McGuire AFB is actually located at Ft. Dix. The internal loads to the shelter are constant non-stop input values of 0 W for electronics equipment load, 1,200 W for lighting load and occupancy of 1 person which equates to 120 W occupancy load. The range of input ECU set-point temperatures for driving the controller using both MPC and manual methods is the following range of values in °F: 64, 65, 66, 67, 68, 69, 70, 71, 72 & 73. These °F values correspond to the integer °C values of the following values respectively: 17.8, 18.3, 18.9, 19.4, 20.0, 20.6, 21.1, 21.7, 22.2 & 22.8.

Figure 49 shows the actual recorded weather data for June 22, 2017 at McGuire AFB, when the MPC application testing was performed. The top graph shows the outdoor dry air bulb temperature input to the model. Specifically, the average recorded outdoor dry air bulb temperature at 12:58 PM EST is 84.2 °F [52].

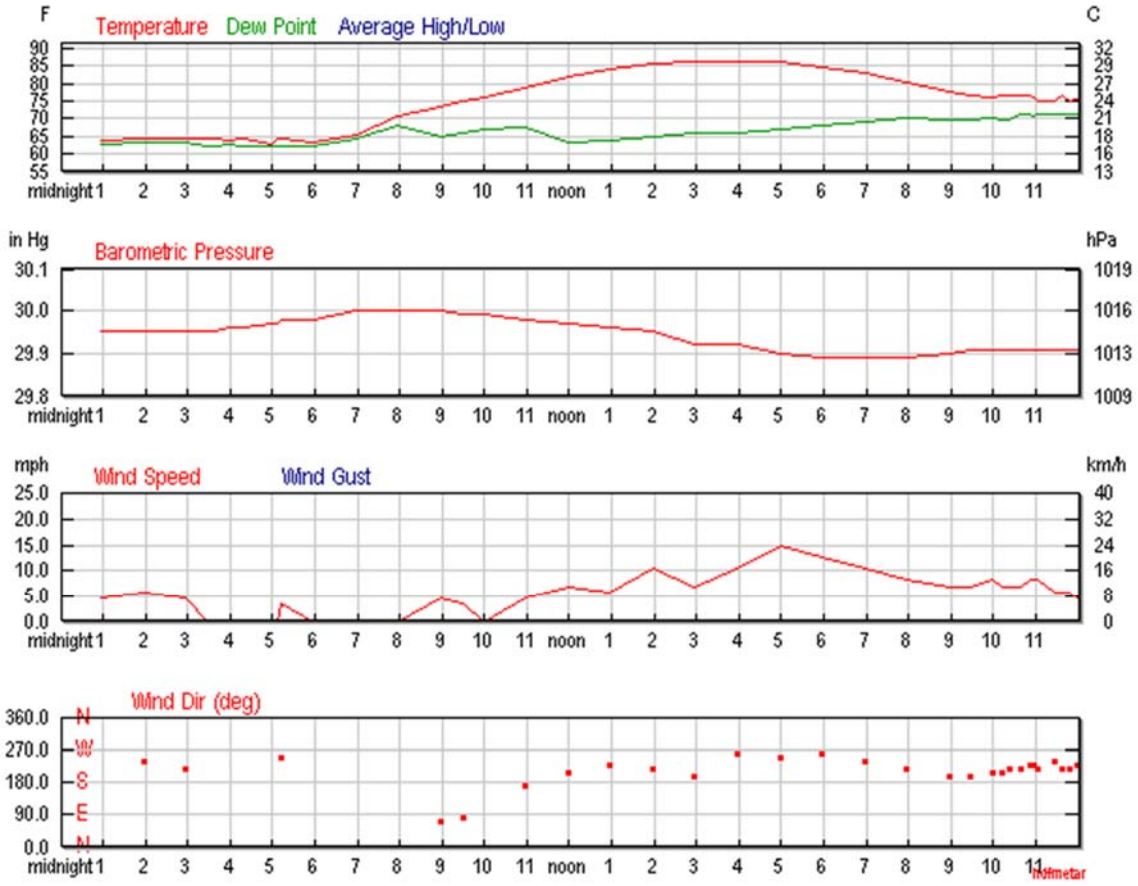

Figure 49 – Actual Weather History of McGuire AFB on June 22, 2017 [52]

Figure 50 shows the actual recorded weather data for July 21, 2017 at McGuire AFB, when the manual control application test was performed. The top graph shows the outdoor dry air bulb temperature input to the model. Specifically, the average recorded outdoor dry air bulb temperature at 12:58 PM EST is 91.2 °F [53].

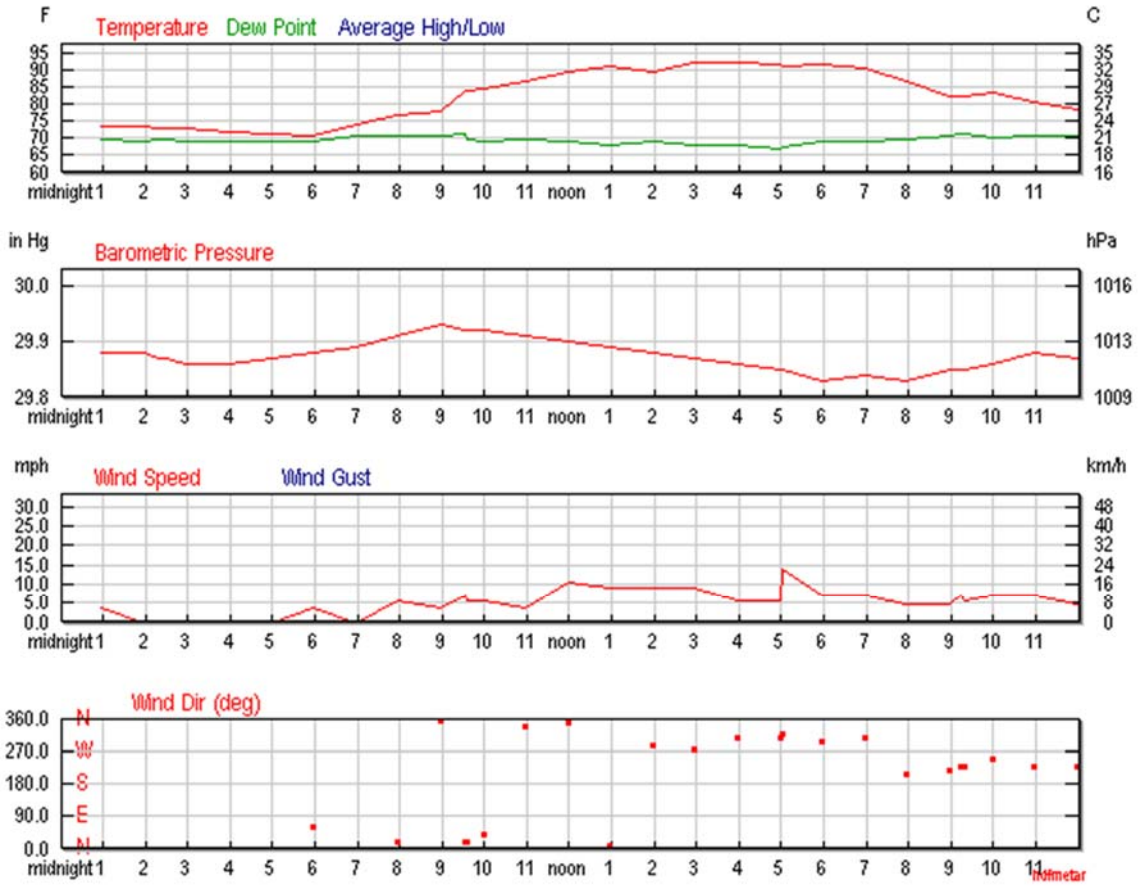

Figure 50 – Actual Weather History of McGuire AFB on July 21, 2017 [53]

Figure 51 shows the user-chosen thermostat set-point schedule for both MPC and manual control. Specifically, this input was provided for the 2 test days (July 21 & June 22) for the 50 minute run-periods (constraint to MPC).

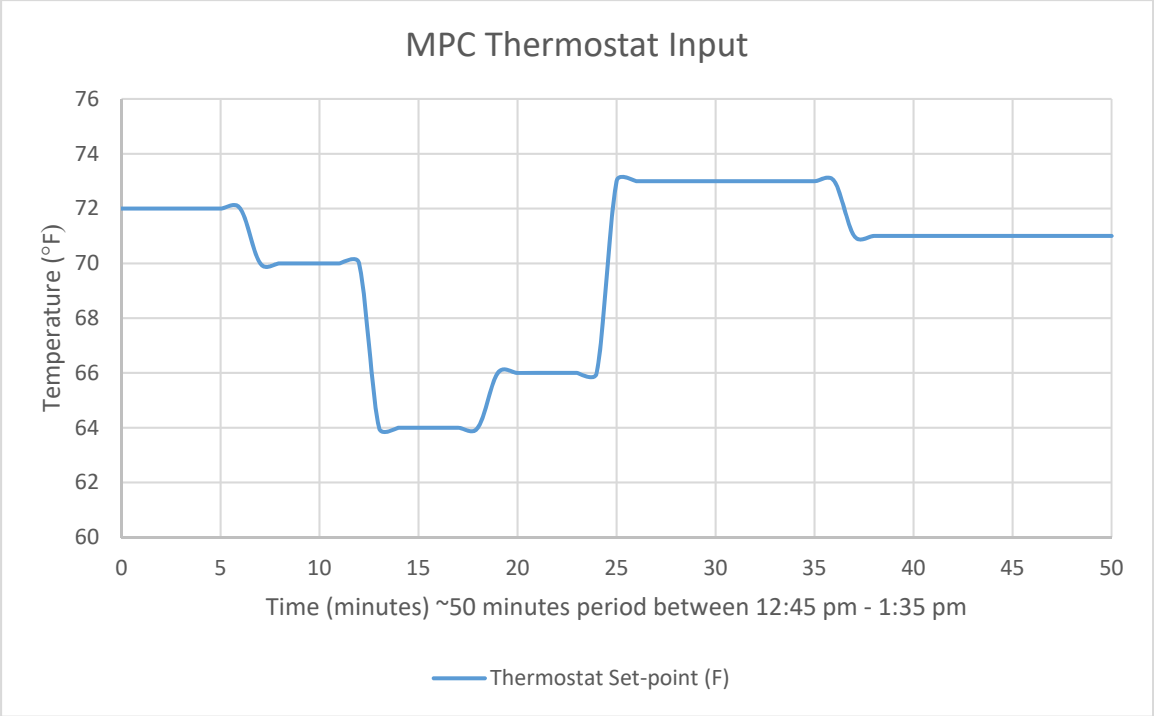

Figure 51 – Controller Input for Application of MPC

5.1.2 Inconsistencies

There are discrepancies involved between the 2 control methods applied to the IECU of the Alaska Shelter. These factors affect the overall results of the implementation effort.

5.1.2.1 MPC Model and Alaska Shelter

The valid model of the baseline Airbeam shelter provided by NREL serves as the input model to the controller for the MPC application. Since both the Alaska shelter and Airbeam shelter belong to the same category of soft-shell shelters, and there is no validated model of Alaska shelter in existence, the Airbeam shelter served as the most suitable model for the purpose.

Beyond having similar soft shell shelter features, the 2 shelters are precisely similar in dimensions. The Alaska shelter dimensions are precisely the same as the Airbeam shelter for the length, width and height [51]. But Alaska shelter uses vinyl as the primary material for the tent structure and aluminum frame for support [51]. Unlike Airbeam shelter, it does not have any vestibule zone. It is a single zone shelter with IECU for ventilating the space.

Considering these discrepancies, the valid Airbeam shelter model was only altered to add the total cubic volume of the vinyl material and aluminum frame as "InternalMass" objects. The architectural construction sets and materials of the Airbeam model were not changed.

5.1.2.2 Run Period

The next discrepancy involves matching the run period of the 2 control techniques. Due to limitations of the EnergyPlus software regarding selection of run periods for a period less than a day [48], the MPC simulation period almost never matches to the real-time control period. This is primarily because any MPC and EnergyPlus simulation session always begins at the midnight hour/minute of the day. Also, the duration of the simulation period never perfectly matches the duration of the real-time control period. This requires precise trial and error calibration of simulation run-time with actual application run-time, which was not performed for the application.

Another source of disparity in the application testing, is the difference between the summer season dates of July 21 for manual control and June 22 for MPC. Even though the two test dates are of the same summer season, there are climatic variations between the 2 different dates.

5.1.3 Results for MPC versus Manual Control

The results presented are for the June 22nd with MPC, and July 21st with manual control in McGuire AFB, NJ. With the thermostat set-point schedule entered into the model as a hard constraint, the resultant EnergyPlus and MPC predictions of ventilated shelter temperature and equivalent ECU power consumption are compared.

5.1.3.1 Zone Temperature

Figures 52 & 53 show the resultant Main Zone temperature from both manual control and MPC. On both Figures, red line represents temperature of the zone while blue line represents thermostat set-point temperature. By observation, it is evident that for the summer application dates of July 21 for manual control and June 22 for MPC, both controller applications roughly tend to overlap the thermostat set-point temperature. MPC outperforms manual control by displaying faster and precise IECU system response to the thermostat set-point schedule.

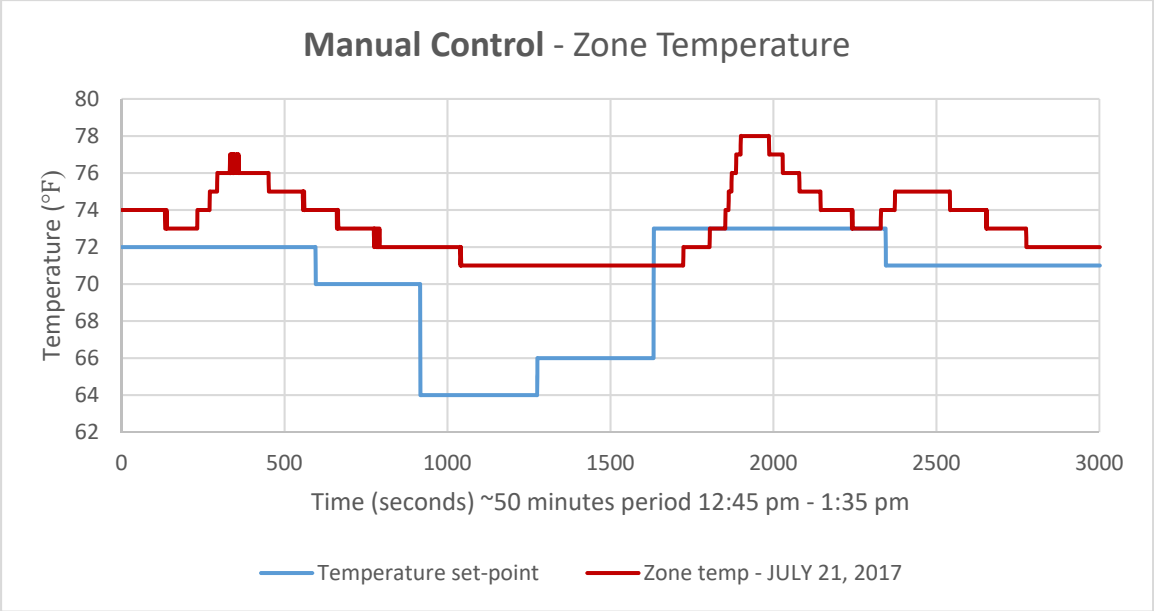

Figure 52 – Manual Control – Zone Temperature – JULY 21

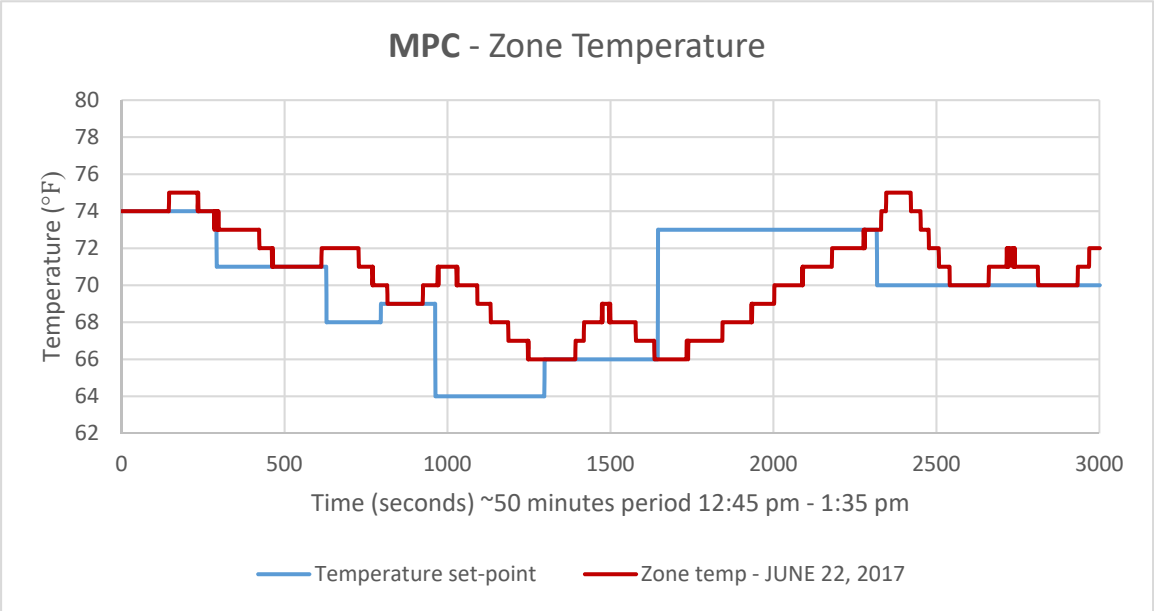

Figure 53 – MPC – Zone Temperature - JUNE 22

5.1.3.2 Power Consumption

For both manual control and MPC, Figure 54 shows the resultant IECU power consumption. This output variable combines the electric power consumption of the heating and cooling coils with the power consumption of the active fan. The power consumption of the ECU is the net load generated from the fan, compressor and heating coil. Unique to the IECU programmatic control, the fan and the compressor cyclically shutoff operation when the return-air shelter temperature reaches the ECU set-point temperature, to restart operation when the return-air shelter temperature offsets from the ECU set-point temperature. This operational trait of the IECU is proven by the load peaks in the power consumption data set. On the figure, red line represents manual control while blue line represents MPC. By observation, it is evident that for the summer season application dates of July 21 for manual control and June 22 for MPC, the IECU power consumption with MPC is significantly lower than the IECU power consumption with manual control.

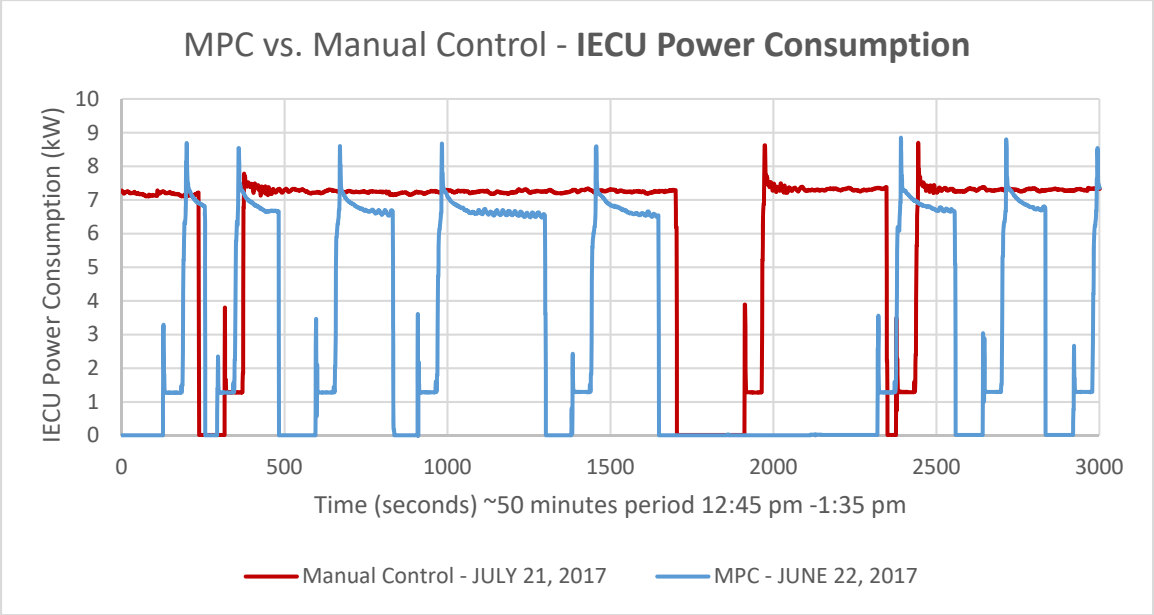

Figure 54 – MPC vs. Manual Control – IECU Power Consumption – JUN 22

5.1.3.3 Zone Temperature and Power Consumption – Superimposed

For further assessment of the results, Figures 55 & 56 show the Main Zone temperature (in units of °F) superimposed with the ECU power consumption (in units of kW), for both manual control and MPC. On both Figures, red line represents temperature of the zone, blue line represents thermostat set-point temperature and dashed green line represents IECU power consumption.

On Figure 55, the double y-axis results of the manual control case on July 21 for ventilated zone temperature, thermostat set-point temperature and the corresponding ECU power consumption are displayed. Each time the ECU operation terminates, the zone temperature rises above the set-point temperature and ECU power consumption instantaneously drops to zero. This system shutoff occurs around the 250th, 1700th and 2400th second instants across the run period. Each time the ECU operation resumes/restarts,

the zone temperature drops to reach the set-point temperature. The system restart occurs in 2 stages. At 1st stage, the fan turns on and stabilizes which occurs around the 350^{th}, 1950^{th} and 2400^{th} second instants across the run period. At 2^{nd} stage, the compressor turns on and stabilizes which occurs around 400^{th}, 2000^{th} and 2500^{th} second instants across the run period. Due to large inrush current, the short ECU load peaks occur for the fan, followed by long ECU load peaks which occur for the compressor.

Due to high inconsistencies in the efficiency of the ECU operation, the cooling component or compressor could not reach temperature set-points below 71°F. Hence, during run period from 400 to 1,700 seconds, the ECU operates continuously however, the zone temperature in the shelter is unable to reach the lower ECU set-point temperature values. The cyclic system termination and resumption of the ECU properly occurs during run period from 1,700 to 3,000 seconds. During the manual control operation, the ECU set-point temperature is only altered at the beginning of each thermostat set-point temperature band (6 times). After each ECU set-point temperature input, the system is left unchanged due to which the precise system update/check does not take place. The slow system response time of the controlled zone temperature in the shelter is due to the delay in forthcoming input ECU set-point temperature entries to the controller. This delay in input signal entry is resolved by the discretely rapid, predictive and optimized selection of ECU set-point temperature during MPC operation.

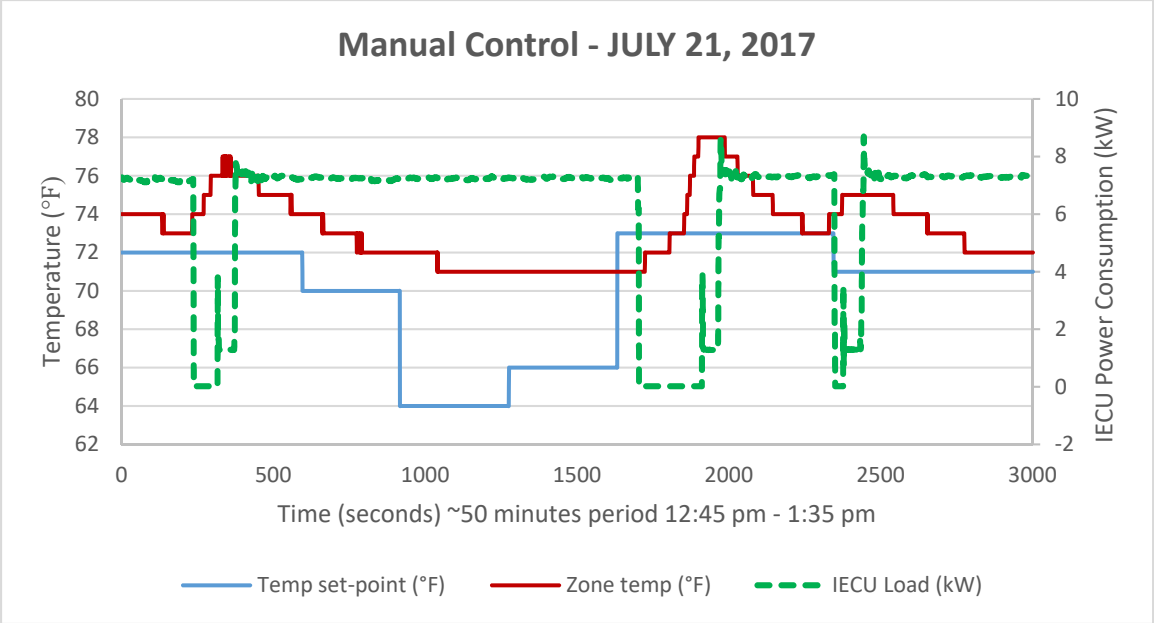

Figure 55 – Manual Control – Zone Temperature & Power Consumption – Superimposed

On Figure 56, the double y-axis results of the MPC case on June 22 for ventilated zone temperature, thermostat set-point temperature and the corresponding ECU power consumption are displayed. Each time the ECU operation terminates, the zone temperature rises above the set-point temperature and ECU power consumption instantaneously drops to zero. This system shutoff occurs around the 250th, 500th, 800th, 1300th, 1600th, 2550th and 2800th second instants across the run period. Each time the ECU operation resumes/restarts, the zone temperature drops to reach the set-point temperature. The system restart occurs in 2 stages. At 1st stage, the fan turns on and stabilizes which occurs around the 150th, 300th, 600th, 950th, 1450th, 2400th, 2600th and 2900th second instants across the run period. At 2nd stage, the compressor turns on and stabilizes which occurs around 200th, 350th, 650th, 1000th, 1500th, 2450th, 2700th and 3000th second instants across the run period. Due to large

inrush current, the short ECU load peaks occur for the fan, followed by long ECU load peaks which occur for the compressor.

Due to low inconsistencies in the efficiency of the ECU operation, the cooling component or compressor could reach temperature set-points below 71°F. During the operation of the ECU, the cyclic system termination and resumption systematically occurred during the entire duration of the run period. The discretized input of thermostat set-point temperature, roughly after each minute under predictive MPC optimized selection, significantly improved the system response time of the controlled zone temperature in the shelter. Unlike the manual control operation, a fresh ECU set-point temperature signal is sent to the ECU at roughly each minute during the MPC operation. This signal is either the same ECU set-point temperature from previous time-step or an entirely new ECU set-point temperature. This precisely discrete update to the system fastens the system response time of the ECU.

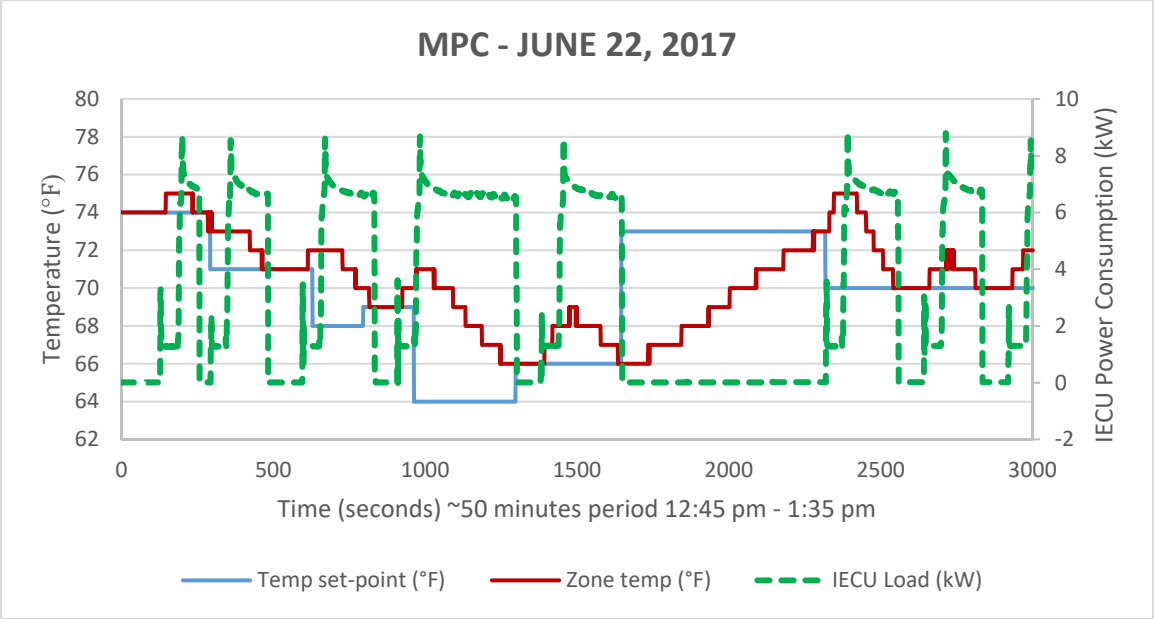

Figure 56 – MPC – Zone Temperature & Power Consumption – Superimposed

5.2 Discussion of Results for Alaska Shelter with IECU

The results obtained for the shelter and ECU combination are further analyzed by determining the net kWh each MPC and manual control for the run period of 50 minutes. Collected raw data for both tests was stored in the second-by-second time-step. The approach of trapezoidal numerical integration resulted in the values shown in Table 8.

Table 8 – MPC vs. Manual Control Net Load (kWh) Comparison – IECU

Day	Net Load (kWh)	MPC	Manual Control
July 21st	IECU	---	18502.7
June 22nd	IECU	9115.7	---

For summer season application days of June 22nd for MPC and July 21st for manual control, net load with manual control on IECU significantly exceeds the net load with MPC on IECU. The difference between the net loads for the power consumption of MPC versus manual control is 9387.1 kWh.

5.3 Verification of Application of MPC versus Manual Control

The Airbeam shelter model, adjusted with Alaska shelter inputs and equipped with IECU, is tested for minute-by-minute EnergyPlus simulations for June 22 as well as July 21. For all simulation cases with EnergyPlus, doubled IECUs/dual capacity IECU is used to account for unmet hours of load in the baseline EnergyPlus model of the ECU. The purpose of this simulation study is to establish a credible system model of the shelter for actual MPC application to the Alaska shelter. Since the MPC application run was performed on June 22nd while the manual control application run was performed on July 21st, this study is to establish the accuracy of comparing the results of the 2 applications. The precise net load effects between the 2 test dates is the focus of the approach taken with the minute-by-minute EnergyPlus simulation over the 50 minute run period. Since Alaska shelter is also a soft-shell shelter with similar features to Airbeam shelter, the valid model of Airbeam shelter was implemented in the study. Due to its ease of use, OpenStudio software is used to perform the simulations for the EnergyPlus cases. The testing is done for the 2 summer weather days, June 22 and July 21, which represent the actual MPC test date and manual control test date respectively. Also, the time-step for all simulations in the study is set to 1 minute. The simulations correspond to the weather of McGuire AFB, NJ.

5.3.1 Loads Applied to the Model

Since the simulations are performed for two individual days representing a summer season, the environmental load profile is heavily dependent on the chosen two days of the weather file. The date June 22nd corresponds to the summer day at the site when MPC application was performed whereas the date July 21st corresponds to the summer day at the site when manual control application was performed. Hence, the simulation dates were also set to the same historical weather dates of the geographical location of McGuire, AFB. Figure 57 shows the outdoor dry air bulb temperature input to the model, which is extracted from the EPW file. The internal loads to the model are constant 24 hour input values of 0 W for electronics equipment load, 1200 W for lighting load and occupancy of 1 person which equates to 120 W occupancy load.

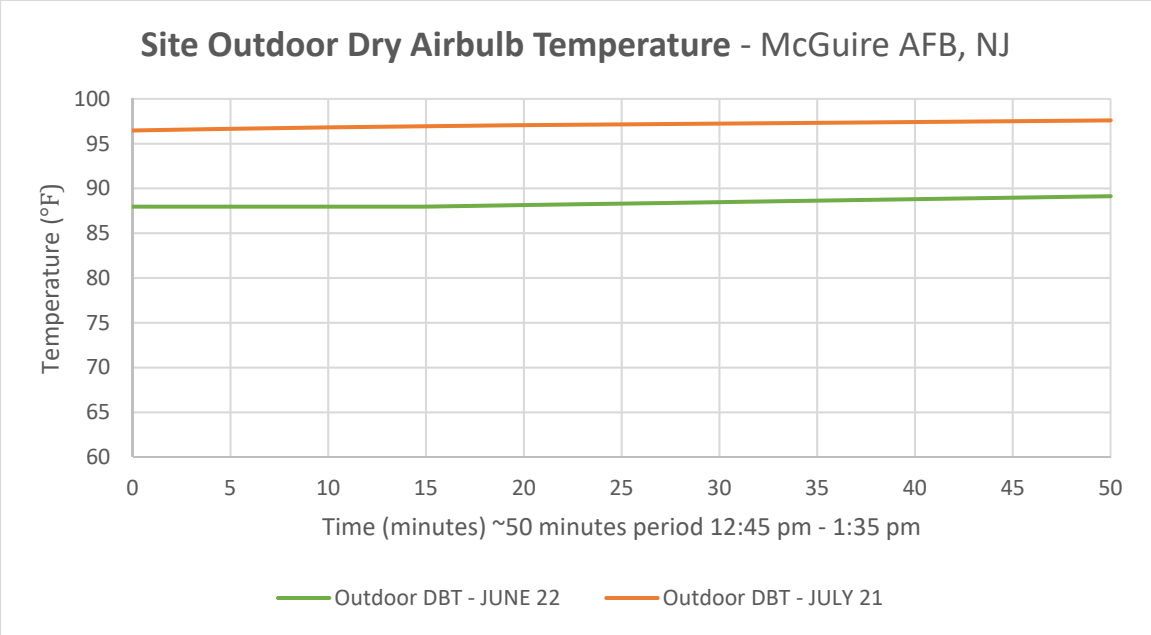

Figure 57 – Site Outdoor Dry Air Bulb Temperature – McGuire AFB, NJ

5.3.2 Results

The set of results presented is for the June 22nd and July 21st minute-by-minute cases in McGuire AFB, NJ. With the thermostat set-point schedule entered into the model as a hard constraint, the resultant EnergyPlus predictions of ventilated shelter temperature and equivalent ECU power consumption are compared.

5.3.2.1 Main Zone Temperature

Figure 58 shows the resultant Main Zone temperature from both EnergyPlus simulations. Green line represents June 22nd of MPC test date while orange line represents July 21st of manual control test date. The blue line represents the hard constraint of thermostat set-point and the dashed lines represent the historical site outdoor temperature. By observation, it is evident that for both summer season simulation dates, both zone temperature results precisely overlap the thermostat set-point temperature.

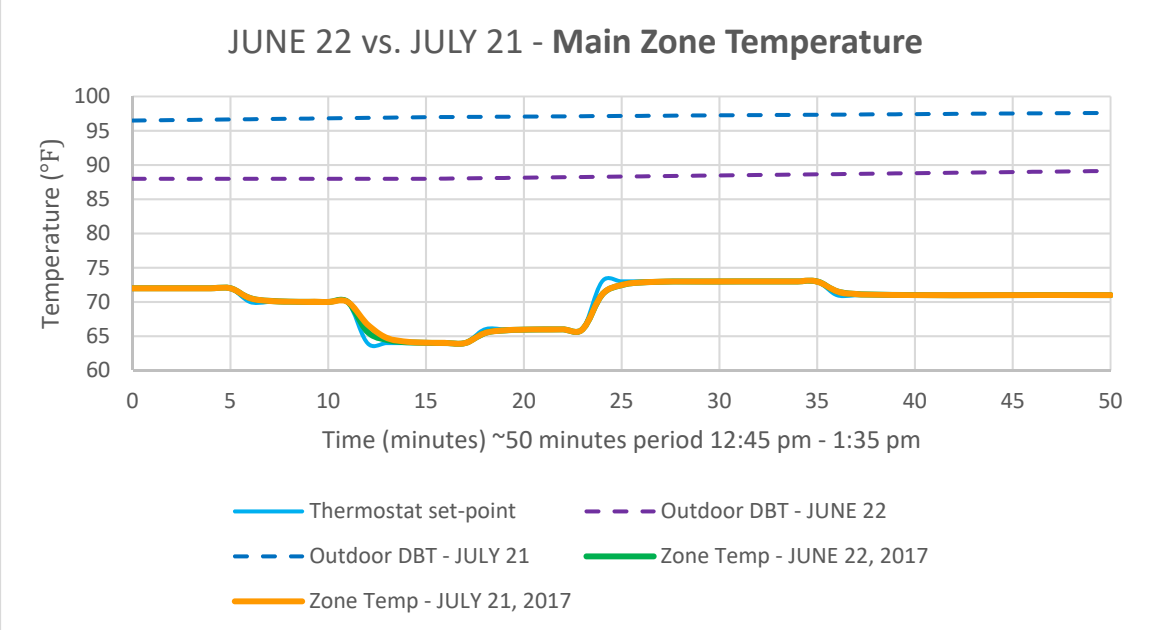

Figure 58 – June 22 vs. July 21 – Main Zone Temperature – EnergyPlus Simulations

5.3.2.2 Power Consumption

For both EnergyPlus simulations, Figure 59 shows the resultant unitary system electric power consumption. This output variable combines the electric power consumption of the heating and cooling coils with the power consumption of the active fan. On the figure, red line represents June 22nd of MPC test date while blue line represents July 21st of manual control test date. By observation, it is evident that for both summer season simulation dates, the cooling coil electric power is active throughout the run period while heating coil electric power is nearly negligible. By comparison, the unitary system electric power of June 22nd roughly overlaps the unitary system electric power of July 21st. This definite similarity in power consumption confirms the summer season simulation characteristics, which further justifies the application of MPC and manual control on the 2 separate summer days of the season.

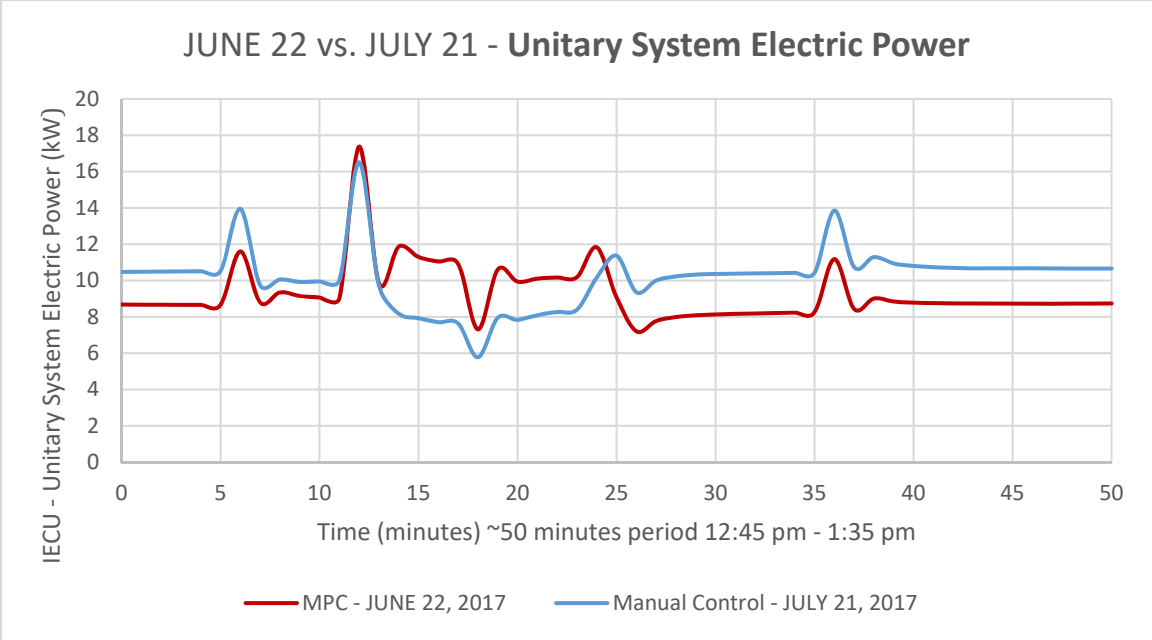

Figure 59 – June 22 vs. July 21 – Unitary System Electric Power – EnergyPlus Simulations

For both EnergyPlus simulations, Figures 60 & 61 show the resultant cooling coil electric power and heating coil electric power respectively. On both figures, red line represents June 22nd of MPC test date while blue line represents July 21st of manual control test date. By observation, it is evident that for the summer season simulation dates, the cooling coil electric power is active throughout the run period while the heating coil electric power is nearly negligible. By comparison, the cooling coil electric power of June 22nd roughly overlaps the unitary system electric power of July 21st. Furthermore, the heating coil electric power of June 22nd precisely overlaps the unitary system electric power of July 21st at that single peak in this operation. These definite similarities in cooling and heating coil power consumptions confirm the summer season simulation characteristics, which further justifies the application of MPC and manual control on the 2 separate summer days of the season.

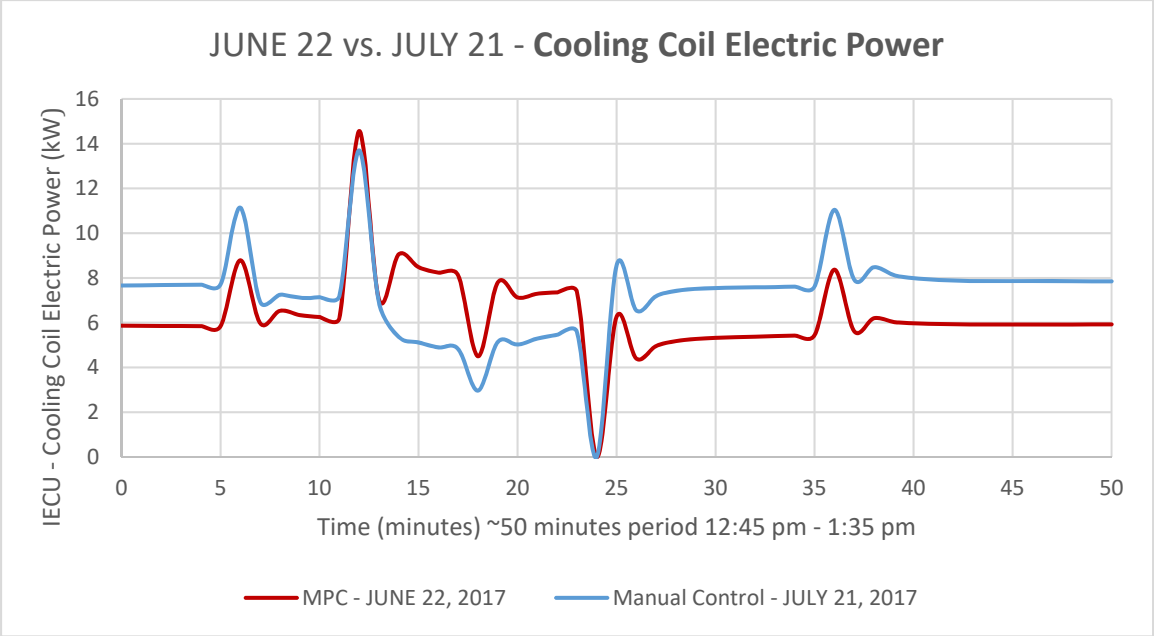

Figure 60 – June 22 vs. July 21 – Cooling Coil Electric Power – EnergyPlus Simulations

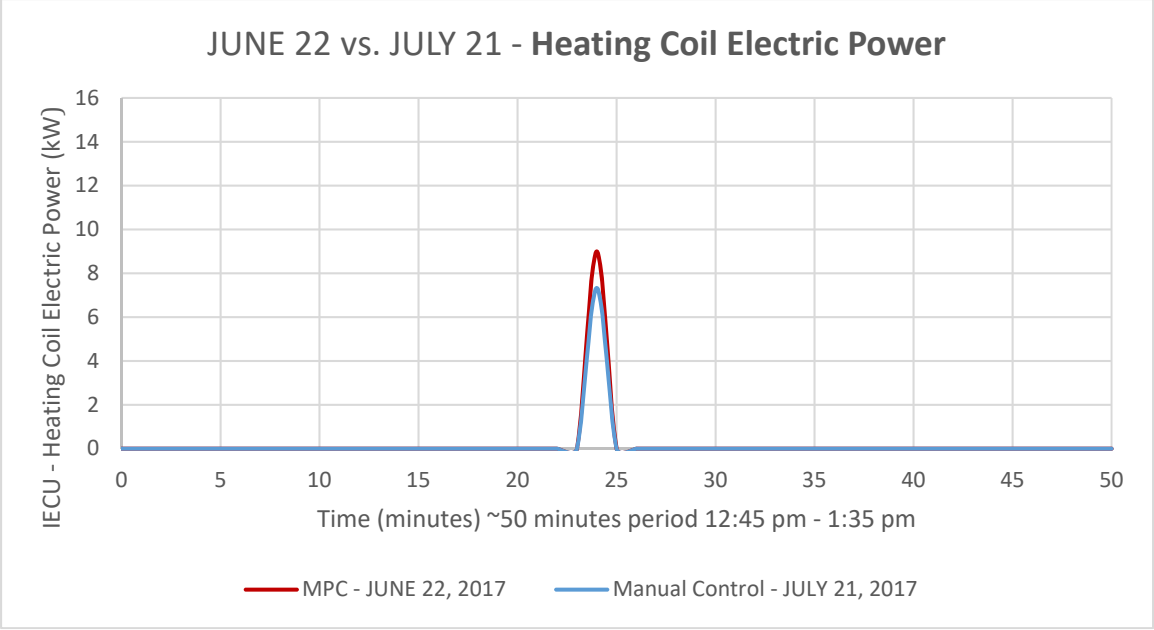

Figure 61 – June 22 vs. July 21 – Heating Coil Electric Power – EnergyPlus Simulations

5.4 Discussion of Results for Verification of MPC Application

The results obtained for the shelter and ECU combination are further analyzed by determining the net kWh of both EnergyPlus simulation cases for the run period of 50 minutes. The approach of trapezoidal numerical integration resulted in the values shown in Table 9.

Table 9 – June 22 vs. July 21 Net Load (kWh) Comparison – IECU

Day	Net Load (kWh)	EnergyPlus
June 22nd – MPC	Unitary System	465.7
	Cooling	316.1
	Heating	9.0
July 21st – Manual Control	Unitary System	508.3
	Cooling	360.3
	Heating	7.3

For summer season simulations with EnergyPlus, net load on July 21st for the output variables unitary system electric power and cooling coil electric power slightly exceed the net load for the same output variables on June 22nd. However, the net load on June 22nd for the output variable heating coil electric power slightly exceeds net load for the same output variable on July 21st. The difference between the net loads for the unitary system, cooling coil and heating coil of MPC versus EnergyPlus is 42.6 kWh, 44.2 kWh and 1.7 kWh

respectively. The higher power consumption with July 21st simulation is not significant in value as it still precisely simulates a summer season day similar to the June 22nd simulation. Since the load profiles match and the net load values are at the same order of magnitude, the results justify the accuracy in implementing MPC study versus manual control study on the 2 separate summer season dates.

5.5 Real-Time Load Profile Live-Updates during MPC Operation

A considerable limitation of the MPC application to actual ECU with an inhabitable shelter, is the inability to live-update the MPC controller in operation with actual changes to the load profile, weather profile, occupancy profile and thermostat schedule profile. For the current MPC controller, the validated EnergyPlus shelter model is updated with the hypothetically predicted load profile, weather profile, occupancy profile and thermostat schedule profile of the system. Hence in reality, a model is used in place of a real system to predict system behavior under future control actions. Due to this, the predicted behavior and the results obtained by predictive control will only be as good as the fidelity of the model with respect to the physical system.

Since the system model/EnergyPlus model of the shelter and ECU is the most important input to the MPC controller, the accuracy of the model significantly affects the performance of the controller. A more advanced MPC controller with the functionality to live-update the statuses of internal equipment load, lighting load, occupancy load, outside weather conditions and thermostat schedule, will truly represent the real system model. The advancement to such high-level of control workflow requires an advanced software for heat transfer calculations of the system model, higher processor for performing the

MPC optimization calculations with the system model and a much more advanced military software for receiving and sending such extreme assortment of data feedback. Moreover, the actual ECU and the shelter require to be highly advanced and equipped with every sophisticated transducer, for live-recordings of system states to be fully-accessible by the military software. The ability to attain such state-of-the-art hardware and supporting software would definitively enhance the performance of MPC operation.

CHAPTER 6. CONCLUSION & FUTURE WORK

This chapter summarizes and concludes the thesis along with remarking upon prospective work which remains to be pursued.

6.1 Conclusion

This thesis developed the MPC framework which executed the predictive modeling optimization approach on an ECU of an off-grid soft shell shelter. At each time-step, the framework investigated the future outputs of the validated EnergyPlus shelter and ECU model to determine the most fuel efficient output that also conformed to the constraining comfort criteria. Detailed simulations using the Airbeam shelter and HDT F100 ECU model for various seasons were performed with MPC framework as well as baseline EnergyPlus control framework. The resultant ECU power consumption and ventilated zone temperature outputs were quantified and compared for each seasonal case of the simulations.

The first MPC simulation case tested was the foremost optimization sequence in the controller of zero temperature overshoot outside the constraints of the thermostat schedule. Similar to the baseline EnergyPlus control, the ventilated zone temperature with MPC simulations are favorable to the constraining thermostat comfort criteria. The ECU power consumption with MPC was significantly lower than the EnergyPlus control for the seasonal cases of winter and spring. For the seasonal case of summer, the power consumption with MPC for the cooling coil was lower than the power consumption with EnergyPlus for the cooling coil. The second MPC simulation case tested was the foremost

optimization sequence in the controller of least energy consumption by the ECU during the operation of its fan, heating cycle and cooling cycle. Unlike EnergyPlus simulations, thermal comfort criteria was not met with the MPC simulations. However, the ECU power consumption with MPC was significantly lower than the EnergyPlus control for all seasonal cases of winter, spring and summer. The 2 forms of MPC optimization selection sequence resulted in overall much lower ECU power consumption than EnergyPlus simulation, regardless of the foremost selection priority given to thermal comfort criteria.

In addition, the thesis also developed the MPC framework software integration with EIO Application, which is the military GUI control system for hardware at FOBs. At each time-step, the MPC-chosen fuel efficient temperature set-point for the ECU was programmatically commanded to the actual ECU in operation for a shelter. Enhanced Airbeam shelter model with Alaska shelter inputs and HDT IECU input was provided as the system model input to the controller. Definite applications of both MPC and manual control on the IECU were performed for a 50 minute run period with each method. The resultant ECU power consumption and ventilated zone temperature outputs with MPC outperformed the resultant ECU power consumption and ventilated zone temperature outputs with manual control. In other words, MPC resulted in much higher energy efficiency and thermal comfort criteria than manual control.

Lastly, the exercise of implementing autonomous predictive modeling control on an actual ECU at a FOB is the first successful application of its kind. This is a significant contribution to the industry of military heating/cooling system as well as to the energy efficiency of off-grid shelters at forward operating bases (FOBs), disaster relief camps, refugee aid camps and other encampments.

6.2 Future Work

Among the many possibilities for forthcoming work with the framework, further refinement of the system model input to the MPC controller presents the most promising scope for improvement. Among the 3 input types to the controller, the validated EnergyPlus model of the shelter and ECU has the highest impact on the system outputs with the framework. The more accurate and precise modeling of the actual ECU and shelter characteristics is established, the more accurately fuel-efficient is the output prediction(s) determined by the controller.

Another scope for future work is implementing the framework on other validated shelter and ECU model types. An assortment of the simulation studies for all the available system model input options would certainly improve the fidelity of the current framework. Moreover, the different system model characteristics, unique to each individual shelter and ECU combination, could be analyzed for establishing the suitability aspects to the framework.

A major area of work left to be addressed is the consequences of the following variations to the controller –

- using an exact thermostat schedule followed by the occupant(s)
- reducing prediction time-step
- increasing prediction horizon
- increasing range of input ECU set-point temperatures

An actual operative thermostat schedule versus a presumptive thermostat schedule would validate the system model responses. Since reduction of prediction time-step considers more precise model response to a user-chosen thermostat schedule, in theory it should increase the fidelity of model response resulting in higher fidelity in MPC-chosen outcome(s). Since increase in prediction horizon considers a larger future forecast period of a model response to a user-chosen thermostat schedule, in theory it should refine the MPC-chosen outcome(s). Since in the range of input ECU set-point temperatures considers model response to set-point temperature choices for both integer and decimal cases, in theory it should results in more precise MPC-chosen outcome(s).

REFERENCES

[1] K. M. Gebo, "A Comparison of the Lifecycle Cost and Environmental Impact of Military Barracks Huts in Deployed Environments Constructed from Structural Insulated Panels (SIPs) versus Traditional Techniques," Sustainable Engineering (MS) Masters, Industrial and Systems Engineering (KGCOE), Rochester Institute of Technology http://scholarworks.rit.edu/theses/7848/, 2014.

[2] Eduardo F. Camacho., Carlos Bordons., 2007, "Model Predictive Control," 2nd edition, Springer London.

[3] D. Sturzenegger, D. Gyalistras, M. Morari, and R. S. Smith, "Model Predictive Climate Control of a Swiss Office Building: Implementation, Results, and Cost–Benefit Analysis," *IEEE Transactions on Control Systems Technology,* vol. 24, pp. 1-12, 2016.

[4] F. Oldewurtel, A. Parisio, C. N. Jones, D. Gyalistras, M. Gwerder, V. Stauch*, et al.*, "Use of model predictive control and weather forecasts for energy efficient building climate control," *Energy and Buildings,* vol. 45, pp. 15-27, 2// 2012.

[5] F. Oldewurtel, C. N. Jones, A. Parisio, and M. Morari, "Stochastic Model Predictive Control for Building Climate Control," *IEEE Transactions on Control Systems Technology,* vol. 22, pp. 1198-1205, 2014.

[6] I. Hazyuk, C. Ghiaus, and D. Penhouet, "Optimal temperature control of intermittently heated buildings using Model Predictive Control: Part I – Building modeling," *Building and Environment,* vol. 51, pp. 379-387, 5// 2012.

[7] I. Hazyuk, C. Ghiaus, and D. Penhouet, "Optimal temperature control of intermittently heated buildings using Model Predictive Control: Part II – Control algorithm," *Building and Environment,* vol. 51, pp. 388-394, 5// 2012.

[8] J. Široký, F. Oldewurtel, J. Cigler, and S. Prívara, "Experimental analysis of model predictive control for an energy efficient building heating system," *Applied Energy,* vol. 88, pp. 3079-3087, 9// 2011.

[9] J. D. Álvarez, J. L. Redondo, E. Camponogara, J. Normey-Rico, M. Berenguel, and P. M. Ortigosa, "Optimizing building comfort temperature regulation via model predictive control," *Energy and Buildings,* vol. 57, pp. 361-372, 2// 2013.

[10] J. Ma, J. Qin, T. Salsbury, and P. Xu, "Demand reduction in building energy systems based on economic model predictive control," *Chemical Engineering Science,* vol. 67, pp. 92-100, 1/1/ 2012.

[11] M. Wallace, R. McBride, S. Aumi, P. Mhaskar, J. House, and T. Salsbury, "Energy efficient model predictive building temperature control," *Chemical Engineering Science,* vol. 69, pp. 45-58, 2/13/ 2012.

[12] S. Prívara, J. Široký, L. Ferkl, and J. Cigler, "Model predictive control of a building heating system: The first experience," *Energy and Buildings,* vol. 43, pp. 564-572, 2// 2011.

[13] Y. Ma, F. Borrelli, B. Hencey, B. Coffey, S. Bengea, and P. Haves, "Model Predictive Control for the Operation of Building Cooling Systems," *IEEE Transactions on Control Systems Technology,* vol. 20, pp. 796-803, 2012.

[14] S. C. Bengea, A. D. Kelman, F. Borrelli, R. Taylor, and S. Narayanan, "Implementation of model predictive control for an HVAC system in a mid-size commercial building," *HVAC&R Research,* vol. 20, pp. 121-135, 2014.

[15] L. Fabietti, "Control of HVAC Systems via Explicit and Implicit MPC: an Experimental Case Study," Master's School of Electrical Engineering, KTH Royal Institute of Technology, Stockholm, Sweden, www.diva-portal.org/smash/get/diva2:712334/FULLTEXT01.pdf, 2014.

[16] J. Rehrl and M. Horn, "Model Predictive Control for Heating Ventilating and Air Conditioning Systems," *PAMM,* vol. 11, pp. 833-834, 2011.

[17] D. Schwingshackl, J. Rehrl, and M. Horn, "Model predictive control of a HVAC system based on the LoLiMoT algorithm," in *Control Conference (ECC), 2013 European*, 2013, pp. 4328-4333.

[18] G. Pattarello, "Model Predictive Control of HVAC Systems: Design and Implementation on a Real Case Study," Master's, University of Padua, http://tesi.cab.unipd.it/43642/, 2013.

[19] A. Beghi, L. Cecchinato, M. Rampazzo, and F. Simmini, "Energy efficient control of HVAC systems with ice cold thermal energy storage," *Journal of Process Control,* vol. 24, pp. 773-781, 6// 2014.

[20] G. P. Henze and M. Krarti "Predictive Optimal Control of Active and Passive Building Thermal Storage Inventory," University Of Nebraska, http://www.osti.gov/scitech/biblio/894509-GH9Mqf/2005.

[21] T. Zakula, P. R. Armstrong, and L. Norford, "Modeling environment for model predictive control of buildings," *Energy and Buildings,* vol. 85, pp. 549-559, 12// 2014.

[22] J. Zhao, K. P. Lam, and B. E. Ydstie, "ENERGYPLUS MODEL-BASED PREDICTIVE CONTROL (EPMPC) BY USING MATLAB/SIMULINK AND MLE+," presented at the 13th Conference of International Building Performance Simulation Association, Chambéry, France, 2013.

[23] C. D. Corbin, "Assessing Impact of Large-Scale Distributed Residential HVAC Control Optimization on Electricity Grid Operation and Renewable Energy Integration," PhD, Department of Civil, Environmental and Architectural Engineering, University of Colorado, https://mpra.ub.uni-muenchen.de/58318/, 2014.

[24] S. Prívara, J. Široký, L. Ferkl, and J. Cigler, "Model predictive control of a building heating system: The first experience," *Energy and Buildings,* vol. 43, pp. 564-572, 2// 2011.

[25] I. Hazyuk, C. Ghiaus, and D. Penhouet, "Optimal temperature control of intermittently heated buildings using Model Predictive Control: Part II – Control algorithm," *Building and Environment,* vol. 51, pp. 388-394, 5// 2012.

[26] J. Rehrl and M. Horn, "Model Predictive Control for Heating Ventilating and Air Conditioning Systems," *PAMM,* vol. 11, pp. 833-834, 2011.

[27] D. Sturzenegger, D. Gyalistras, M. Morari, and R. S. Smith, "Model Predictive Climate Control of a Swiss Office Building: Implementation, Results, and Cost–Benefit Analysis," *IEEE Transactions on Control Systems Technology,* vol. 24, pp. 1-12, 2016.

[28] M. Gruber, A. Trüschel, and J.-O. Dalenbäck, "Model-based controllers for indoor climate control in office buildings – Complexity and performance evaluation," *Energy and Buildings,* vol. 68, Part A, pp. 213-222, 1// 2014.

[29] Sinha, A., Joshi, Y K., "Model Predictive Control of Military Soft Shelter Environment Control Units,". IN PROGRESS.

[30] Sinha, A., Joshi, Y K., "Modeling of military soft shelters for HVAC control purposes,". IN PROGRESS.

[31] Druby B. Crawley, Linda K. Lawrie, F.C.W. W.B.Y., "Energyplus: creating a new generation building energy simulation program," in Energy and Building, vol.33, pp.319-331, Elsevier Science B.V., 2001.

[32] "Getting Started with EnergyPlus," EnergyPlus Documentation, vol 8.7.0, NREL, 2016.

[33] Eguaras-Martínez, María, Marina Vidaurre-Arbizu, and César Martín-Gómez. "Simulation and Evaluation of Building Information Modeling in a Real Pilot Site." Applied Energy 114 (2014): 475-84. Web.

[34] "OpenStudio," OpenStudio | OpenStudio. NREL. Web. 15 Jul. 2017. <https://www.openstudio.net/>

[35] Athinodoros Tzoulis, "Performance assessment of building energy modelling programs and control optimization of thermally activated building systems," Delft University of Technology, 2014.

[36] "MATLAB Primer," rev 9.2 (R2017a), pp. 2-4, The MathWorks, Inc., 2017.

[37] Willy Bernal, Madhur Behl, Truong Nghiem, and Rahul Mangharam, "MLE+: A Tool for Integrated Design and Deployment of Energy Efficient Building Controls",. October 2012.

[38] "Oracle VM VirtualBox User Manual," ver 5.1.22, pp. 12-18, Oracle Corporation, 2017.

[39] “Getting Started with Ubuntu 14.04,” rev 100, pp. 5-19, The Ubuntu Manual Team, 2014.

[40] “Energy Informed Operations Sensor Service API,” version 7.0, CERDEC CP&I, 2016.

[41] “EIO Application Installation and Administration Guide Ubuntu – Linux,” version 1.0, CERDEC CP&I, 2016.

[42] Deru, M., Bonnema, E., Barker, G., Hancock, E., & Kumar, A. (2015). “Energy Performance Measurement and Simulation Modeling of Tactical Soft-Wall Shelters (No. ERDC/CERL-TR-15-13),” Engineer Research and Development Center Champaign IL, Construction Engineering Research Lab.

[43] “HDT 60K IECU AND S60K IECU,” rev 1, pp. 1-2, HDT Global, 2017.

[44] “F100-60K Commercial ECU,” rev 2, pp. 1-2, HDT Global, 2012.

[45] Lee, Daniel (IN PROGRESS). “Energy Usage Modeling for Heating and Cooling off Off-Grid Shelters,” Georgia Institute of Technology.

[46] “Auxiliary Programs,” EnergyPlus Documentation, vol 8.7.0, NREL, 2016.

[47] “Engineering Reference: The Reference to EnergyPlus Calculations,” EnergyPlus Documentation, vol 8.7.0, NREL, 2016.

[48] “Input Output Reference: The Encyclopedic Reference to EnergyPlus Input and Output,” EnergyPlus Documentation, vol 8.7.0, NREL, 2016.

[49] Kusuda, T., & Achenbach, P. R. (1965). “Earth temperature and thermal diffusivity at selected stations in the United States (No. NBS-8972),” National Bureau of Standards Gaithersburg MD.

[50] “Environmental Control Unit Data Model,” revision 1.3, CERDEC CP&I Energy Informed Operations Program, 2015.

[51] "Alaska XP Shelter System," Alaska Structures. Web. 20 Jul. 2017. <https://www.aks.com/military-division/aks-xp-shelter-system/>

[52] “Weather History for KWRI - June, 2017,” Weather Underground. Web. 6 Aug. 2017. < https://www.wunderground.com/history/airport/KWRI/2017/6/22/DailyHistory.html?req_city=Fort+Dix&req_state=NJ&req_statename=&reqdb.zip=08640&reqdb.magic=1&reqdb.wmo=99999>

[53] “Weather History for KWRI - July, 2017,” Weather Underground. Web. 6 Aug. 2017. < https://www.wunderground.com/history/airport/KWRI/2017/7/21/DailyHistory.html?req_city=Fort+Dix&req_state=NJ&req_statename=&reqdb.zip=08640&reqdb.magic=1&reqdb.wmo=99999>